NTNU
Norwegian University of
Science and Technology

Simulation of Anchor Loads on Pipelines

Kristbjörg Edda Jónsdóttir

Marine Technology
Submission date: June 2016
Supervisor: Svein Sævik, IMT

Norwegian University of Science and Technology
Department of Marine Technology

MASTER PROJECT WORK SPRING 2016

for

Stud. tech. Kristbjörg Jónsdóttir

Simulation of anchor loads on pipelines

Simulering av ankerlaster på rørledninger

Anchor loads on pipelines is in general a rarely occurring event, however, the severity when it occurs could easily jeopardize the integrity of any pipeline. It is considered as an accidental load in the design of pipelines. In the Norwegian Sea there are several locations where the subsea pipeline density is high, also in combination with high vessel density. The vessels usually know where pipelines are located and avoid anchoring, but anchors might be dropped in emergencies, lost in bad weather or due to technical failures. In these cases, the drop might not be noticed before the anchor hooks, e.g. in a pipeline.
The master thesis work is to be carried out as a continuation of the project work as follows:

1. Literature study on pipeline technology, relevant standards for pipeline design, with particular focus on impact loads. Aspects related to vessel size, frequencies and corresponding anchor equipment is to be included also using previous thesis by Wei Ying and Stian Vervik as starting points.
2. Study the theoretical background for and get familiarized with the computer program SIMLA
3. Define the basis for a case study considering anchor geometry, pipeline mechanical properties, soil interaction parameters, wire chain capacity, water depth, friction and hydrodynamic coefficients
4. Establish SIMLA models for the hooking event that allows for sliding under friction along the pipeline and perform simulations to demonstrate the performance of the model.
5. Then perform parametric studies in order to categorize the anchor contact behaviour as follows:
    a. Assume two pipe diameters 30 inch and 40 inch with D/t = 35
    b. Assume ship velocities 2 knots and 10 knots
    c. Look at the anchor chain lengths and identify contact scenarios as a function of water depth for three water depths
    d. Assume the pipe to be continuously supported and identify hooking scenarios for tow direction/pipeline relative angles 90, 60 and 30 deg (using a stiff model).
    e. Based on identified hooking scenarios, make a refine FE model to study the overall detailed behaviour including the pipeline global response.
6. Conclusions and recommendations for further work

All necessary input data are assumed to be delivered by Statoil.
The work scope may prove to be larger than initially anticipated. Subject to approval from the supervisors, topics may be deleted from the list above or reduced in extent.
In the thesis the candidate shall present his personal contribution to the resolution of problems within the scope of the thesis work

Theories and conclusions should be based on mathematical derivations and/or logic reasoning identifying the various steps in the deduction.
The candidate should utilise the existing possibilities for obtaining relevant literature.

Thesis format
The thesis should be organised in a rational manner to give a clear exposition of results, assessments, and conclusions. The text should be brief and to the point, with a clear language. Telegraphic language should be avoided.
The thesis shall contain the following elements: A text defining the scope, preface, list of contents, summary, main body of thesis, conclusions with recommendations for further work, list of symbols and acronyms, references and (optional) appendices. All figures, tables and equations shall be numerated.
The supervisors may require that the candidate, in an early stage of the work, presents a written plan for the completion of the work.
The original contribution of the candidate and material taken from other sources shall be clearly defined. Work from other sources shall be properly referenced using an acknowledged referencing system.
The report shall be submitted electronically on DAIM:

- Signed by the candidate
- The text defining the scope included
- In bound volume(s)
- Drawings and/or computer prints which cannot be bound should be organised in a separate folder.

Ownership
NTNU has according to the present rules the ownership of the thesis. Any use of the thesis has to be approved by NTNU (or external partner when this applies). The department has the right to use the thesis as if the work was carried out by a NTNU employee, if nothing else has been agreed in advance.

Thesis supervisors:
Prof. Svein Sævik, NTNU
Dr. Erik Levold, Statoil

Deadline: June 10, 2016

Trondheim, January, 2016

Svein Sævik

Candidate – date and signature:

Preface

This thesis is based on research carried out during the spring semester of 2016 at the Department of Marine Technology, NTNU, as part of my Master's degree in Marine Technology, with Underwater Technology as specialization. The thesis is a continuation on the work I carried out during the autumn semester of 2015 in the course *TMR4580: Marine Subsea Engineering, Specialization Project.*

The main topic of this thesis is to inspect how and which parameters affect anchor-pipeline interaction through simulation of the interaction using the computer software SIMLA. This was done by carrying out a parameter study and eleven case studies.

This thesis is a continuation of Master theses by Stian Vervik (2011) and Ying Wei (2015). The initial SIMLA input files were received from Wei (2015). A large amount of time has gone into understanding these input files and modifying them, as old drafts were received for the parametric study. Modifying and updating the input files was by far the most time consuming part of this thesis. The scope of the thesis was narrowed compared to the work description presented above, by altering point 5 C). Only one water depth was investigated to determine the minimum anchor length for interaction.

I would like to thank my supervisor Prof. Svein Sævik at the Department of Marine Technology, NTNU, for his guidance during this project with regards to theoretical understanding and the computer software SIMLA. I would also like to thank Dr. Erik Levold from Statoil for the input parameters, and I would like to acknowledge MARINTEK regarding the license of SIMLA. Lastly, a special thanks to my parents and the girls in office A2.027 for help with the thesis.

Trondheim, June 2016

Kristbjörg Edda Jónsdóttir

Summary

Incidents where anchor and pipeline interact are rare, but such an event can have drastic consequences. In the report, *Pipeline and Riser Loss of Containment* by HSE, published in 2001 for the UK sector, 44 incidents involving anchors and pipelines were found for the period 1990-2000. Furthermore, The International Cable Protection Committee reported that between 2007-2008, there were ten cases of submarine cables damaged due to anchor damage. All of these cases were due to vessels being unaware of their anchors being deployed during transit.

The objective of this thesis is to study the anchor's and the pipeline's response to such interactions. The response of the anchor was investigated by performing a parametric study and categorizing the anchor's behaviour. The pipeline was modelled as a 10 meter long constrained rigid body in this study. The literature usually defines anchor behaviour as impact, hooking or pull over. In this study a new system was made for the categorization of the behaviour. The behaviour was either categorized as brief or lasting contact. If categorized as brief, the contact was further defined as either pull over or bounce over. If lasting contact, it was defined either as hooking or sliding, with or without twisting.

Seventy-eight models were analysed in the parametric study. The parameters investigated were the anchor's mass and geometry, towing speed of the anchor, size of pipeline and angle of attack between anchor and pipeline. Forty-eight new models were created to investigate the minimum chain length for the towed anchor to reach the subsea pipeline. A constant water depth of 200 meters was applied in all studies.

The pipeline's global response was studied by performing eleven case studies. The parameters applied in these cases were based on the results from the parametric study and the minimum chain length study. In the eleven cases studied, the pipeline was modelled to be 10 kilometer long, with elastoplastic material properties. The pipeline was constrained at the ends, but otherwise allowed to displace and globally deform. The effect of the interaction on the pipeline was investigated by studying the longitudinal strains in the cross-section. The results were

compared with DNV's design load strain for combined loading, and with the pipeline's characteristic strain resistance.

The study of minimum chain length revealed that for an anchor towed at 2 knots, a chain length approximately 3 meters longer than the water depth was required. For the 10 knot case, due to drag forces, the chain needed to be roughly 110 meters longer than the water depth. However, these results are only valid when the anchor is dropped 100 meters away from the pipeline.

The general trend of the anchor behaviour seen in the parametric study, points towards an increase in hooking and sliding with increased mass of anchor, smaller pipe diameter and lower vessel speed. The largest amount of hooking scenarios in the parametric study occurred for 60 degrees angle of attack, as the anchor twisted and hooked. No hooking occurred for the 30 degrees cases, while all sliding events occurred for this angle.

Three of the eleven case studies resulted in hooking. In all of these cases, the longitudinal strain in the cross-section of the pipeline exceeded both DNV's design load criteria for combined loading and the pipeline's characteristic strain resistance. Exceeding the characteristic strain resistance puts the integrity of the structure at risk for local buckling. However, a more detailed FEA is necessary to determine the actual response of the cross-section, and which failure mechanisms it may initiate.

In the case studies with the full-length pipeline, no hooking was obtained for the attack angle of 60 degrees, which contradicts the results from the parametric study. This may indicate that the rigid modelling of the pipeline, rather than the anchor's response, caused the hooking response in the parametric study.

The three of the eleven case studies that resulted in hooking, revealed that the global displacement of the pipeline is much greater when the anchor is towed at a lower velocity. For higher velocities, the hooking case with minimum chain length displaced the pipeline farther, both laterally and vertically, than the anchor towed with maximum chain length.

Sammendrag

Ulykker hvor undersjøiske rørledninger blir utsatt for ankerlaster er sjeldne, men kan ha dramatiske konsekvenser. Ulykker som Kvitebjørn gassrør-ulykken i 2007, kombinert med den økende skipstrafikken over rørledninger i Nordsjøen, gjør ankerinteraksjon med rørledninger til et svært relevant tema.

Formålet med denne oppgaven er å analysere responsen ved interaksjon mellom anker og rørledning. For å undersøke ankerresponsen, ble en parameterstudie utført. Syttiåtte modeller ble analysert for å undersøke effekten av ankermasse og -geometri, størrelse på rørledning, ankerets angrepsvinkel og tauehastighet. Ved undersøkelse av ankerets respons ble rørledningen modellert som et 10 meter langt fastinnspent stivt legeme.

Tradisjonelt blir interaksjonen mellom anker og rørledning beskrevet som «impact», «hooking» eller «pull over». Basert på denne terminologien ble et nytt system utviklet og brukt for å kategorisere interaksjon. Ankerets adferd ble først kategorisert basert på om kontakten mellom ankeret og rørledninger var kort- eller langvarig. Hvis den var kortvarig, ble den videre definert som enten «pull over» eller «bounce over». Om kontakten var langvarig, ble den kategorisert som enten «hooking» og «sliding», med eller uten vridning.

Etter å ha kategorisert adferden til ankeret ble 48 modeller laget for å undersøke effekten av tauehastighet på ankerkjetting med ulik lengde. Formålet med disse 48 analysene var å definere minimum lengde på ankerkjettingen for at ankeret skal treffe rørledningen på 200 meters dyp.

DNVs kriteria for maksimal tøyning hvis en rørledning er utsatt for kombinerte laster, har blitt benyttet for å bedømme rørledningens respons. Hvis tøyningen i tverrsnittet overskrider denne verdien, kan lokal knekking oppstå. Elleve casestudier ble opprettet på grunnlag av funn fra parameterstudiet og studiet av minimum lengde på ankerkjetting. I casestudiene ble rørledningen modellert som 10 kilometer lang med elastoplastiske material egenskaper, kun fastinnspent ved endene.

Minimum lengde på ankerkjetting for at ankeret skal treffe et rør på 200 meters dyp, er avhengig av tauehastigheten. Resultatene viste at ved lav hastighet, 2 knot, må kjettingen være minst 3 meter lengre enn vanndybden for at ankeret skal treffe røret. Ved høy hastighet, 10 knot, må kjettingen være minst 110 meter lengre enn vanndybden. Disse resultatene er kun gyldige hvis ankeret starter maksimalt 100 meter unna røret.

Resultatene fra parameterstudiet viser en økning i «hooking»- og «sliding»-responser ved økt ankermasse, lavere tauehastighet og mindre diameter på rørledningen. Flertallet av interaksjonene som resulterte i en «hooking»-respons, forekom når angrepsvinkelen var 60 grader. «Sliding» forekom kun når angrepsvinkelen var 30 grader.

Tre av de elleve casestudiene resulterte i «hooking». I disse overskred den langsgående tøyningen i tverrsnittet DNV's kriteria for tillatt tøyning, og rørets karakteristiske tøyningsmotstand. Dette setter rørledningens tverrsnitt i fare for lokal knekking.

Det forekom ingen «hooking»-respons i casestudiet når angrepsvinkel var 60 grader. Dette kan indikere at «hooking»-responsen i parameterstudiet var forårsaket av hvordan rørledningen ble modellert, og ikke av ankerets respons.

Fra casestudiene som resulterte i «hooking» er det tydelig at den globale forskyvningen av rørledningen er større når ankeret taues ved lavere hastighet. For casene med høyere hastighet, ble rørledninger forskjøvet lengre lateralt og vertikalt når ankeret ble tauet med kortest mulig ankerkjetting.

Table of Contents

List of Figures

List of Tables

Nomenclature

Abbreviations

ALS	Accidental Limit State
DNV	Det Norske Veritas
FEA	Finite Element Analysis
FEM	Finite Element Method
FLS	Fatigue Limit State
HSE	Health and Safety Executive (UK)
MARINTEK	Norwegian Marine Technology Research Institute
SLS	Serviceability Limit State
ULS	Ultimate Limit State

Roman Letters

Unfortunately many of the same roman letters have been used for more than one purpose, the exact meaning of each letter is therefore explained in the text.

a_1	Fluid acceleration
A	Area
A	Projected area
c	Damping
$c_{critical}$	Critical damping
C	Impulse shape factor
$\boldsymbol{C}$	Damping matrix
$\boldsymbol{C_0}$	Diagonal damping matrix
C_M	Mass coefficient
C_D	Drag coefficient
D	Outside diameter
E	Young's modulus

$\boldsymbol{E}$	Green strain tensor
$\boldsymbol{E^e}$	Elastic strain tensor
$\boldsymbol{E^p}$	Plastic strain tensor
EN	Equipment number
$dF_{horizontal}$	Horizontal forces
$dF_{inertia}$	Inertia forces
dF_{drag}	Drag forces
f_0	Initial ovality
f_c	Characteristic material strength
$\boldsymbol{f}$	Related volume force vector
F	Maximum impact load
F_{lift}	Lift force
$\boldsymbol{F}$	Deformation gradient
I	Second moment of inertia
I	Impulse load
$\boldsymbol{K}$	Stiffness matrix
L	Length of cylinder
L_i	Load effects
L_{Sd}	Design load
m	Mass
$\boldsymbol{M}$	Mass damping matrix
p_b	Bursting pressure
p_c	Collapse pressure
p_e	External pressure
p_{min}	Minimum external pressure
$\boldsymbol{r}$	Displacement
R_{Rd}	Design resistance
$\boldsymbol{R}$	Load vector
$\boldsymbol{R^I}$	Internal force
$\boldsymbol{R^E}$	External force
$\boldsymbol{S}$	2nd Piola-Kirchhoff stress tensor
$\boldsymbol{t}$	Traction on the volume surface
t_2	Wall thickness corrected for corrosion
t_c	Characteristic thickness
t_d	Duration of impact

u	Fluid velocity
u_x	Displacement in X-direction
u_y	Displacement in Y-direction
u_z	Displacement in Z-direction
$\boldsymbol{u}$	Displacement
$\delta\boldsymbol{u}$	Virtual displacement
v_0	Initial velocity
v_i	Velocity at time i

Greek Letters

$\boldsymbol{\alpha_1}$	Mass damping ratio
$\boldsymbol{\alpha_2}$	Stiffness damping ratio
α_h	Train hardening
α_{gw}	Girth weld factor
γ_i	Load effect factor
γ_m	Material resistance factors
γ_{SC}	Safety class resistance factor
γ_ε	Strain resistance factor
Δ	Displacement
$\delta\varepsilon$	Virtual natural strain
ε_c	Characteristic bending strain resistance
ε_{Sd}	Design loads strain
θ_x	Rotation about X-axis
θ_y	Rotation about Y-axis
θ_z	Rotation about Z-axis
κ	Strain-hardening parameter
ξ	Damping ratio
ρ	Density
ρ_0	Density of undeformed configuration
$\boldsymbol{\sigma}$	Natural stress tensor
σ_0	Initial stress tensor
σ_e	Von Mises stress
σ_{xx}	Longitudinal stress
$\sigma_{\varphi\varphi}$	Hoop stress

Chapter 1

Introduction

1.1 Motivation

Incidents where anchor and pipeline interact are rare, but can have drastic consequences. In the report *Pipeline and Riser Loss of Containment* published in 2001 for the UK sector, 44 incidents involving anchors and pipelines were found for the time period 1990-2000 (HSE, 2009). The largest amount of incidents occurred near offshore platforms, followed by incidents further than 100 meters from the platform (HSE, 2009). Eighteen of the incidents were caused by supply boats, and eleven by construction vessels. The International Cable Protection Committee could also report that between 2007-2008 ten submarine cables were damaged due to anchor damage in the UK sector (*Damage to Submarine Cables Caused by Anchors*, 2009). In all of these cases, the vessels were unaware that their anchors were deployed during transit.

An example of an anchor-pipeline accident in the Norwegian sector, is the Kvitebjørn gas pipeline incident (Gjertveit, Berge, & Opheim, 2010). During inspection in 2007, it was discovered that the pipeline had been dented and local buckling had occurred. It was concluded that this was due to impact with an anchor as an overwhelming amount of evidence was found, including a 10 ton anchor retrieved beside the pipeline (Gjertveit et al., 2010).

Despite the small amount of interactions, the consequences of these and the increasing amount of pipelines and ship traffic across these in the North Sea, makes the topic of anchor-pipeline interaction highly relevant. Additionally, there is currently a limited coverage of anchor hazards within both UK Codes/Standards and other publicly available guidance (HSE, 2009).

1.2 Objective

There is limited literature regarding anchor-pipeline interaction, however most of this literature classify the interaction as either: impact, hooking or pull over. This classification may prove to be somewhat simplistic, and cause loss of information regarding the behaviour of the anchor and the pipeline's response. This thesis therefore attempts to categorize and analyse the anchors behaviour when exposed to different parameters, but also to improve the categorization of the behaviour. Understanding the anchors behaviour, may increase the knowledge about the pipeline's response to the interaction.

Once having determined how the parameters affect the anchor's behaviour, it is of interest to inspect the pipeline's response to the different behaviours, and to determine the consequences of such an event. The main objective here is to investigate whether the strain in the pipeline's cross-section exceeds DNV's criteria for the characteristic bending strain and design load. Exceeding this value indicates that the pipeline's cross-section may experience local buckling (DNV-OS-F101, 2013).

1.3 Scope and limitations

The master (MA) theses by Vervik (2011) and Wei (2015) create the foundation for this master thesis. Vervik (2011) studied the likelihood of hooking for the Kvitebjørn gas pipeline and the impact of anchor hooking on the pipeline. Wei (2015) investigated the effect of parameters on the probability of hooking and the pipeline's global response.

To study the interaction, a Finite Element Analysis (FEA) needs to be carried out. To do this MARINTEK's software SIMLA was chosen, as it was applied by both Vervik (2011) and Wei (2015). A draft for the input file used in Wei's (2015) parametric study, and the input files for the model including elastoplastic materials, were received by Wei (2015). These input files were modified and used to study the anchor's and pipeline's response to an interaction.

Statoil defined the parameters that are of interest in the attached work description to be: pipe size, anchor size, anchor chain length, water depth, vessel speed and angle of attack between anchor and pipeline. The given parameters are summarized in Table 1.1.

Table 1.1: Given parameters from Statoil

Pipe Diameter [Inches]	**Vessel velocity [Knots]**	**Angle of Attack [Degrees]**
30	2	90
40	10	60
		30

A parameter study was performed to determine which combination of parameters cause hooking, sliding and pull over, and by improving the categorization, get a better impression of the anchors' behaviour. The scope of the thesis is narrowed by only inspecting six different anchor sizes and only one water depth.

Due to time limitations and the complexity of the topic, modelling of the soil has been simplified quite extensively. The seabed is also modelled as completely flat. The local response of the pipeline is not studied, as that would require a more detailed analysis.

The scope of the thesis was also narrowed by inspecting only one water depth of 200 meters. This choice had particular significance for point 5 C) in the attached work description presented at the beginning of the thesis. The water depth was not altered in the second study, which investigates the minimum chain length for the anchor to reach the subsea pipeline, when towed. Instead, the chain's length was varied.

1.4 Outline of Thesis

Before describing the modelling of the anchor-pipeline interaction, an overview of the problem is presented through a brief introduction to anchor-pipeline interaction, subsea pipelines and anchors in Chapter 2.

Relevant literature in the form of rules and regulations by DNV, scientific papers, and the two master thesis by Vervik (2011) and Wei (2015) are reviewed in Chapter 3.

Non-linear finite element theory used in the SIMLA software to analyse the interaction are reviewed in Chapter 4.

To inspect the anchor's and pipeline's response to an interaction, two main analysis were carried out. The first, to determine the anchor's response, was the parametric study, which was divided into two segments. The first segment inspects all parameters, except the anchor chain length and depth, and the second segment only inspects only chain length and depth. The second

analysis, to study the pipeline's global response, consists of eleven case studies. The eleven cases were created based on results from the two previous studies, and investigates the strain in the pipeline's cross-section. A description of these analyses, the modelling of the interaction and calculations procedures are presented in Chapter 5.

Results and discussion for each of the analyses are presented in Chapter 6. The conclusion of the thesis is presented in Chapter 7, and lastly, further work is discussed in Chapter 8.

Chapter 2

Anchor-Pipeline Interaction

Several situations may lead to anchor-pipeline interaction. The anchor can be accidentally dropped, or if there are severe weather conditions during deployment and recovery, the anchor may be dragged along the seabed. Anchors can also experience dragging along the seabed should they lose hold of the soil (HSE, 2009).

Interactions between anchors and pipelines have traditionally been classified into three main categories: impact, pull over and hooking. All anchor-pipeline interaction start with an initial impact. A dropped anchor will either rest on the pipeline or slide of after the impact. A towed anchor will either be pulled over or hook on to the pipe. The initial impact may cause local dents, damage to coating or large local deformations (DNV-RP-F111, 2010). A hooking event may cause large deformations such as the pipe being displaced laterally or lifted several meters (DNV-OS-F101, 2013). This can cause the pipeline to rupture and leave the pipeline unfit to operate (Sriskandarajah & Wilkins, 2002).

Pipelines exposed to external interference will generally experience failure mechanisms immediately after the interference (DNV Energy Report, 2010). However, in the case of an anchor impact, the damage to coating will not necessarily induce failure at once, but rather allow corrosion, which could lead to leaking or rupturing with time (DNV Energy Report, 2010). Anchor-pipeline interaction can therefore cause both instantaneous and long-term consequences.

Before inspecting the literature and modelling of the anchor-pipeline interaction, some general background regarding subsea pipelines and anchors will be reviewed.

2.1 Subsea Pipelines

The main purpose of any pipeline is to carry a fluid from one end to the other, without losing any of the substance. Pipelines are exposed to hydrostatic pressure from the water column and internal pressure from the fluid within, which cause stresses in the pipewall as seen in Figure 2.1.

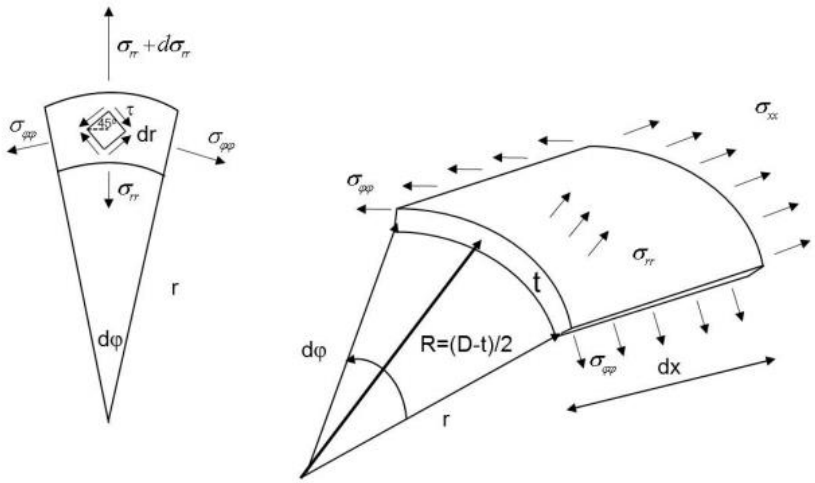

Figure 2.1: Stress components in cross-section segment of the pipewall (Sævik, 2014)

There are three contributions to the stress in the pipewall; these are the hoop stress, longitudinal stress and radial stress. Hoop stress is defined as the stress that goes in the circumferential direction of the pipe ($\sigma_{\varphi\varphi}$), longitudinal stress goes along the pipe (σ_{xx}) while radial stress (σ_{rr}) works perpendicular to the surface. There are two methods to calculate these, either thin walled theory, as done by DNV, or by thick walled shell theory (Sævik, 2014). Independently of which method is applied to find the longitudinal and hoop stress, the results can be used to find the Von Mises equivalent stress, see equation (2.1), to assess yielding in the steel material.

$$\sigma_e = \sqrt{\sigma_{xx}^2 + \sigma_{\varphi\varphi}^2 - \sigma_{xx}\sigma_{\varphi\varphi}} \tag{2.1}$$

The pressure and external loads that the pipelines may be exposed to, can cause several forms of failures such as bursting, excessive yielding (collapse), buckling and denting. To prevent bursting, the pipeline needs to be able to withstand the internal pressure, while to prevent collapse it needs to be able to withstand the external pressure (Sævik, 2014). To prevent denting, if exposed to impacts loads, sufficient thickness is required. Buckling propagating and plastic straining must also be prevented. Other failure modes that can affect pipelines, but are of less

importance when discussing the immediate consequences of anchor-pipeline interaction, are fatigue and corrosion (Sævik, 2014).

When a pipeline is exposed to an anchor load, several of the above mentioned failure modes become important. The interaction can cause gross deformations of the pipeline, such as denting and buckling. The anchor can also damage the coating, cause large deformations and displace the pipeline by several meters, creating large internal stresses which may rupture the pipeline.

Assessing the effect on the pipeline is usually done by use of Load Factored Resistance Design (LRFD) or Allowable Stress Design (ASD) (Sævik, 2014). These two methods are used to inspect how the combinations of different loads will affect the pipeline. The main difference is that the LRFD is based on realistic loading conditions and material properties, while ASD is based on prescribed loading and stress limits (Wong, 2009). The LRFD method will be inspected in more detail in Subchapter 3.1.1, as this method is described and recommended by DNV (DNV-OS-F101).

2.2 Anchors

The most popular anchors used for vessels, according to anchor manufacturer SOTRA, are the stockless fluke anchors, particularly the Hall and Spek type (SOTRA, 2014a). These anchors consists of a fluke, shank, shackle and forerunner. The collective term for these anchors are embedment anchors, and these are the most common types applied for temporary mooring (Sriskandarajah & Wilkins, 2002). The Kvitebjørn gas pipeline was damaged by interaction with an anchor similar to the Spek type anchor (Gjertveit et al., 2010), and hence this anchor will be utilized in this thesis. The geometry of the Spek anchor is seen in Figure 2.2, while some of the dimensions are listed in Table 2.1.

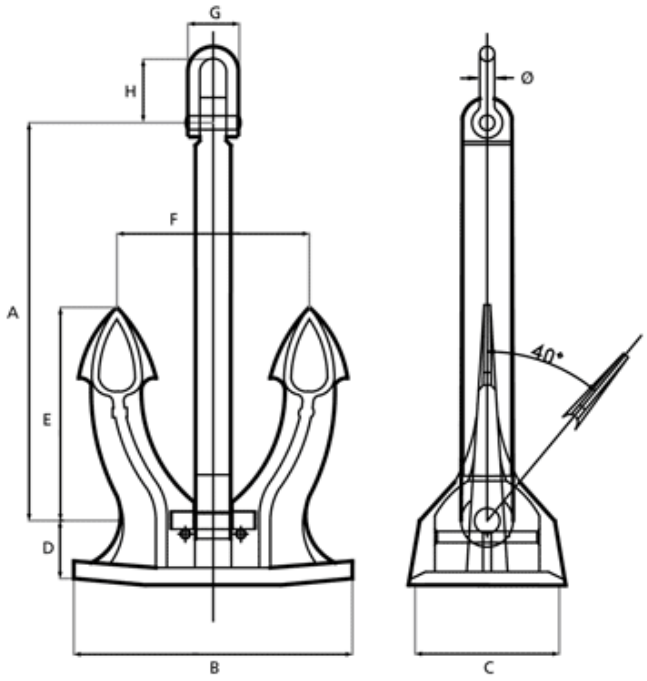

Figure 2.2: Spek anchor (SOTRA, 2014a)

Table 2.1: Dimensions in Figure 2.2 for different anchor masses (SOTRA, 2014a)

Mass	**A**	**B**	**C**	**D**	**E**	**F**	**G**	**H**	**Ø**
[kg]	[mm]	[mm]	[mm]	[mm]	[mm]	[mm]	[mm]	[mm]	[mm]
3780	2430	1850	810	393	1350	1350	310	385	90
6000	2700	2060	900	446	1500	1500	350	450	100
9900	3160	2332	1020	510	1700	1700	421	580	124
15400	3690	2824	1230	615	2050	2050	498	680	150

For the anchor to sink to the seabed, it needs to be of sufficient mass, and the chain long enough. The anchor will be exposed to a buoyancy force, due to its mass, and a drag force, particularly important if the anchor is being towed by a moving vessel. This effect is seen in Morrison's equation (Faltinsen, 1990) seen in Equation (2.2).

$$dF_{horizontal} = dF_{inertia} + dF_{drag} = \frac{\pi}{4}\rho D^2 dz C_M a_1 + \frac{\rho}{2} C_D D dz |u| u \qquad (2.2)$$

In Morrison's equation, C_D and C_M are the drag and mass coefficients respectively, D is the outer diameter of the cylinder, u and a are respectively the undisturbed fluid velocity and acceleration at the midpoint of the strip, either caused by waves or current. The expression in Equation (2.2) is written for a stationary cylinder. Despite the simplistic forms of the equation above, the important element to note is the dependency of velocity. The equation shows how the velocity of the vessel directly affects the forces the anchor is exposed to.

The mooring lines can either be made of chains, fiber or steel rope. The most common option is chains, with the option of studless or studlink chains. For mooring lines where the anchor needs to be reset many times, as for most vessels, studlink chains are the preferred option (Sriskandarajah & Wilkins, 2002). A studlink chain is shown in Figure 2.3.

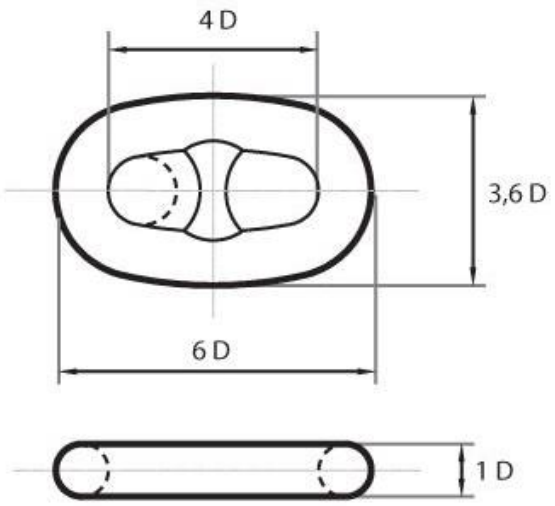

Figure 2.3: SOTRA Chain (SOTRA, 2014b)

To summarize, the environmental loads from waves, winds and currents are transferred from the vessel through the mooring system to the anchor, meaning environmental conditions should be considered to obtain a realistic model.

Chapter 3

Rules, Regulations and Literature Review

To obtain an overview of literature regarding anchor-pipeline interaction, two offshore standards and one recommended practice by DNV, which were of direct relevance to the topic, were inspected. Following this, the research papers *Effect of Ship Anchor Impact in Offshore Pipeline* (Al-Warthan, Chung, Huttelmaier, & Mustoe, 1993) and *Assessment of Anchor Dragging on Gas Pipelines* (Sriskandarajah & Wilkins, 2002), and the two master theses by Vervik (2011) and Wei (2015) were reviewed.

The research papers reviewed in this chapter were found using NTNUs library search engine ORIA. By use of this search engine, the database OnePetro was found, which had all of the more recent papers from International Society of Offshore and Polar Engineering (ISOPE) and Offshore Technology Conferences (OTC). Relevant papers were found using the search words "Anchor, Pipeline, Impact".

3.1 DNV Rules and Regulations

Despite the lack of DNV rules or regulations directly addressing anchor-pipeline interaction, three are of relevance. The first one is rules and regulations regarding submarine pipeline system, DNV-OS-F101 (2013), which describes how to classify scenarios, and which limit states to take into consideration. The second one is for position mooring, DNV-OS-E301 (2010), which describes how to classify anchors, and which requirements are made for each class. The final publication is the recommended practice for interference between trawl gear and pipelines, DNV-RP-F111 (2010), which displays a method for calculating impact loads

from trawl gear on pipelines. The relevant sections of these publications are inspected in more detail.

3.1.1 DNV-OS-F101

The first rules and regulations for submarine pipeline systems by DNV were published in 1976, and have been updated several times since then, last time in October 2013. The Offshore Standard *Submarine Pipeline Systems* dictates criteria and recommendations regarding concept development, design, construction, operation and abandonment of subsea pipelines. The DNV Offshore Standard ensures the pipeline's safety by applying a safety class methodology and limit state design (DNV-OS-F101, 2013). The safety class methodology defines the safety classes by the consequences of a failure of the system, as seen in Figure 3.1. The limit states applied in the limit state design are defined as conditions where the pipeline no longer satisfies the requirements (DNV-OS-F101, 2013).

Safety class	*Definition*
Low	Where failure implies insignificant risk of human injury and minor environmental and economic consequences
Medium	Where failure implies low risk of human injury, minor environmental pollution or high economic or political consequences.
High	Classification for operating conditions where failure implies risk of human injury, significant environmental pollution or very high economic or political consequences

Figure 3.1: Definition of safety classes (DNV-OS-F101, 2013)

The design principle used by DNV is the Load Factored Resistance Design (LFRD). This principle gives the opportunity to inspect if the pipeline has sufficient characteristic resistance to withstand the different loads during different limit states. The formulation of the principle and the design load effect are described by Equation (3.1) (DNV-OS-F101, 2013).

$$f\left(\left(\frac{L_{Sd}}{R_{Rd}}\right)_i\right) \leq 1 \tag{3.1}$$

R_{Rd} is the design resistance, seen in Equation (3.2), and is a function based on the characteristic resistance, material strength, thickness, and ovality of the pipeline (DNV-OS-F101, 2013).

$$R_{Rd} = \frac{R_c(f_c t_c, f_0)}{\gamma_m \gamma_{SC}} \tag{3.2}$$

R_C is the characteristic resistance, f_c is the characteristic material strength, t_c is the characteristic thickness, f_0 is initial ovality, and $\gamma_m \gamma_{SC}$ is the partial resistance factors consisting of a material

resistance factor and a safety class resistance factor. The values for the factors depend on which limit state is being investigated.

L_{Sd} in Equation (3.1) is the design load described by load effects L_i, as seen in Equation (3.3).

$$L_{Sd} = L_F\gamma_F\gamma_c + L_E\gamma_E + L_I\gamma_F\gamma_c + L_A\gamma_A\gamma_c \tag{3.3}$$

The load effects are the resulting cross-sectional loads due to applied loads. These are combined by use of load effect factors γ_i that are determined by which limit state is considered. The loads used in these calculations are placed in four categories (DNV-OS-F101, 2013):

1. Functional loads (F)
2. Environmental loads (E)
3. Interference loads (I)
4. Accidental loads (A)

The functional loads are those imposed on the structure during operations due to the structures physical existence, such as weight, external hydrostatic pressure and internal pressure. Environmental loads are those from winds, hydrodynamics, ice and earthquakes. Interference forces are those imposed on the pipeline by 3rd party activities that have a probability of occurrence higher than 10^{-2}. Those that have a probability lower than this are classified as accidental loads. The final factor is the condition load effect factor $\gamma_{c,}$ which depends on the conditions surrounding the pipeline when inspecting the loads. That is, conditions such as "the pipeline is resting on uneven seabed", or "exposed to pressure test" (DNV-OS-F101, 2013).

The limit states are categorized into two major classes (DNV-OS-F101, 2013):

1. Serviceability Limit State Category (SLS)
2. Ultimate Limit State Category (ULS)
    a. Fatigue Limit State (FLS)
    b. Accidental Limit State (ALS)

FLS and ALS are undercategories of ULS. Which scenarios are included in which limit states, are seen in Figure 3.2. Depending on which limit state is being inspected, the load factors have to be chosen according to Figure 3.3.

	Ultimate Limit States						Serviceability Limit States			
Scenario	Bursting	Fatigue	Fracture	Collapse	Propagating buckling	Combined loading	Dent	Ovalisation	Ratcheting	Displacement
Wall thickness design	X			X	X					
Installation		X	X	X	X	X		X		X
Riser	X	X	X	X	X	X		X		X
Free-span	(X)	X	X			X				
Trawling/3rd party	(X)	X				X	X			
On bottom stability	(X)	(X)	(X)			(X)	(X)	(X)		X[1]
Pipeline Walking		X				X				
Global Buckling	(X)	X	X			X			X	
1) Typically applied as a simplified way to avoid checking each relevant limit state										

Figure 3.2: Typical link between scenarios and limit states (DNV-OS-F101, table 5-8)

Limit State / Load combination	*Load effect combination*		*Functional loads* [1]	*Environmental load*	*Interference loads*	*Accidental loads*
			γ_F	γ_E	γ_F	γ_A
ULS	*a*	System check[2]	1.2	0.7		
	b	Local check	1.1	1.3	1.1	
FLS	*c*		1.0	1.0	1.0	
ALS	*d*		1.0	1.0	1.0	1.0
1) If the functional load effect reduces the combined load effects, γ_F shall be taken as 1/1.1.						
2) This load effect factor combination shall only be checked when system effects are present, i.e. when the major part of the pipeline is exposed to the same functional load. This will typically only apply to pipeline installation.						

Figure 3.3: Load effect factor combinations (DNV-OS-F101, table 4-4)

Anchor hooking is by definition an interference load as it is caused by a 3rd party, but is classified as an accidental load due to its low probability of occurring. Furthermore, the safety class of the system can be defined as high, as a possible leakage could results in significant environmental pollution.

If anchor load is defined as an accidental load, the design against such a load is to be performed by either "direct calculation of the effects imposed by the loads on the structure, or indirectly, by design of the structure as tolerable to accidents" (Sec.5, D1001, DNV-OS-F101, 2013). There are however, no specific requirements for design against anchor loads by DNV, and it is therefore reasonable to assume that the first approach must be applied.

For accidental limit states all load effects have to be applied when calculating the design load. Furthermore, if one assumes that anchor loads are similar to trawling/3rd party loads, bursting, fatigue, combined loading and denting have to be inspected. In this thesis however, only the combined loading limit state is investigated when inspecting the pipeline's response to an anchor impact.

The design criteria for local buckling when the pipeline is exposed to combined loading is expressed in Equation (3.4) and Equation (3.5), for internal and external overpressure respectively.

$$\varepsilon_{Sd} \leq \frac{\varepsilon_c\left(t_{2,}\, p_{min} - p_e\right)}{\gamma_\varepsilon} \tag{3.4}$$

$$\left(\frac{\varepsilon_{Sd}}{\frac{\varepsilon_c\left(t_{2,}0\right)}{\gamma_\varepsilon}}\right)^{0.8} + \frac{p_e - p_{min}}{\frac{p_c(t_2)}{\gamma_m \gamma_{sc}}} \leq 1 \tag{3.5}$$

$$\varepsilon_c(t, p_e - p_{min}) = 0.78\left(\frac{t}{D} - 0.01\right)\left(1 + 5.75\frac{p_e - p_{min}}{p_b(t)}\right)\alpha_h^{-1.5}\alpha_{gw} \tag{3.6}$$

ε_{Sd} is the design loads strain, ε_c is the characteristic bending strain resistance described in Equation (3.6), p_e is the external pressure, p_{min} is the minimum internal pressure that can be continuously sustained, p_c is the collapse pressure, γ_ε resistance strain factor and t_2 is the pipewall's thickness removing corroded thickness. p_b is the bursting pressure, α_h is the train hardening and α_{gw} is the girth weld factor. The design load strain describes the maximum strain that the pipeline should be exposed to, without any consequences for the pipeline's safety, and this should not be exceeded. The characteristic bending strain resistance is the actual maximum strain that the pipeline can experience without local buckling.

The pipeline's response to the impact in this thesis will be inspected by studying the strain in the pipeline's cross-section and comparing the results with the design strain load and characteristic bending strain resistance, seen in Equation (3.4), (3.5) and (3.6).

3.1.2 DNV-OS-E301

This Offshore Standard covers the design of position mooring. It describes the three limit states considered: Ultimate Limit State (ULS), Accidental Limit State (ALS) and Fatigue Limit State (FLS), and which methods to apply, loads to consider and analyses to perform when designing mooring lines.

The standard describes the different equipment necessary for the mooring system, and the requirements for these. The standard states that studlink chain qualities K1, K2 and K3 are intended for temporary mooring of ships (DNV-OS-E301, 2010), and should not be used on offshore units.

Section 2 in this Offshore Standard describes equipment selection, certification and how to classify anchors. The classification is based on equipment numbers defined in Equation (3.7) (DNV-OS-E301, 2010).

$$EN = \Delta^{2/3} + A_c \tag{3.7}$$

Δ is the moulded displacement in saltwater measured in tons of the vessel, on maximum transit draught, A_c is the projected area given in m^2 of all wind-exposed surfaces above the units light transit draught. Once having found equipment number, the tables presented in DNV-OS-E301 (2010) are employed to find required mass of anchor, length of chain and diameter, as seen in the Figure 3.4. In this thesis, the K3 grade anchor chain is applied. More properties of K3, and how the information from Figure 3.4 is applied, is described in Subchapter 5.2.2.

Equipment number Exceeding – not exceeding	*Equipment letter*	*Stockless anchors*		*Chain cables*					
		Number	*Mass per anchor (kg)*	*Total length (m) 2)*	*Diameter and grade*				
					NV R3 or K3 1)	*NV R3S*	*NV R4*	*NV R4S*	*NV R5*
720 – 780	S	2	2 280	467.5	36				
780 – 840	T	2	2 460	467.5	38				
840 – 910	U	2	2 640	467.5	40				
910 – 980	V	2	2 850	495	42				
980 – 1 060	W	2	3 060	495	44				
1 060 – 1 140	X	2	3 300	495	46				
1 140 – 1 220	Y	2	3 540	522.5	46				
1 220 – 1 300	Z	2	3 780	522.5	48				
1 300 – 1 390	A	2	4 050	522.5	50				
1 390 – 1 480	B	2	4 320	550	50				
1 480 – 1 570	C	2	4 590	550	52				
1 570 – 1 670	D	2	4 890	550	54				
1 670 – 1 790	E	2	5 250	577.5	56	54	50		
1 790 – 1 930	F	2	5 610	577.5	58	54	52		
1 930 – 2 080	G	2	6 000	577.5	60	56	54		
2 080 – 2 230	H	2	6 450	605	62	58	54		
2 230 – 2 380	I	2	6 900	605	64	60	56		
2 380 – 2 530	J	2	7 350	605	66	62	58		
2 530 – 2 700	K	2	7 800	632.5	68	64	60		
2 700 – 2 870	L	2	8 300	632.5	70	66	62		
2 870 – 3 040	M	2	8 700	632.5	73	68	64		

Figure 3.4: Part of the table describing equipment requirements (DNV-OS-E301)

3.1.3 DNV-RP-F111

Interference Between Trawl Gear and Pipelines (DNV-RP-F111, 2010) is the recommended practice for calculating loads induced by trawl gear on pipelines. The interaction is described as a two-stage situation. First, the anchor causes an impact on the pipeline, which is then followed by either a pull over or a hooking. The recommended practice explains how to calculate the impact force, the depth of the local dent and the energy absorbed by the pipeline. For the pull over, it also illustrates how to calculate the pull over duration. For the hooking situation, it simply states that the response during hooking should be found by applying relevant and conservative models, without going into more detail.

It is clearly stated in the recommended practice that the loads and load effects found are related to size, shape, velocity and mass of the trawling gear. The equations presented can therefore not be directly applied to calculate anchor loads, but they can be used to calculate the approximate impact force and denting caused on the pipelines.

As the loads and load effects are affected by size, shape, velocity and mass of the impacting object, it is reasonable to assume that these parameters will have an effect on the anchor-pipeline interaction.

3.2 Research Papers

Two research papers have particular relevance for the modelling and study of anchor-pipeline interaction. The first one, *Effect of Ship Anchor Impact in Offshore Pipeline* (Al-Warthan et al., 1993), investigates the dynamic pipeline response, within the elastic range, in the event of anchor-pipeline interaction. The analysis is performed by using Discrete Element Method (DEM). The paper's main focus is on how the span length, that is the free span of the pipeline, may affect the outcome of such a situation.

In the second one, *Assessment of Anchor Dragging on Gas Pipelines* (Sriskandarajah & Wilkins, 2002), the authors assess the force needed to initiate lateral movement of a subsea pipeline, force needed for the pipeline to reach its maximum allowable design stress and force needed to cause local buckling. This is done for pipelines resting on the seabed, and buried, by performing a dynamic non-linear FEA using ABAQUS.

Al-Warthan et al. (1993) model a 16-inch pipeline with rigid body elements connected with lumped axial, shear and bending stiffness. Plastification and local buckling are excluded in the

study, as is environmental loading by applying a constant vessel velocity of 1 knot. The results are found using time integration scheme with an updated Lagrangian approach. Sriskandarajah and Wilkins (2002) on the other hand model a 10 km long pipeline using an element that enables prediction of collapse buckling. The outer diameter is not listed.

Al-Warthan et al. (1993) define two different interaction modes: dropped anchor and hooking, while Sriskandarajah and Wilkins (2002) define two phases of the interaction: initial impact followed by dragging of the pipeline. The latter authors also establish drag embedment anchors as the type of anchor most likely to cause a hooking event, as in the case with the Kvitebjørn pipeline (Gjertveit et al., 2010). Al-Warthan et al. (1993) simplify the modelling of the interaction by not modelling the anchor, but instead defining three load cases for an anchor of 4310 kg. The initial impact caused by a dropped anchor is modelled as an impulse load with either a triangular impulse shape factor or a ramp loading. The basic expression for an impulse is shown in Equation (3.8) (Al-Warthan et al., 1993).

$$I_I = \int_{t_1}^{t_2} F dt = mv_2 - mv_1 \tag{3.8}$$

$$I_I = mv_0 = C_I F t_d \tag{3.9}$$

m is the anchor mass, v_1 and v_2 are the initial and final velocities respectively. The alternative way of writing the equation, seen in Equation (3.9), employs the initial velocity of the anchor v_0, or the maximum impact load F, duration of impact t_d and the impulse shape factor C_I. Hertz theory is applied to find the duration of the impact, as seen in Equation (3.10). k_1 is a function dependent on the Young's modulus, Poisson's ratios and the mass for pipe and anchor.

$$t_d = k_1 v_0^{-\frac{1}{5}} \tag{3.10}$$

Al-Warthan et al. (1993) model the hooking load by use of catenary equations, and the expression seen in Equation (3.11), to express the upward vertical tension applied to the pipeline.

$$T = T_x \left[1 + \sqrt{\sinh\left(W_c \frac{x - (x_r - x_t)}{T_x} \right)^2} \right] \tag{3.11}$$

$$x_r = \frac{T_x}{W_c} \tanh^1\left(\frac{h}{L}\right) + \frac{x_t}{2} \tag{3.12}$$

T_x is the horizontal tension, x_t is the downstream excursion, W_c is the total chain and anchor weight, L is the total chain length and h is the water depth. This approach finds the tension in the cable and applies it to the pipeline as a load increasing with time, as the horizontal tension increases due to towing.

The approach of calculating tension transmitted onto the pipeline from the vessel when the mooring lines take on the form of a catenary, is supported by Sriskandarajah and Wilkins (2002). Sriskandarajah and Wilkins (2002) also claim that the worst case scenario would be if the mooring line does not contact the seabed, as the full force from the vessel motion would be exerted onto the pipeline.

The article by Al-Warthan et al. (1993) applies the same basic concepts as in the Recommended Practice DNV-RP-F111 (2010) to calculate the initial loads on the pipeline, but simplifies it by ignoring all effects of size and shape of the anchor. Sriskandarajah and Wilkins (2002) also applies a simplified approach by applying internal and external pressure, followed by a prescribed lateral displacement of 50 meters at the hooking location. This displacement was applied statically.

Al-Warthan et al. (1993) demonstrates that the stresses increase with decreasing span length, and that the highest amount of stresses are caused when the pipeline is exposed to a ramp impulse load. A ramp impulse load is a dropped anchor that remains on the pipe. The results indicate that the bending stress is always higher than the axial stress, independently of span length. The article concludes that stresses exceed yield stress for the pipeline grade API X-65, which would result in local buckling and yielding, making the pipeline unable to operate.

Sriskandarajah and Wilkins (2002) show that for a pipeline resting on the seabed, results indicate a lateral force of 73 kN is necessary to displace the pipeline 1 meter in lateral direction, while 150 kN is necessary to reach the design stress limit. A force of 525 kN is necessary to begin the onset of lateral buckling. For the buried pipe, a lateral force of 400 kN is necessary to

displace the pipeline 1 meter, indicating the effectiveness of burying pipelines. Local effects on the pipeline are not considered in this text.

Neither of the research papers model the anchor when simulating the interaction. Instead, impulse loads are applied to inspect initial impact, and catenary calculations and prescribed lateral displacements applied to inspect hooking. The effect of size and shape of anchor are thus excluded from the studies.

3.3 Master theses

3.3.1 "Pipeline Accidental Load Analysis"

Vervik's MA-thesis (2011) is based on the anchor hooking incident at the Kvitebjørn Gas Pipeline. The thesis' main goal is to predict the most probable loads induced by anchors if hooking occurs, investigating what type and size of anchors can cause hooking and the probability of a vessel with such an anchor passing the Kvitebjørn gas pipeline.

Similarly to *Assessment of Anchor Dragging on Gas Pipelines* (Sriskandarajah & Wilkins, 2002) drag embedment anchors of different classes are inspected, specifically classes of the Spek anchor. Following DNV-OS-E301 rules and applying Equation (3.7), the anchors are divided into six classes based on their equipment number described in Subchapter 3.1.2, seen in Table 3.1 below.

Table 3.1: Equipment letter and class in Vervik's (2011) thesis

	Equipment Letter	**Anchor Mass [kg]**
Class 1	z - G	3780 – 6000
Class 2	G – L	6000 – 8300
Class 3	L – O	8300 – 9900
Class 4	O – X	9900 – 15400
Class 5	X – A*	15400 – 17800
Class 6	A* - E*	17800 – 23000

$$D_{max} = \frac{2L(1 - cos\alpha)}{sin\alpha} \tag{3.13}$$

The Spek anchor's geometry, seen in Figure 2.2, has a maximum angle of 40 degrees between the shank and the fluke. This makes the anchor optimal for hooking. By use of Equation (3.13) Vervik (2011) shows that due to its geometric dimensions, anchors smaller than 3780 kg will

not manage to hook onto a pipeline with a steel diameter of 30 inches. In Equation (3.13) D_{max} is the maximum pipe diameter the anchor can hook onto; L is the fluke's length and α is the angle between the fluke and shank. For this reason anchors smaller than 3780 kg are excluded in the following analyses.

For anchor hooking to occur, several key parameters are identified. These are vessel velocity, anchor mass, pipe diameter, chain length versus water depth and chain breaking strength. Inspecting the Norwegian Coastal Administration's (NCA), Automatic Identification System (AIS), reveals that in the period from March 2010 to March 2011 there were 237 out of 7160 ships which could cause hooking (Vervik, 2011). This analysis is carried out for all segments of the Kvitebjørn pipeline, which rest at varying depths. The distribution of anchor classes for these 237 vessels is shown in Figure 3.5.

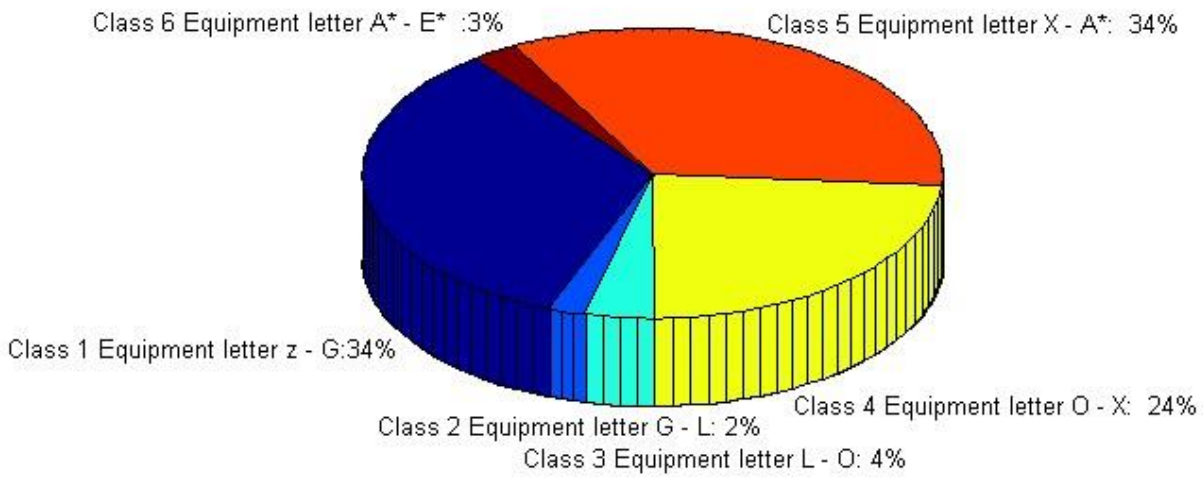

Figure 3.5: Distribution of the 237 vessels which cause hooking, figure by Vervik (2011)

The pipeline section with the largest ship traffic in the vicinity is located at a water depth of 300 meters. Based on the geometry of the Kvitebjørn pipeline and applying Equation (3.13), it is concluded that Spek anchors of type z, G, L, O, X, A* and E* can cause hooking. However, by applying SIMLA and inspecting the drag forces on the anchor when towed, and a water depth of 300 meters, it is determined that only anchors of type O or larger can cause hooking at this depth. This is due to the force exerted on the anchor and chain when towed, as well as the maximum allowable length of anchor chain.

To study the forces applied on the pipeline during hooking, a global analysis is performed in SIMLA. A similar approach to that of Al-Warthan et al. (1993) and Sriskandarajah and Wilkins (2002) is employed as the response of the pipeline is the focus. The anchor-pipeline interaction

is modelled using a linear spring between the pipeline node and the anchor chain node. The resistance properties of the spring is mimicking a triangular impulse load where the maximum force is equal to the maximum anchor chain breaking load. The chain itself is modelled as a single beam element with low bending stiffness to represent the bending flexibility of the chain, and an axial stiffness corresponding to the applied anchor chain diameter (Vervik, 2011). The pipeline is modelled as full-length with elastoplastic material properties.

The largest displacements and strain in the pipeline occurred at 5 knots, and lower values at higher velocities. The large displacements results in the response being dominated by plastic bending and the development of large membrane forces.

3.3.2 "Anchor Loads on Pipelines"

Wei's MA-thesis (2015) is a continuation of Vervik's MA-thesis from 2011. The focus of the thesis is on creating a SIMLA model to inspect parameters necessary for hooking, and the non-linear effects of hooking. The data regarding relevant anchors from Vervik's (2011) thesis is utilized, and the anchors of type z, G, O and X are studied.

Two models are produced for SIMLA. The first models the pipeline as a 10 meter long rigid body, similar to the modelling done by Al-Warthan et al. (1993), and attempts to determine which parameters are necessary to cause hooking. The second model consists of a full-length pipeline of 10 kilometers with elastoplastic material properties, similar to the modelling done by Sriskandarajah and Wilkins (2002) and Vervik (2011). This model attempts to display the actual response of the pipeline when allowing non-linear effects. Unlike the aforementioned research papers and MA-thesis, Wei (2015) models the anchor as a 3D object. The anchor's geometry is simplified, but is modelled using SOTRAs Spek anchor's dimensions as a basis. Which specific values were used to model the different anchors is however not clear.

The parameters inspected in the short model are the diameter of the pipe, anchor mass, span height and the angle of attack between anchor and pipeline. The values used for the different variables are shown in Table 3.2. The measured parameter is the tension in the anchor chain.

Table 3.2: Parameters inspected by Wei (2015)

Anchor mass [kg]	**Pipe Diameter [m]**	**Hooking Angle [°]**	$\frac{\textbf{Span Height}}{\textbf{Diameter}}$ [−]
3780	0.4	90	0
6000	0.6	100	1
9900	0.8	110	2
15400	1.0	120	3

Using SIMLA, 512 simulations are performed. The results show that increasing anchor size, and decreasing pipe dimensions, cause a higher probability of hooking. Furthermore, larger span heights reduces the probability of hooking, because the anchor will twine and bounce off the pipeline. This is a response not seen in the research papers as the anchor is modelled as a load on the pipeline. Lower vessel speed increases the probability for hooking, as in accord with Vervik's (2011) results.

The long pipeline model introduces elastoplastic material, instead of elastic, to inspect the pipeline's bending moment. Four different simulation are performed. The first three simulations with a pipe diameter of 0.4 meters, a hooking angle of 90 degrees and a span height of 1.2 meters. The anchor types z, O and X are assessed. For anchor types z and O, the force in the cables connected to the anchors will exceed their capacity limit, resulting in the cable breaking. For anchor X this does not occur, which results in the conclusion that the pipe will rupture. However, in the final simulation, the pipe diameter was increased from 0.4 to 0.6 meters, and showed that the cable would once more fail. In other words, it is more likely that the cable will break than the pipeline rupturing.

There are some uncertainties regarding the modelling in SIMLA that make it difficult to replicate the results. For instance, it is uncertain exactly how the anchor is modelled. It is uncertain whether the anchor geometry is updated with anchor mass, or the anchor geometry has been held constant. It is also unclear whether the cable geometry and properties are updated when the anchor mass is altered, and which cable length is applied. Which values were used for the pipe's properties is also somewhat uncertain, and if these properties were updated when altering pipe diameter. Furthermore, it is uncertain which drag coefficients were used for the cable. Because of this, comparing results will be difficult.

Despite no DNV rules or regulations specifically assessing anchor-pipeline interaction, general rules regarding subsea pipeline in DNV-OS-F101 apply, and the recommended practice for

calculating trawl loads can be applied to find an approximation of anchor loads. Al-Warthan et al. (1993) showed a simplified approach to calculate anchor loads by excluding anchor size and shape. The loads were modelled either as an impulse load, or as tension applied to hooking location. Sriskandarajah and Wilkins (2002) describes a method to assess the probability of an anchor being dropped, and models the hooking onto the pipeline by applying a prescribed lateral displacement. Vervik (2011) applies the method by Sriskandarajah and Wilkins (2002) to inspect the probability of anchor hooking on the Kvitebjørn gas pipeline, and models the interaction in SIMLA by connecting a spring between the cable and hooking location.

Wei (2015) is the first of these to create a model of the anchor when inspecting which parameters increase the probability of hooking. However, the many uncertainties regarding how the results were obtained may provide difficulties when comparing results. Wei's (2015) model does however create the basis for the modelling of the anchor-pipeline interaction. This is described in more detail in Chapter 5.

The results from the research papers and the MA-theses indicate detrimental effects, such as local buckling (Sriskandarajah & Wilkins, 2002) (Al-Warthan et al., 1993) and rupturing (Wei, 2015), should hooking occur. The two research papers conclude with local buckling, but both ignore the effects of anchor geometry, by not modelling the anchor. The results from this thesis will be compared with the two research papers described, and the two MA-theses.

Chapter 4

Non-linear Finite Element Analysis

To analyse the interaction between anchor and pipeline in this thesis the computer software SIMLA was applied. SIMLA is a specified software used to perform analyses on umbilical structures, such as pipelines. The software was originally created by MARINTEK for Norsk Hydro ASA, after a request made in 2000 (MARINTEK, 2012). Its original purpose was to simulate the structural response of a pipe during laying, and visualize the results. In later years the use was extended, and as it allows for both non-linear static and dynamic analysis, it is an optimal tool for inspecting anchor-pipeline interaction. In this chapter, the basics behind a non-linear analysis are described, with focus on the methods applied in SIMLA.

According to Belytschko, Liu, Moran, and Elkhodary (2014) a non-linear analysis consists of four steps:

1) Development of a model
2) Formulation of the governing equations
3) Solution of the equations
4) Interpretation of the results.

Several non-linear effects need to be considered when inspecting the structural behaviour of subsea pipelines. According to Sævik (2014), these are:

1) Large displacements
2) Non-linear pipe-soil interaction forces
3) Non-linear material behaviour
4) Non-linear hydrodynamic loading
5) Variable boundary conditions
6) Transient temperature and pressure loads due to variable fluid flow conditions

A linear Finite Element Method (FEM) analysis assumes that the displacements are small, and the material linear elastic (Moan, 2003b). This is not the case for anchor-pipeline interaction, as the pipe may be exposed to large displacements. The non-linear effects relevant for anchor-pipeline interaction analysis are large displacement, non-linear pipe-soil interaction forces and non-linear material behaviour.

4.1 Basics of Finite Element Method

FEM is a method to calculate the response of a structure. This is done by discretizing the structure into elements and nodes, calculating the response for the individual nodes and elements, assimilating the responses and applying boundary conditions before calculating the global response (Moan, 2003a). The basic principles of FEM according to Moan (2003b) are:

1) Equilibrium, expressed by stresses
2) Kinematic compatibility, expressed by strains
3) Stress-strain relation

These principles will be inspected in more detail, with focus on how they are implemented in SIMLA.

4.1.1 Equilibrium

The requirement of equilibrium demands that there is always equilibrium between external and internal forces. This is enforced by applying the principle of virtual work, or the principle of virtual displacement. The principle states that (Langen & Sigbjörnsson, 1986, p. 3.1):

> The total virtual work performed by a system in equilibrium when it is subjected to virtual compatible displacements is equal to zero.

This results in the equilibrium expression seen in Equation (4.1) (Sævik, 2014).

$$\int_V (\boldsymbol{\sigma} - \boldsymbol{\sigma_0}) : \delta\boldsymbol{\epsilon} dV + \int_V \rho \ddot{\boldsymbol{u}} \cdot \delta \boldsymbol{u} dV - \int_V \boldsymbol{f} \cdot \delta \boldsymbol{u} dV - \int_V \boldsymbol{t} \cdot \delta \boldsymbol{u} dS = 0 \qquad (4.1)$$

$\delta\mathbf{u}$ is the virtual displacement, $\boldsymbol{\sigma}$ is the natural stress tensor, $\boldsymbol{\sigma_0}$ is the initial stress tensor, $\boldsymbol{\epsilon}$ is the natural strain tensor, **f** is the related volume force vector and **t** is the traction on the volume surface.

In Equation (4.1) natural stress and strain are applied, these refer to the deformed configurations of the element. However, since non-linear effects are included, there is a need for a description of stress and strain within the element that refers to the initial undeformed configurations. The natural stress and strain are hence not preferred for non-linear analysis (Moan, 2003b). The Green strain tensor **E**, and 2nd Piola-Kirchhoff stress tensor **S** refers to the undeformed configurations (Sævik, 2014). These can therefore replace the natural strain and stress tensors respectively. 2nd Piola-Kirchhoff is given by Equation (4.2) (Sævik, 2008).

$$\boldsymbol{S} = \frac{\rho_0}{\rho}\boldsymbol{F}^{-1} \cdot \boldsymbol{\sigma} \cdot \boldsymbol{F} \tag{4.2}$$

F is the deformation gradient, $\boldsymbol{\sigma}$ is the natural stress tensor, ρ is the density of the deformed configuration, and ρ_0 is the density of the undeformed configuration. For strains smaller than roughly 2%, the difference between 2nd Piola-Kirchhoff and the natural stress tensor will be small, and hence are assumed equal.

4.1.2 Kinematic Compatibility

To obtain convergence of the solution for the finite element analysis, when reducing mesh size, the element must be complete and compatible (Belytschko et al., 2014). Complete means that the displacement function must be able to represent all rigid body modes and constant strain modes (Moan, 2003a). Compatibility means that there is continuity over the element boundaries and at the nodes, that is: there are no gaps or overlaps in the deformed body (Belytschko et al., 2014). This principle dictates the appearance of the element's shape or displacement functions.

In SIMLA it is assumed that Bernoulli-Euler and Navier's hypothesis apply for the pipe elements and that strain is expressed by Green strain tensor **E**. As the pipelines response will be both elastic and plastic, it is assumed that the elements are classified as elastoplastic, which is discussed in more detail in the following Subchapter 4.1.3. The displacements and longitudinal Green strain which replaces the natural strain tensor in Equation (4.1) is expressed in equation (4.3) (Sævik, 2008).

$$E_{xx} = u_{x0,x} - yu_{y0,xx} - zu_{z0,xx} + \frac{1}{2}\left(u_{y0,x}^2 + u_{z0,x}^2\right) + \theta_{,x}\left(yu_{z0,x} - zu_{yo,x}\right) + \frac{1}{2}\theta_{,x}^2(y^2 + z^2) \tag{4.3}$$

$$u_x(x,y,z) = u_{x0} - yx_{y0,x} - zu_{z0,x} \tag{4.4}$$

$$u_y(x,y,z) = u_{y0} - z\theta_x \tag{4.5}$$

$$u_z(x,y,z) = u_{z0} - y\theta_x \tag{4.6}$$

4.1.3 Constitutive Equations

The constitutive equations explain the relation between stress and strain. For a linear elastic material, Hooke's law describes this relation, but for a plastic material, the situation becomes more complicated due to plastic effects. The expression for total strain is seen in Equation (4.7) (Sævik, 2014).

$$\boldsymbol{E} = \boldsymbol{E}^e + \boldsymbol{E}^p \tag{4.7}$$

$\mathbf{E}^e$ is the elastic strain expressed by elastic material law, and $\mathbf{E}^p$ is the plastic strain. Plastic strain is the strain which results in permanent deformation. The relation between these is seen in the stress-strain graph in Figure 4.1, where strain is denoted ϵ.

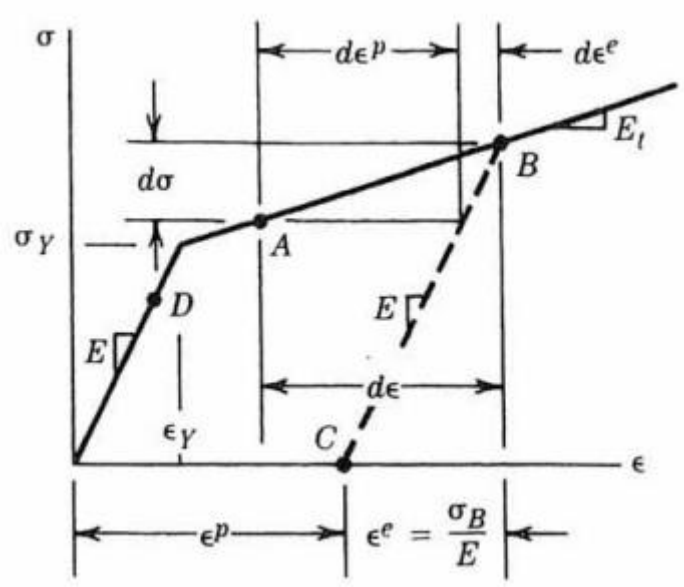

Figure 4.1: Stress-strain showing elastic and plastic strain contribution (Moan, 2003b)

To find the plastic strain one needs to define (Moan, 2003b):

1) A yield criterion
2) A hardening rule
3) A flow rule

The yield criterion defines when the material is plastic and which combinations of multi-axial stresses are necessary to move in plasticity. The flow rule describes the plastic strain increments, while the hardening rule defines how the yield condition changes as plastic flow proceeds (Sævik, 2008). These will now be described in more detail.

The yield criterion defines at which stress level plastic deformation first occurs, and is described by Equation (4.8) (Sævik, 2008).

$$f(\boldsymbol{S}, \kappa) = 0 \tag{4.8}$$

Where the equation describes a scalar function of **S** and κ, which are the stress tensor of 2nd Piola-Kirchhoff stress, and a strain-hardening parameter dependent on the history of the loading in the plastic range. It is assumed that the yield surface is a closed surface, and the equation above expresses this in the six-dimensional stress space (Sævik, 2008). A consistency condition is necessary to describe that stress points remain on the yield surface during loading in the plastic range. The consistency condition is given by Equation (4.9) (Sævik, 2008).

$$\dot{f} = \frac{\partial f}{\partial \boldsymbol{S}} : \dot{\boldsymbol{S}} + \frac{\partial f}{\partial \kappa}\dot{\kappa} \tag{4.9}$$

The hardening rule is necessary to describe how the yield criterion changes with the onset of plastic deformation. In SIMLA both kinematic and isotropic hardening are included in the material model (Sævik, 2008). Kinematic hardening means that one assumes that the yield point and the effects of work hardening are the same in tension and compression (Moan, 2003b). This is unlike isotropic hardening, where the material remembers the hardening, and requires an unloading which is equal to twice the stress prior to unloading (Sævik, 2008). Isotropic hardening also means that yield surface expands isotropically, while staying centred at origin (Kyriakides & Corona, 2007). Kinematic and isotropic hardening are seen in Figure 4.2.

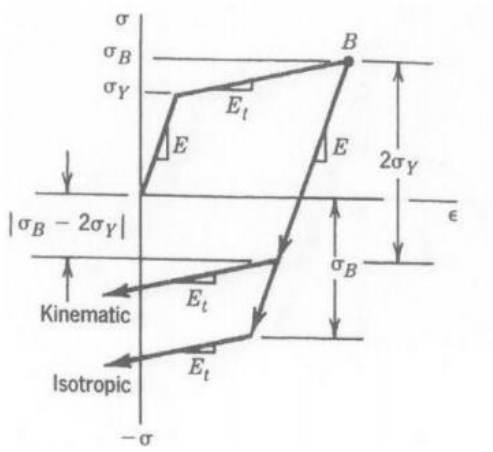

Figure 4.2: Kinematic and isotropic hardening (Moan, 2003b)

As metal plasticity is path dependent, the flow rule is needed to express the relation between the strain increments to the stress increments. The flow rule is based on Drucker's postulate that (Kyriakides & Corona, 2007):

1) Yield-surfaces are convex,
2) The instantaneous plastic strain increment at σ is normal to the yield surface,
3) The strain increments are linearly related to the stress increments.

4.2 Co-rotational Total Lagrangian Formulation

When describing non-linear problems the choice of reference system needs to be carefully considered. In SIMLA a Co-rotated Total Lagrangian system is applied (Sævik, 2008). A Lagrangian description of the motion uses the material particle as a reference point (Moan, 2003b). There are two main types of Lagrangian formulation: Total and Updated. The basic idea behind these two formulations is to separate rigid body motions from the local deformation of the element (Sævik, 2008). The difference between the two formulations is that total Lagrangian is based on a fixed coordinate system, where all deformations refer to the initial configuration (Moan, 2003b), while updated Lagrangian operates with a local coordinate system that has to be updated when the geometry changes due to deformations (Sævik, 2008). Deformations in the latter formulation do not refer to the initial configuration, but rather the previous configuration.

The Co-rotational formulation is a combination of the two described above. All quantities refer back to the initial configuration, but there is a local coordinate system attached to the element

that is allowed to both translate and rotate with the element (Sævik, 2008). The Co-rotated system then employs four base vector systems. The first one is a fixed global system with axis X_i and base vectors $\mathbf{I}_i$, where i is the directions 1, 2 or 3. The second is a local coordinate system attached to each node of the element and continuously updated to capture the rotations at the nodes. This system is defined with axis x_i and base vectors $\mathbf{i}_i$. The third one is an element end coordinate system that defines how the different elements connected to the node are oriented relative to the nodal coordinate system. This system is only defined once and not updated. The last one is a local element system at each element used to find the element deformations with coordinate axes y_i and base vectors $\mathbf{j}_i$ (Sævik, 2008). The large displacements are accounted for by continuously updating the element and node orientation, as well as the position of the end coordinates. In Figure 4.3 the global coordinate system is seen at the top, with a node centred between three elements below. In this node one can see the nodal coordinate system base vectors (**i**) and the element end base vectors (**j**).

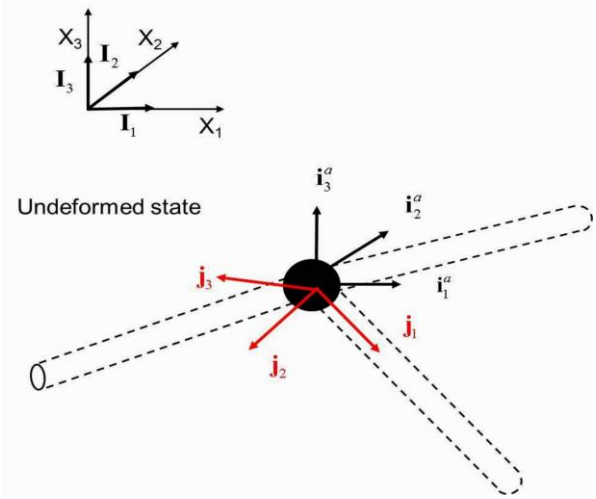

Figure 4.3: Global (**I**), nodal (**i**) and element base (**j**) vector (Sævik, 2008)

The incremental equilibrium expressed by Equation (4.10) below is used as the basis for the stiffness matrix. This equations is found from Equation (4.1), by applying the Co-rotational Total Lagrangian formulation and the basics of the FEM described in Subchapter 4.1, while neglecting higher order terms and assuming that the difference between two neighbouring equilibrium states are small (Sævik, 2008).

$$\int_V \boldsymbol{C}: \Delta\varepsilon: \delta\varepsilon dV_0 + \int_V \boldsymbol{\sigma}: \delta\Delta\boldsymbol{E} dV_0 - \int_S \Delta\boldsymbol{t} dS_0 = 0 \tag{4.10}$$

C is the elasticity tensor, **S** is the 2nd Piola-Kirchhoff, **E** is the Green strain tensor, δ is the virtual quantity, Δ is the increment between two configurations, **t** is the referential surface traction vector and $\boldsymbol{\sigma}$ is the Cauchy stress tensor. The first term describes the material stiffness, while the second term describes the geometric stiffness matrix. The material stiffness reflects the alteration of the stiffness caused by change in geometry due to deformation, while the geometric stiffness is the stiffness caused by initial member forces prior to displacement (Moan, 2003b).

4.3 Solution Methods

As the anchor's impact on the pipeline is a dynamic load dependent on time, a dynamic analysis has to be performed. Before this, a static analysis has to be performed to ensure that the system is in equilibrium before the onset of the dynamic load. The main difference between dynamic loads and static loads are (Langen & Sigbjörnsson, 1986, p. 1.2):

1) Dynamic loads imply a time dependent solution
2) Dynamic loads introduce inertia loads throughout the structure

Since large deformations are allowed and non-linearities are included, an incremental approach has to be implemented to find the static and the dynamic solution.

4.3.1 Static Solution

The expression for the static problem is seen in Equation (4.11).

$$\boldsymbol{Kr} = \boldsymbol{R} \tag{4.11}$$

K is the stiffness, **R** is the applied force, and **r** is the displacement. In Equation (4.11) the stiffness **K** is the total global stiffness consisting of all contributions to the stiffness, that is the material or initial stress stiffness and the geometric stiffness seen in Equation (4.10). The contributions are summed together, and transformed from a local to a global matrix using a transformation matrix. The global stiffness matrix is then created by summing together the

contributions. The solution of Equation (4.11) is found by use of user defined load control, with Newton-Raphson equilibrium iteration at each load step (Sævik, 2008). The equation can then be rewritten to incremental form, as seen in Equation (4.12), and solved by applying Equation (4.13) and (4.14) (Moan, 2003b).

$$\Delta \boldsymbol{r}_{k+1}^{\boldsymbol{i}} = \boldsymbol{K}_{T,k+1}^{-\mathbf{1}\boldsymbol{i}} \cdot \Delta \boldsymbol{R}_{k+1}^{\boldsymbol{i}} \tag{4.12}$$

$$\boldsymbol{r}_{k+1} - \boldsymbol{r}_k = \Delta \boldsymbol{r}_{k+1} = \boldsymbol{K}_I^{-1}(\boldsymbol{r}_k)(\boldsymbol{R} - \boldsymbol{R}_{\boldsymbol{int}}) \tag{4.13}$$

$$\boldsymbol{r}_{k+1} = \boldsymbol{r}_k + \Delta \boldsymbol{r}_{k+1} \tag{4.14}$$

This requires an update of the stiffness matrix for each load step. To reduce computational power, modified Newton-Raphson may be applied, here the stiffness matrix is not updated for each load step. The modified Newton-Raphson iteration is seen in Figure 4.4 below.

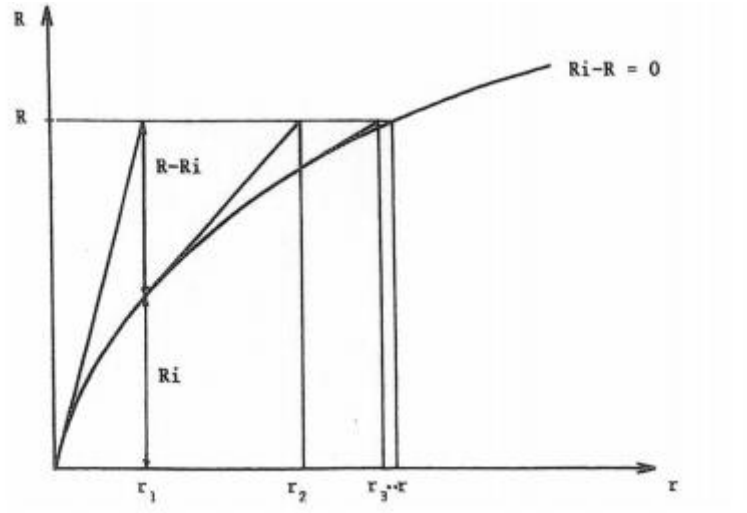

Figure 4.4: Modified Newton-Raphson iterations (Moan, 2003b)

4.3.2 Dynamic Solution

The expression for the dynamic equation of motion is seen in Equation (4.15).

$$\boldsymbol{M}\ddot{\boldsymbol{r}} + \boldsymbol{C}\dot{\boldsymbol{r}} + \boldsymbol{K}\boldsymbol{r} = \boldsymbol{Q} \tag{4.15}$$

M denotes the mass matrix, **C** is the damping matrix, **K** is the stiffness matrix, **Q** is the load vector and **r** is the displacement vector. When non-linear effects are included this equation can be solved by applying modal superposition. This means that the dynamic equation of motion is

expressed as a number of uncoupled equations which may be solved by direct time integration (Moan, 2003b).

The solution to Equation (4.15) can either be found by explicit or implicit methods. The explicit methods use only current and previous time step results to find the results for the next time step. Explicit solution methods are conditionally stable as long as the time steps are small enough, which makes the method appropriate for explosion and impact analysis (Sævik, 2008). If however the analysis requires a long duration, it is more appropriate to apply implicit methods. The expression for an implicit method is seen in Equation (4.16).

$$\boldsymbol{r}_{k+1} = f\left(\ddot{\boldsymbol{r}}_{k+1}, \dot{\boldsymbol{r}}_{k+1,} \ddot{\boldsymbol{r}}_k, \dot{\boldsymbol{r}}_k, \boldsymbol{r}_k, \dots\right) \tag{4.16}$$

These methods will generally have a better numerical stability. Very small time steps will however make this method uneconomical with regards to computational effort and time. For the anchor-pipeline interaction simulation in SIMLA, implicit methods are applied, along with the incremental time integration scheme HHT-α.

The reason for applying this specific scheme is that the lower modes are the most interesting for the response. It is hence desirable to avoid higher and medium modes (Langen & Sigbjörnsson, 1986). If Rayleigh-damping is introduced in the Newmark-β scheme, the medium modes are damped out. Applying Newmark-β will however result in reduced accuracy. This can be counteracted by introducing the HHT-α scheme. Without going into too much detail, HHT-α becomes Newmark-β when α is equal to zero. The HHT-α scheme results in accuracy remaining, while damping out the higher frequencies. The modified equilibrium equation of the system is seen in Equation (4.17) (Moan, 2003b).

$$\begin{aligned} \boldsymbol{M}\ddot{\boldsymbol{r}}_{k+1} + (1+\alpha)\boldsymbol{C}\dot{\boldsymbol{r}}_{k+1} - \alpha\boldsymbol{C}\dot{\boldsymbol{r}}_k + (1+\alpha)\boldsymbol{R}^I_{k+1} - \alpha\boldsymbol{R}^I_k \\ = (1+\alpha)\boldsymbol{R}^E_{k+1} - \alpha\boldsymbol{R}^E_k \end{aligned} \tag{4.17}$$

Where **M** is the mass matrix, $\mathbf{R}^{\mathrm{I}}$ is the internal force, $\mathbf{R}^{\mathrm{E}}$ is the external force, and **C** is the damping matrix consisting of both diagonal damping terms and Rayleigh-damping described by Equation (4.18).

$$\boldsymbol{C} = \boldsymbol{C}_0 + \alpha_1\boldsymbol{M} + \alpha_2\boldsymbol{K} \tag{4.18}$$

$\mathbf{C}_0$ is the diagonal damping matrix, while the two other terms are the Rayleigh-damping where α_1 is the mass proportional damping factor and α_2 is the stiffness proportional damping factor. Equation (4.17) will be unbalanced, and hence, requires equilibrium iterations. The updated Newton-Raphson approach described in Subchapter 4.3.1 is one possible approach to perform these iterations.

Chapter 5

Modelling

The purpose of this chapter is to describe the modelling of the anchor-pipeline interaction. To model the interaction, the anchor, chain and pipeline must be modelled. In addition, the seabed, sea surface and environmental conditions have to be specified. All of the necessary components needed to create the model are seen in Figure 5.1, with the applied coordinate system. The anchor moves in negative Y-direction, the X-axis points into the plane and Z is zero at the sea surface.

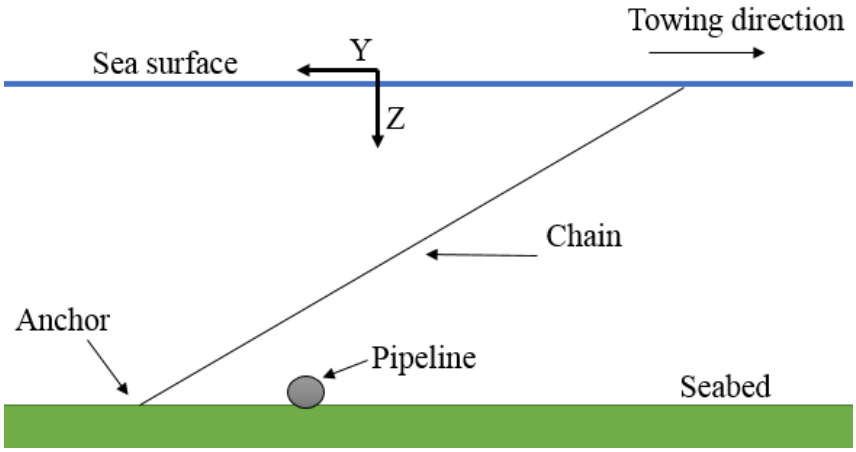

Figure 5.1: All components needed to model the interaction, with coordinate system

A total of three separate analyses were carried out to inspect the anchor-pipeline interaction. The first analysis investigated the effect of anchor mass, anchor geometry, pipe diameter, vessel velocity and angle of attack on the anchor's response. The angle of attack was defined as seen in Figure 5.2. The second analysis determined minimum chain length for the anchors to reach the seabed when towed at 2 and 10 knots. The final analysis consisted of eleven case studies, which investigate the global response of the pipeline when exposed to anchor forces. The collective term for the eleven cases are elastoplastic case studies.

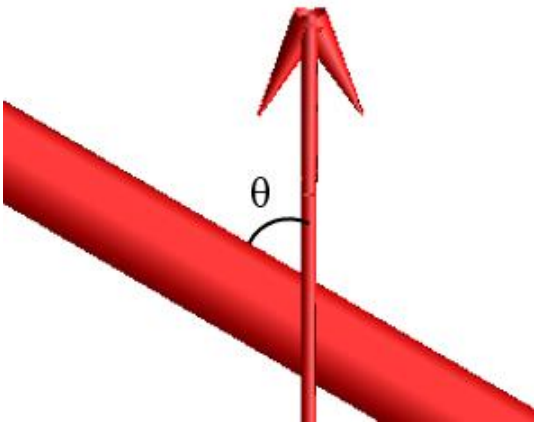

Figure 5.2: Angle of attack between pipeline and anchor

For all of the analyses, the water depth was 200 meters. The pipe was assumed to be grade X-65. All objects made of steel were assumed to have the same general material properties. These and other general properties applied in the analyses are shown in Figure 5.1. The naming system seen in Figure 5.3 was used for the parametric study, and the case studies, to easily distinguish the models. Figure 5.4 displays the naming system used for the study of minimum required chain length.

Table 5.1: General properties applied in the analyses

	Symbol	Value	Unit
Young's Modulus	E	$2.10 \cdot 10^{11}$	*Pa*
Shear Modulus	G	$7.93 \cdot 10^{10}$	*Pa*
Gravitational acceleration	g	9.81	m/s^2
Density seawater	$\rho_{seawater}$	1026	kg/m^3
Density steel	ρ_{steel}	7850	kg/m^3
Water Depth	b	200	*m*

a – Anchor Mass [kg]

b – Water depth [m]

c – Pipe diameter [in]

d – Vessel velocity [kn]

e – Chain length [m]

f – Angle of attack [˚]

akg***b***m***c***in***d***kn***e***m***f***

Example: **4890**kg**200**m**30**in**2**kn**550**m**90**

Figure 5.3: Naming system

a – Anchor Mass [kg]

d – Vessel velocity [kn]

e – Chain length [m]

$\boldsymbol{a}$kg$\boldsymbol{d}$kn$\boldsymbol{e}$m

Example: $\mathbf{4890}$kg$\mathbf{2}$kn$\mathbf{550}$m

Figure 5.4: Naming system for required anchor chain length

All the time-domain analyses were carried out by applying MARINTEK's special purpose computer tool SIMLA. The next subchapter will give an overview over SIMLA's structure, and how a SIMLA analysis is performed. Following this, the elements in SIMLA, and how they were applied to model the components seen in Figure 5.1 is described. This includes simplification of geometry and calculations performed using MATLAB. Finally, the analyses' setup is described.

5.1 SIMLA

To perform a SIMLA analysis several modules are employed, as seen in Figure 5.5. Models are created using FlexEdit, which is a text editor consisting of ASCII characters and based on cards that define specific aspects of the model (Sævik, Økland, Baarholm, & Gjøsteen, 2010). FlexEdit creates a .sif file that is run by SIMLA which produces the output file .sof, the log file .slf, as well as the results database .raf and .dyn. The .raf file is used by XPost to create a 3D visualization. To create plots of the responses, a .spi file is made specifying which responses are to be inspected. SIMPOST takes this .spi file and creates a .mpf file consisting of ASCII characters which can be utilized by MatrixPlot to create plots.

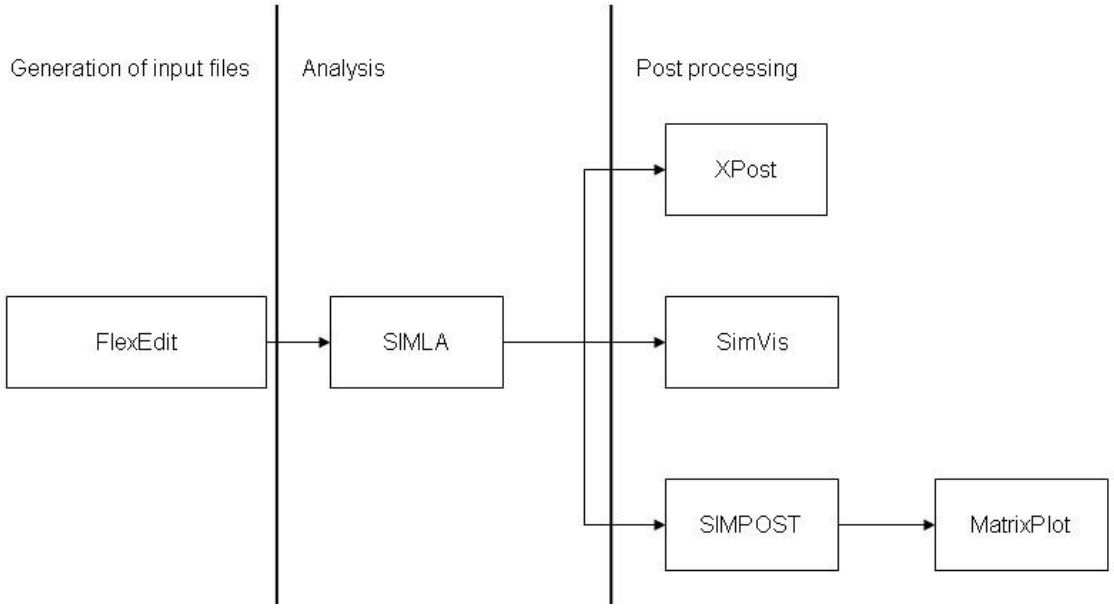

Figure 5.5: Overview over modules from SIMLAs user manual (Sævik et al., 2010)

When creating the model using FlexEdit, one first defines nodal coordinates before attaching elements to these nodes (Sævik, 2008). These elements are organized into element groups, which are given a chosen name and defined by the choice of element and material type. In the modelling of the anchor-pipeline interaction, four different element types were applied. These are PIPE31, PIPE33, CONT126 and CONT164. The first two are pipe elements, used to model the anchor, pipeline and cable. The two latter elements are contact elements applied to model the interaction between the pipe elements and the seabed, and between the pipe elements. These elements will be reviewed.

5.2 Pipe Elements

Pipe elements are 3D elements modelled with two nodes. They are employed to model all physical objects in the models, that is the anchor, anchor chain and pipeline. By default it is assumed that the pipe elements have thin walled tubular cross-sections with constant radius and constant thickness along each element (Sævik, 2008). This can however be bypassed by applying the card NODPROP.

For the pipe elements, the mass matrix is found by applying interpolation functions that assume six degrees of freedom per node; three translational and three rotational degrees of freedom (Sævik, 2008). Raleigh and lumped damping is included for each element. Loads applied to the elements include linear interpolations loads along the element, and hydrodynamic loads

found using Morison's equation (Sævik, 2008). Both pipe elements apply the Co-rotational Total Lagrangian approach, described in Chapter 4.2.

The defining difference between PIPE31 and PIPE33 is the material models and the kinematic representation. PIPE31 assumes an elastic linear material, with plane stress and applies Hooke's law, resulting in two normal stress components and one shear stress component.

PIPE33 is an elastoplastic material that takes into consideration both stresses in axial and hoop direction. The plastic properties of the element follows the outline described in Chapter 4.1.3. The Green strain tensor expressed in Equation (4.3) is valid for PIPE33 elements. However, for the elastic element PIPE31, the coupling between longitudinal strain and torsion is neglected and the Green strain is shortened to the expression seen in Equation (5.1).

$$E_{xx} = u_{x0,x} - yu_{y0,xx} - zu_{z0,xx} + \frac{1}{2}\left(u_{y0,x}^2 + u_{z0,x}^2\right) \tag{5.1}$$

5.2.1 Anchor

In accord with prior work done by Vervik (2011) and Wei (2015), and as described in Chapter 2.2, a stockless SOTRA Spek anchor was applied.

The information required to model the anchor and chain were stored in the excel spreadsheet *Input Anchor*, seen in Appendix F. The anchor shape was simplified to the shape seen in Figure 5.6, and it was assumed that the mass was equally distributed.

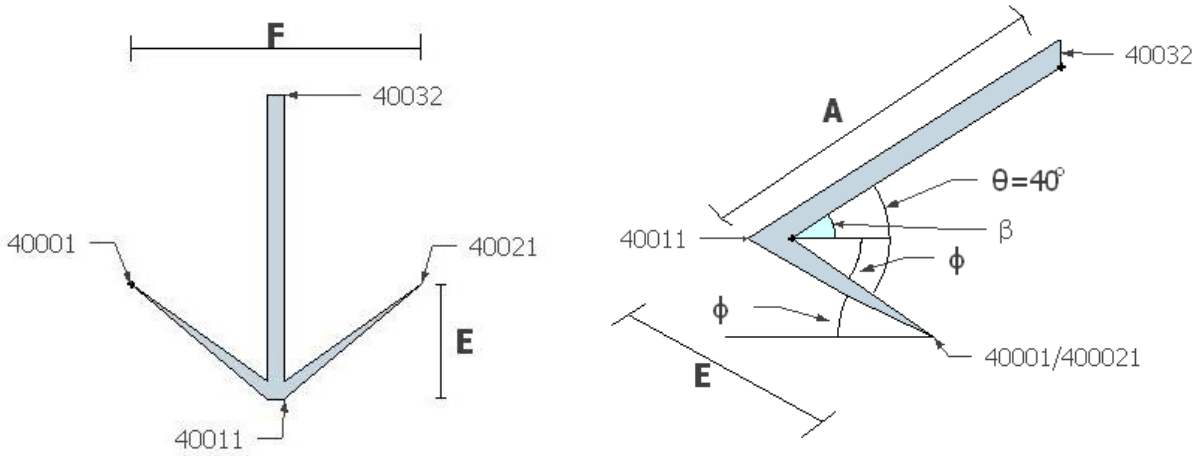

Figure 5.6: Simplified geometry seen above and from the side

Important nodes have been listed with numbers in Figure 5.6, while dimensions taken from SOTRA, seen in Table 2.1, are shown as bolded letters in accord with SOTRAs notation. Node 40011 has a vertical distance from the seabed of 0.2 meters. To model different anchors, the coordinates implemented in the .sif file had to be updated. This was done using the MATLAB script CoorAnchor.m that calculates the nodal coordinates for the anchor. The calculation of the coordinates and distributed mass, is seen in the anchor section of Appendix C. The MATLAB script is seen in Appendix F.

The anchor was modelled using PIPE31 elements, as deformation of the anchor should be small and are hence unimportant. The anchor geometry was split into three parts. The fluke split into two separate parts, and the shank modelled as one piece. The flukes have a varying radius at each node, creating a pointed end at the tips, as can be seen the anchor modelled in Figure 5.7.

Should the anchor appear to deform, an option was to stiffen the anchor by adding three new elements, one along each fluke and one along the shank. These elements have no mass or geometric properties, but have a bending stiffness a hundred times stiffer than the original bending stiffness. This approach can be applied to prevent the deformation of the anchor's flukes. This approach was applied in all of the elastoplastic case studies, but not in the parametric study. This is discussed in more detail in Subchapter 6.1.2.

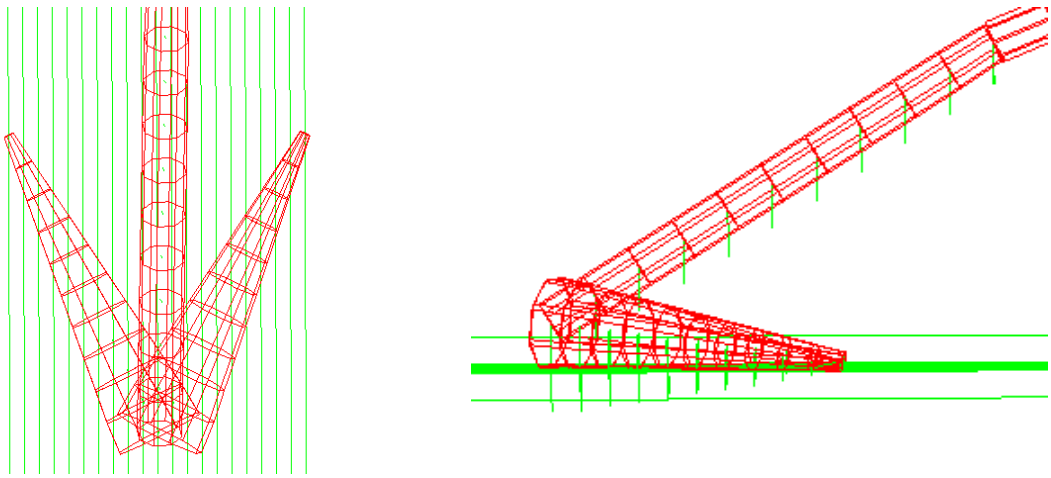

Figure 5.7: Anchor modelled seen in XPost

5.2.2 Chain

As mentioned in Chapter 3.1.2, K3 studlink chain was applied. SOTRA recommends a larger diameter for the chain than DNV requires. In this thesis, DNV's requirements were applied. This means that the mass of the anchor dictates the diameter of the K3 chain found in DNV-OS-E301 (2010), which in return dictates the break load and approximate mass of chain, found in Table E2 in DNV Rules for Classification of Ships (2011). This information was also included in the excel spreadsheet *Input Anchor*, seen in Appendix F. From the same set of rules, the drag coefficients for studlink chains were found to be 2.6 in transverse direction, and 1.4 longitudinal.

When modelled the chain geometry, the shape was simplified to a circular section with a total diameter equal to four times the diameter given for one link's circular cross-section seen in Figure 2.3 as *D*. The axial, bending and torsional stiffness were calculated by use of MATLAB script CoorCable.m. To allow flexibility in the chain, the cross-sectional area of one chain segment was found by multiplying the cross-sectional diameter of one link two.

The chain was modelled with 1000 PIPE31 elements. In the parametric study and the case studies these 1000 elements were divided into three segments. The first segment was the one attached to the anchor. The elements here were the same length as one chain link, that is:

$$l_{element} = 6 \cdot D_{chain}\ [m] \tag{5.2}$$

The next two segments consisted of the remaining elements. The second segment contained two-thirds of the elements, and the last segment one-third. In the models, the chain was separated into two element groups. This was to enable the possibility of making the top elements stiffer than the others. However, this was not used and will not be described further. In the required anchor chain length study the 1000 elements were modelled equally long.

The calculations performed in the MATLAB scripts to determine the properties of the chain, size of chain elements and chain coordinates, can be seen in Appendix C, while the scripts are seen in Appendix F.

5.2.3 Pipeline

To create a realistic model of the pipeline, certain assumptions were made regarding material of the coating and content. These are seen in Table 5.2. As mentioned earlier it was assumed that the pipeline was of grade X-65, in accord with Vervik (2011), and that the given parameters

from Statoil were the outer steel pipe diameter. The total outer diameter for the 30- and 40-inch pipeline with protective coating are seen in Table 5.2.

Table 5.2: Important pipeline parameters

Property	**Value**	**Unit**
Density steel	7850	kg/m^3
Density asphalt	1300	kg/m^3
Density concrete	2500	kg/m^3
Density content	800	kg/m^3
Thickness asphalt layer	6	*mm*
Thickness concrete layer	45	*mm*
Total outer diameter (30-inch)	864	*mm*
Total outer diameter (40-inch)	1118	*mm*

The distributed weight of the pipe, as well as submerged weight, was calculated by use of MATLAB function PipeMass.m seen in Appendix F. The calculations are summarized in Appendix C.

As the main purpose of the parametric study was to investigate the anchor's behaviour, PIPE31 elements were chosen for the pipeline. The pipe was modelled as a 10 meter long rigid body, using two elements constrained against all displacements. When inspecting the actual response of the pipeline in the eleven case studies, PIPE33 elements were chosen for modelling of the pipeline. This was to create a more realistic response where the pipeline was modelled with elastoplastic material. The pipeline was modelled as 10 kilometer long, only constrained at the end nodes, allowing displacements otherwise. The pipeline was not modelled in the minimum chain length study.

5.3 Contact elements

Contact elements calculate the gap between a prescribed master group and a slave group. If the gap is sufficiently small to ensure contact, the elements will calculate the force between the two contacting elements. The force is based on relative velocity and prescribed stiffness found from the material curves (Sævik, 2008).

In the analyses, two contact element types were applied. The CONT126 element type was applied to model general interaction between the physical objects and the seabed, where the

physical objects are anchor, pipeline and cable. To model the contact between the physical objects, CONT164 was used.

CONT164 is a 3D 3-noded roller element, where one node is attached to the contacted element, and shown as a user-defined cylinder. The two remaining nodes are defined as two nodes on the contacting pipe or beam element. These two nodes are thus not fixed, but rather updated when a pipe or beam element comes into vicinity of the master node (Sævik, 2008). CONT126 on the other hand is a 1-noded element, which is linked to a predefined contact surface, where the material properties start to function when in contact or when the surface is pierced

The material type applied to model the seabed contact with CONT126, is R_CONTACT. R_CONTACT allows for user-defined descriptions of the material curve. For CONT164, the material type ISOCONTACT is of interest, as it allows for the modelling of isotropic friction behaviour.

The material curves are defined by using SIMLA's material models HYCURVE and EPCURVE. These models describe how much force is needed to cause a given displacement. HYCURVE describes a non-linear elastic behaviour, giving a one-to-one function between the resultant and associated deformation (Sævik, 2008) by ignoring history effects. That means ignoring the effect of previous loads on the material properties. EPCURVE provides an elastoplastic description of the contact, including history effects. EPCURVE material description requires a yield surface and a hardening rule, as described in Subchapter 4.1.3 regarding plastic strain and constitutive equations.

Contact elements were applied in the parameter study and in the eleven case studies. There were no contact elements in the study of minimum chain length. Any difference in how the contact was modelled in the two relevant studies will be specified in the subsections below.

5.3.1 Contact between physical objects

The roller element CONT164 was applied for contact between objects. The outer diameter of the roller elements were set equal to the total outer diameter of the covered pipeline. The material type ISOCONTACT was chosen for all roller elements with the exception of contact between anchor chain and pipeline in the eleven case studies. CONTACT was applied in the case studies to avoid friction between anchor chain and pipeline, as the friction induced small motions in the pipeline, making the system unstable.

ISOCONTACT was chosen for all roller elements, with the exception mentioned above, to include friction when inspecting impact and sliding. The friction coefficient in local XY-direction for the anchor was defined as 0.50, and as 0.38 for the anchor chain, as recommended by supervisor Prof. Sævik. To ensure that the anchor would not penetrate the pipeline, the material curves of the roller elements, connected to the pipeline, were made sufficiently stiff.

For the parametric study, three CONT164 roller elements were created to model the contact between the anchor segments and the pipeline, and one roller group was created to model the contact between chain and pipeline. All of these element groups were attached to one of the pipe elements and was roughly 100 meters long. This was to allow the anchor to slide along the pipeline.

In the elastoplastic cases studied, the same approach as above was applied when the angle of attack was 90 degrees, with the exception of case 15400kg200m30in2kn660m90 due to erroneous results. For this case, and the cases where the angle of attack was 60 or 30 degrees, the total number of roller elements were increased to 28. One element was for contact with the cable, and was 20 meters long, connected to the element where the anchor would hit the pipeline. The remaining 27 elements were divided into three groups of nine elements each. One group for each fluke, and one for the shank. These elements were eleven meters long, and overlapped with one meter, so that the anchor would be able to slide along the pipeline.

5.3.2 Contact with seabed

In the models created for the parametric study and the elastoplastic case studies, six contact element groups were created to model interaction with the seabed. One contact element for each of the three segments of the anchor, two for the cable and one for the pipeline. All of these element groups share the same properties in regards to friction coefficients. The friction coefficient in X-direction was set to 1.0, and in Y-direction to 0.3. However, the anchor chain and the seabed contact element was rotated by 90 degrees. This means that the cables friction coefficient in X-direction works in Y-direction, and the friction in Y-direction is valid for motion in X-direction. The friction coefficient for the anchor when moving along the Y-axis towards the pipeline would be 0.3, while the friction coefficient would be 1.0 for the cable. The reason for doing this was DNV's recommendation to use a friction coefficient of 1.0 between chain and sea bottom (DNV-OS-E301, 2010). For the analyses where sliding was a possible

response, the friction coefficient in X-direction was altered from 1.0 to 0.3 when allowing sliding. This is to ensure correct friction coefficient when the anchor slides.

The cable was also exposed to damping from the seabed due to soil material. To create this effect damping was also included. The calculation for damping is seen in Equation (C-19) to (C-21) in Appendix C.

The material curves used for soil stiffness were taken directly from Wei (2015), and have not been altered. Hence, the soil stiffness was stiffer than it should be in the case of normal clay, meaning that the anchor and pipeline do not penetrate the seabed as much as they should. Due to time limitations, the material curves were not inspected in detail, and the material modelling was not updated. This is however not a problem, as the largest effect of the soil stiffness, on the interaction, is where the anchor hits the pipeline. That is, if the anchor penetrates the soil considerably, it will have a different attack point on the pipe, than if it doesn't penetrate the soil. This effect can be produced by altering the span height of the pipeline. This was however outside the scope of this thesis.

5.4 Environmental conditions and other parameters

The environmental conditions need to be defined for all of the analyses. However, they do not have any effect on the simulation as the vessels movement was modelled as a constant velocity applied at the top of the anchor chain. The motion of the vessel was thus modelled by applying a PDISP card on the top of the cable. This card defines a factor, which is multiplied with a time history, to calculate the displacement of the top of the anchor chain. The factor is dependent on the chosen vessel velocity. Two different time histories were defined for the two velocities. This was to prevent a too rapid acceleration of the 10 knot scenario, which could cause an unrealistically large force in the anchor chain. Additionally, the top of the anchor chain had to be moved backwards towards the anchor to create a catenary shape before the onset of motion. This was to avoid large tension in the chain. To ensure this, the time histories were modified so that the anchor chain would achieve a catenary shape, and the acceleration of the chain would increase linearly until reaching desired velocity. The catenary shape was not necessary for the required anchor length study as the chain started in a vertical position.

Other parameters that needed to be modelled was the angle of attack between anchor and pipeline. In the parametric study this was done by applying a PDISP card to rotate the pipeline

elements. The rotation was performed during the second static analysis. For the elastoplastic case studies, the coordinates for the pipeline after rotation were calculated and applied.

5.5 Specifics of Analyses

5.5.1 Parametric study

Model Setup

All components seen in Figure 5.1 were included in the parametric study, and modelled as described above. The pipe was modelled using PIPE31 elements, extra stiffness was not applied to the anchor, and the contact between physical objects was modelled with four roller elements. The parameters studied were pipe diameter, anchor mass and geometry, vessel speed and angle of attack between pipe and anchor. The chain length was set to the maximum value corresponding to requirements in DNV-OS-E301 (2010) set by anchor mass, see Figure 3.4. Six anchor classes were chosen to be applied in the parametric study, based on the study by Vervik (2011). Parameters investigated are summarized in Table 5.3. The anchor chain length in Table 5.3 is the maximum anchor chain length recommended by DNV for the anchor mass listed to the left in the table.

Table 5.3: Parameters investigated

Anchor Mass [kg]	Anchor Class	Pipe Diameter [Inches]	Vessel velocity [knots]	Anchor Chain Length [m]	Angle of Attack [deg]
3780	Z	30	2	522.5	90
4890	D	40	10	550	60
6000	G			577.5	30
7800	K			632.5	
9900	O			660	
15400	X			742.5	

The anchors starting point, relative to the pipelines, was determined based on chain length. The longer the chain, the further away it would start. To investigate all combinations of the parameters, 72 analyses were carried out.

Analysis Setup

The analysis sequence is controlled by use of TIMECO cards in the .sif file. For this analysis the sequence was: static, static, dynamic and dynamic. The first sequence performed a basic static analysis of the system, while the second static sequence was a two second long analysis where the pipeline was rotated to obtain desired angle of attack. The first dynamic sequence was performed to obtain contact between the anchor and the pipeline. The restart time for the final dynamic sequence was determined through inspection of the 3D visualization, and was as close to the onset of the impact as possible.

If the angle of attack was different from 90 degrees, the second dynamic analysis would allow sliding of the anchor by releasing boundary conditions on the anchor and cable. If the angle of attack was 90 degrees, the restart was performed to inspect the response in more detail by reducing the size of the the time steps.

The time step for the static analysis was 0.01 seconds where the results were saved every 0.1 seconds. For the onset of the dynamic analysis, however, the time step was reduced to 0.001 and results were saved every 0.01 seconds for the first 3 seconds. This reduction was also performed for the final restart that starts when the anchor reaches the pipeline.

For the static sequence, the convergence criterion was set to ALL, meaning that displacement, forces and energy would be checked. The strictest criterion of the three dictates whether the results of the calculation has reached convergence. For the dynamic sequences, this criterion was set to DISP, which means that only displacement was checked for convergence. The specific convergence criterion for both types was set to 10^{-5} in agreement with supervisor Prof. Sævik.

To efficiently investigate the effect of the parameters, MATLAB was employed. The MATLAB setup is described in Appendix B, and all scripts are seen in Appendix F.

5.5.2 Minimum Chain Length

Model Setup

The purpose of this analysis was to find the minimum chain length that would cause anchor-pipeline interaction. The pipeline, seabed and contact were hence not modelled in this analysis. A constant depth of 200 meters was applied, and the anchor chain lengths varied between 200

meters and 350 meters. All parameters applied are seen in Table 5.4. All listed anchor chain lengths were tested with each anchor mass.

Table 5.4: Parameters investigated in chain length versus depth

Anchor Mass [kg]	**Anchor Class**	**Vessel velocity [knots]**	**Anchor Chain Lengths [m]**
3780	Z	2	200
4890	D	10	250
6000	G		300
7800	K		350
9900	O		
15400	X		

Unlike the parametric study, the anchor was modelled directly beneath the starting point for the vessel. The anchor chain then started as a straight line before the top of the chain was set in motion. A complete model in SIMLA is seen in Figure 5.8.

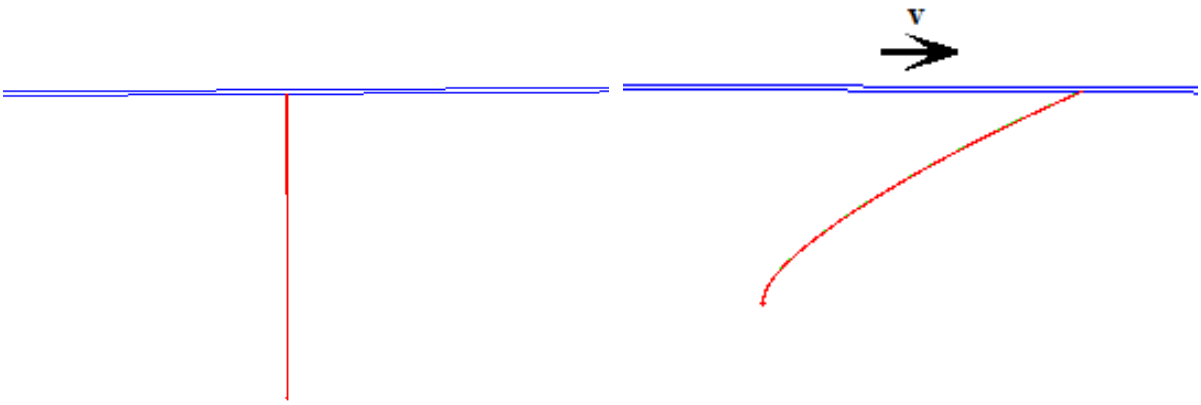

(a) Time 0 [s] (b) Time 66.9 [s]

Figure 5.8: Complete model in the required anchor chain length study

Analysis Setup

For this study only one static and one dynamic analysis were necessary. The static analysis and the dynamic analysis were exactly similar to that of the parametric study. The anchor was dragged for 75 seconds. Once the analyses was finished, the .raf file was inspected to ensure that the anchor had obtained constant speed. The same convergence criterion as in the parametric study were applied. MATLAB was also applied in this study. The MATLAB setup for this analysis is also described in Appendix B, and all scripts are seen in Appendix F.

5.5.3 Elastoplastic Case Studies

Model Setup

All of the segments modelled in the parametric study were included in the elastoplastic case studies. The main difference to the parametric study was the modelling of the pipeline. Instead of 10 meters long, the pipeline was modelled as 10 kilometer. The pipeline was also modelled with PIPE33 elements, with elastoplastic material properties, instead of PIPE31. The pipeline was only constrained at the end nodes, meaning the pipeline was allowed to globally deform and be displaced. As mentioned, extra roller elements were applied, and the anchor was made extra stiff by applying extra elements.

Eleven cases were analysed. The parameters inspected were chosen based on the results of the parametric study and the required length of chain study. These results are discussed in Subchapter 6.1 and 6.2 respectively. The parameters studied are seen in Table 5.5. The alternative length for the anchor chain was only applied to the 15400 kg anchor, in combination with varying angles of attack. A complete list of cases studied are seen in

Table 5.6.

Table 5.5: Parameters studied in the elastoplastic study

Anchor Mass [kg]	Anchor Class	Pipe Diameter [Inches]	Vessel velocity [knots]	Anchor Chain Length [m]	Angle of Attack [deg]
9900	O	30	2	660	90
15400	X	40	10	742.5	60
				350	30

Table 5.6: Complete list of analyses carried out in the elastoplastic study

Name of models	
9900kg200m30in2kn660m90	15400kg200m30in10kn350m90
-660m60	-350m60
9900kg200m30in10kn660m90	-350m30
9900kg200m40in2kn660m90	15400kg200m40in2kn743m90
15400kg200m30in2kn743m90	15400kg200m40in10kn743m90
15400kg200m30in10kn743m90	
-743m60	

Analysis Setup

As the desired output of the analysis was the strain, the VISRES card was applied to gather information regarding longitudinal strain. The analysis sequence for the elastoplastic study was: Static, dynamic and dynamic. Unlike the parametric study, there was only one static analysis sequence. This was because the pipeline was not rotated, as in the parametric study. Instead, the coordinates of the pipeline, when rotated, were calculated and directly implemented in the input file. The pipeline was thus in final position when performing the static analysis. The starting point for the final dynamic analysis was determined by visually inspecting the 3D visualization. The final restart releases the constraints put on the anchor and anchor chain, allowing the anchor to move freely and slide. This is equal to the approach in the parametric study. The same convergence criteria used in the previous studies were applied.

MATLAB was not applied directly in the case studies. All input files are therefore uploaded to the electronical Appendix F.

Chapter 6

Results and Discussion

6.1 Parametric Study

The results from the parametric study were gathered by inspecting the 3D visualisation of each model in XPost. The response of each simulation was categorized by interaction type, and classified as either realistic or unrealistic.

Several simulations showed unrealistic responses after the contact between the anchor and pipeline had ceased. The realism of the response was thus evaluated for the anchor-pipeline interaction itself. The simulation is ruled as unrealistic if the anchor pierces the pipeline, or the anchor deforms grossly. Small deformations at the tip of the flukes were ignored. The responses in the non-realistic analyses were included in the results, as the response before the non-real behaviour was evaluated.

There is no clear consensus on how to define the different responses of an anchor-pipeline interaction. In DNV-RP-F111 (2010) the interaction between the trawl gear and pipeline are classified as pull over or hooking, while Wei (2015) classifies the interaction between anchor and pipeline as either hooking or unhooking. Wei (2015) signifies hooking as any interaction where the anchor remains in contact with the pipeline for a longer period, this means that sliding is also defined as hooking.

To categorize the responses seen in the parametric study a new system was developed. The responses were divided into two main categories: Brief contact and lasting contact. Brief contact was further divided into two subcategories: Bounce over and pull over. Pull over is when the anchor remains in contact with the pipeline while being tilted over. An example is seen in Figure 6.1. A pull over can also occur if the initial impact causes the anchor to twist, and rest

on its back, on top of the pipeline. A bounce over is a response where the anchor loses contact with the pipeline as seen in Figure 6.2.

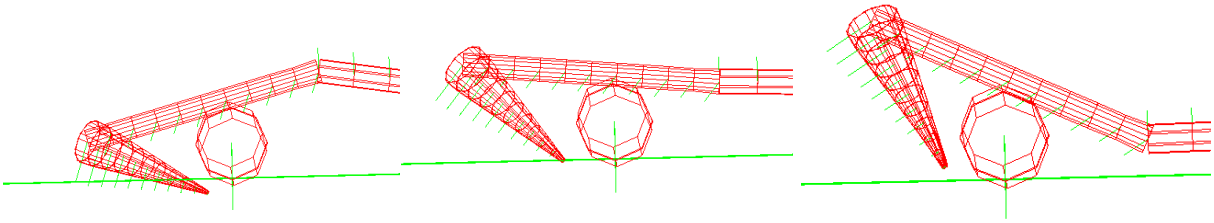

(a) Time 128.4 [s] (b) Time 128.62 [s] (c) Time 128.87 [s]

Figure 6.1: Simulation snapshots of realistic pull over in model 9900kg200m30in2kn660m90 response

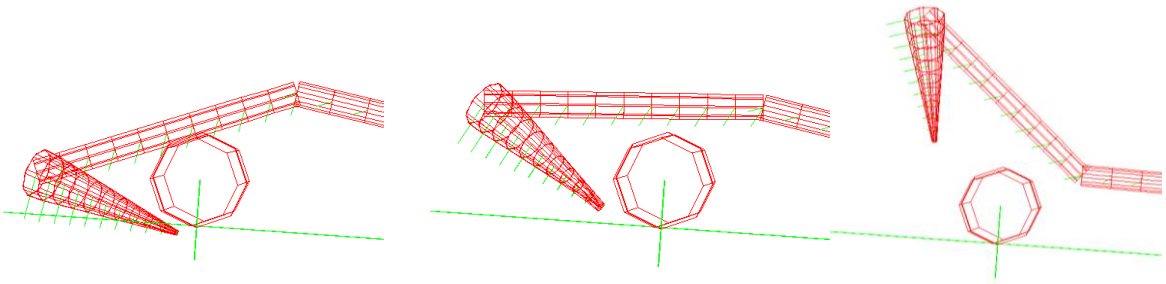

(a) Time 64.65 [s] (b) Time 64.72 [s] (c) Time 64.89 [s]

Figure 6.2: A realistic bouncing off response seen in model 6000kg200m30in2kn578m90

Lasting contact was divided into two categories: Hooking and sliding. Both of these responses can include twisting of the anchor, resulting in the anchor hooking or getting pulled over. A typical example of hooking, with and without twisting, is seen in Figure 6.3. The twisting in Figure 6.3 (b) resulted in the anchor hooking. A typical example of sliding with twisting and finally pull over, is seen in Figure 6.4. Sliding is not visible in the figure.

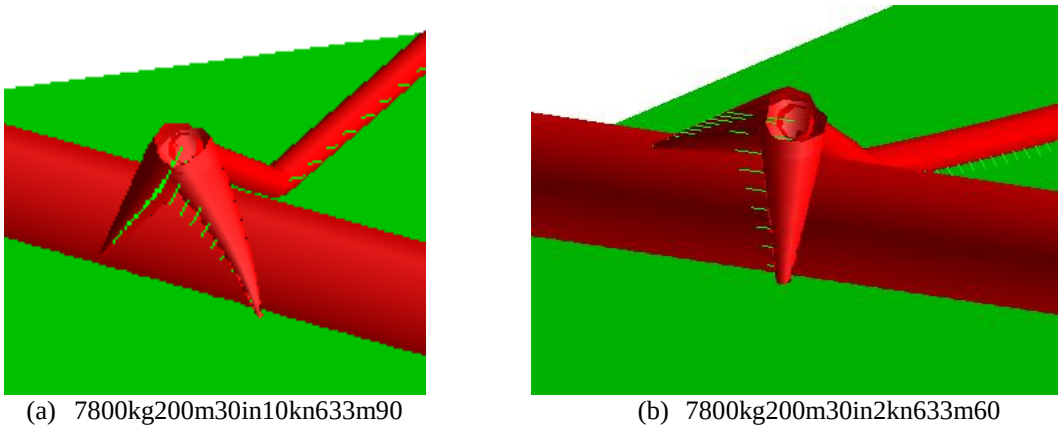

(a) 7800kg200m30in10kn633m90 (b) 7800kg200m30in2kn633m60

Figure 6.3: Two realistic cases of hooking, (a) without twisting and (b) with twisting

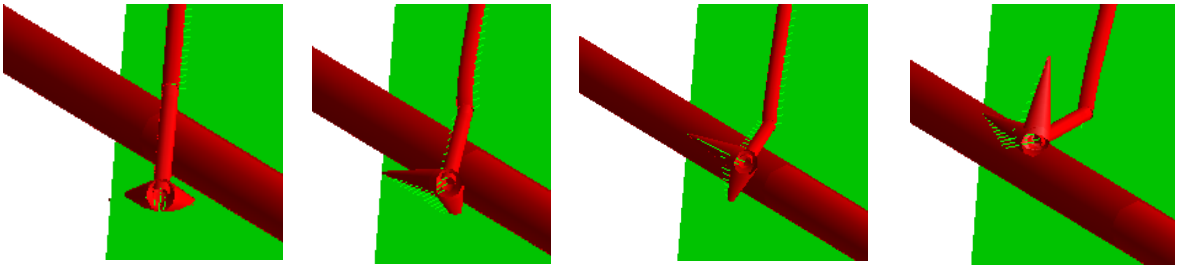

(a) Time 62.4 [s] (b) Time 62.67 [s] (c) Time 62.84 [s] (d) Time 63.4 [s]

Figure 6.4: Sliding with twist and pull over response in 7800kg200m30in10kn633m30

The defining difference between a hooking and sliding response is that the motion of the anchor is stopped during hooking. Thus, if the anchor remains in place for several seconds, the response was registered as hooking, independent of the following behaviour. This is because the eventual sliding or twisting following a hooking response, are due to increased tension in the cable, which would have displaced the pipeline. A flowchart showing how the results were categorized is seen in Figure 6.5.

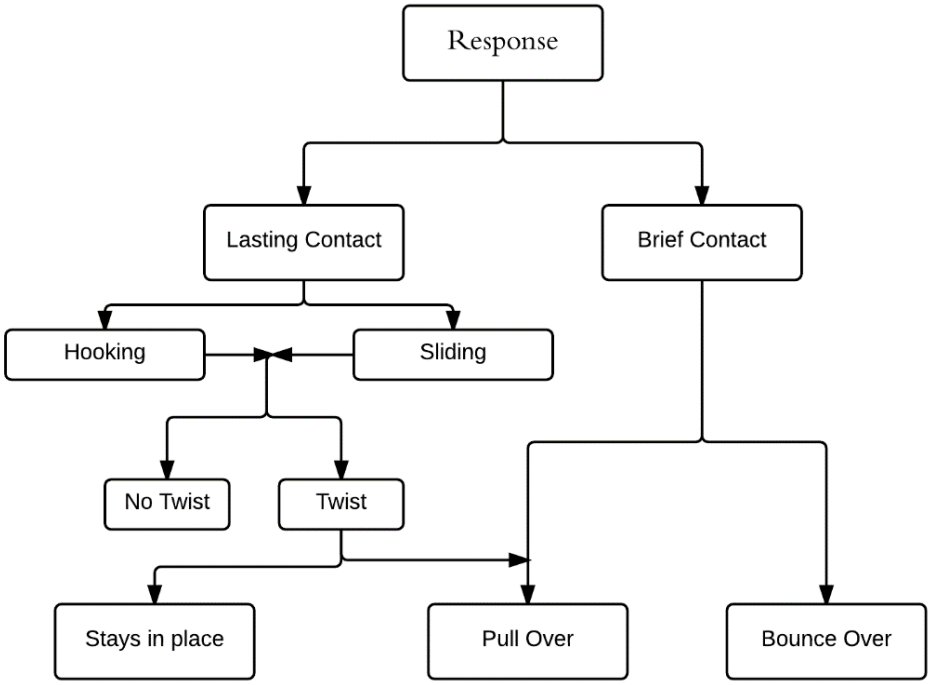

Figure 6.5: Summary of categorisation

6.1.1 Results

Seventy-two models were created and analysed using SIMLA, twelve models created for each mass, varying the parameters listed in Chapter 5.5.1. The categorisation of each model is seen in Appendix D. Table 6.1 summarize how many of the models showed realistic, non-realistic and inconclusive responses.

Table 6.1: Overview of usable results in parametric study

	Mass [kg]					
	3780	**4890**	**6000**	**7800**	**9900**	**15400**
Realistic	1	2	6	7	8	12
Non-realistic	11	9	3	3	1	-
Inconclusive	-	1	3	2	2	-
Total number included in results	12	11	9	10	9	12

There were eight models that were inconclusive as the visualization broke after few time steps and displayed unrealistic behaviour. These are listed in Table 6.2. Seven of the models encountered numerical issues that were solved by increasing the bending stiffness of the chain by a factor 10. These are clearly marked in Appendix D. The total number of models taken into account were 64.

Table 6.2: List of inconclusive models

Inconclusive	
4890kg200m40in2kn550m90	7800kg200m40in2kn633m60
6000kg200m40in2kn578m60	7800kg200m40in10kn633m60
6000kg200m40in10kn578m60	9900kg200m40in2kn660m60
-30	9900kg200m40in10kn660m60

To give insight into the trends seen in the results, a ratio system was applied. The ratio was calculated as seen in Equation (6.1).

$$Ratio = \frac{Number\ of\ responses}{Total\ number\ of\ responses}\ [\%] \tag{6.1}$$

For example, the number of responses can be the number of hooking responses for anchors of 15400 kg and angle of attack of 60 degrees, while the total number of responses would then be the total number of hooking responses. The failed and inconclusive results listed in Table 6.2 are excluded when calculating the ratios.

Overall Results

Figure 6.6 shows the distribution of hooking, sliding and brief contact responses for each anchor mass, while Figure 6.7 shows the distribution of responses within the brief contact category. The distribution, in addition to bounce over and pull over ratios, are summarized in Table 6.3 for the different anchor masses.

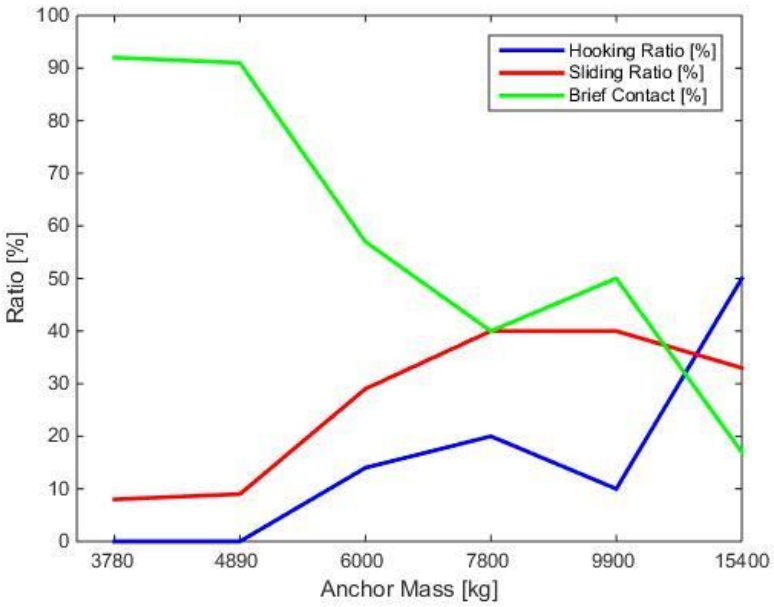

Figure 6.6: Ratio for hooking, sliding and bouncing off

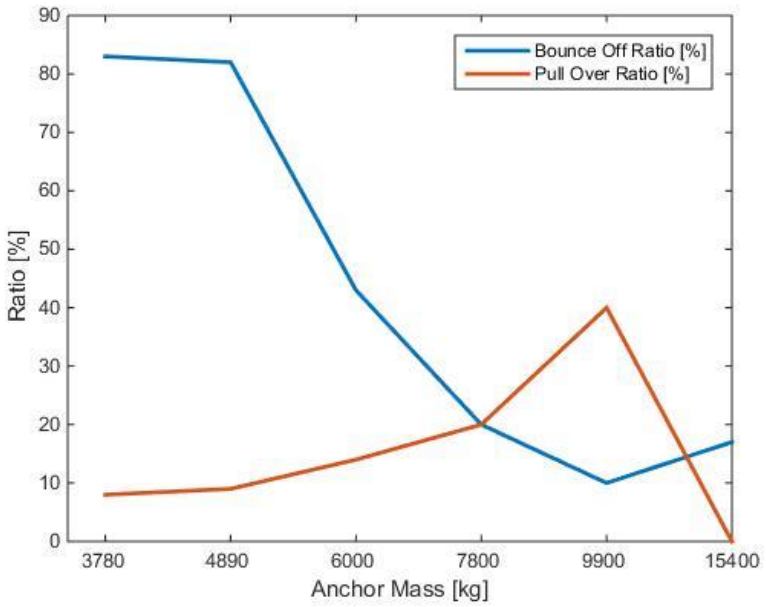

Figure 6.7: Distribution of Brief Contact Ratio seen in Figure 6.6

Table 6.3: Response ratios for different anchor sizes

	Anchor Mass [kg]					
	3780	**4890**	**6000**	**7800**	**9900**	**15400**
Hooking	0 %	0 %	14 %	20 %	10 %	50 %
Sliding	8 %	9 %	29 %	40 %	40 %	33 %
Bounce over	83 %	82 %	43 %	20 %	10 %	17 %
Pull Over	8 %	9 %	14 %	20 %	40 %	0 %
Sum	100 %	100 %	100 %	100 %	100 %	100 %

Effect of angle of attack

Three angles of attack were applied: 90 degrees, 60 degrees and 30 degrees. Figure 6.8 shows the hooking ratios for different angles of attack and anchor masses. Figure 6.9 shows the sliding ratio for different angles and anchor masses.

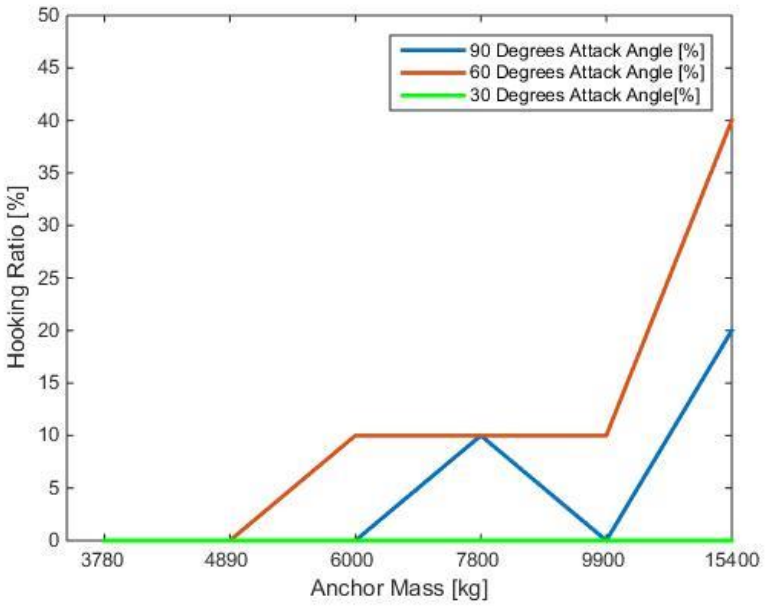

Figure 6.8: Hooking ratio depending on angle of attack and anchor mass

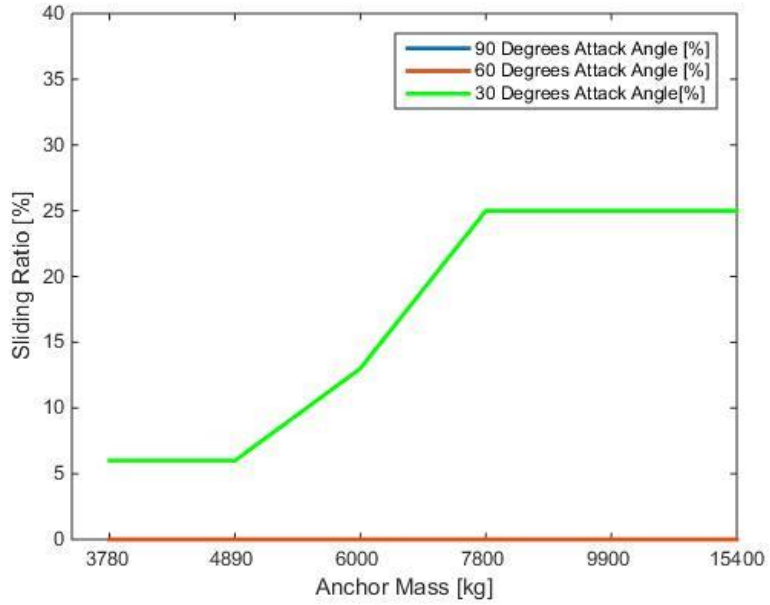

Figure 6.9: Sliding ratio depending on angle of attack and anchor mass

Effect of angle of attack, pipe size and vessel velocity

There were no hooking responses when the angle of attack was 30 degrees. This angle was therefore excluded when inspecting hooking ratio. A complete summary of how angle of attack, pipe size, vessel velocity and anchor mass affects the hooking ratios is seen in Table 6.4. Similarly, there were no sliding responses for the 60 and 90 degrees angle of attack, and they were hence excluded when inspecting sliding. Table 6.5 shows the effect of pipe size, vessel velocity and anchor mass on the sliding ratio when the angle of attack was set to 30 degrees.

Table 6.4: Hooking ratio distribution for all parameters, excluding 30 degrees

Angle of attack [Degrees]	**Pipe Size [Inches]**	**Vessel Velocity [Knots]**	**Anchor Mass [kg]**						
			3780	**4890**	**6000**	**7800**	**9900**	**15400**	**SUM**
90	30	2	-	-	-	-	-	10 %	10 %
		10				10 %		10 %	20 %
	40	2							
		10							
60	30	2			10 %	10 %	10 %	10 %	40 %
		10						10 %	10 %
	40	2						10 %	10 %
		10						10 %	10 %
		SUM			10 %	20 %	10 %	60 %	100%

Table 6.5: Sliding ratio distribution for all parameters excluding, 60 and 90 degrees

Angle [Degrees]	Pipe Size [Inches]	Velocity [Knots]	Anchor Mass [kg] 3780	4890	6000	7800	9900	15400	SUM
30	30	2	6 %	6 %	6 %	6 %	6 %	6 %	38 %
		10				6 %	6 %	6 %	19 %
	40	2				6 %	6 %	6 %	25 %
		10				6 %	6 %	6 %	19 %
		SUM	6 %	6 %	13 %	25 %	25 %	25 %	100 %

The effect of pipe size and velocity on hooking is seen in Figure 6.10, with figure (a) showing the hooking ratio for different vessel velocities and pipe sizes, with an angle of attack of 90 degrees, and figure (b) showing with an angle of attack of 60 degrees. Figure 6.11 summarises the effect of pipe size and vessel velocity on the sliding ratio when the angle of attack is 30 degrees.

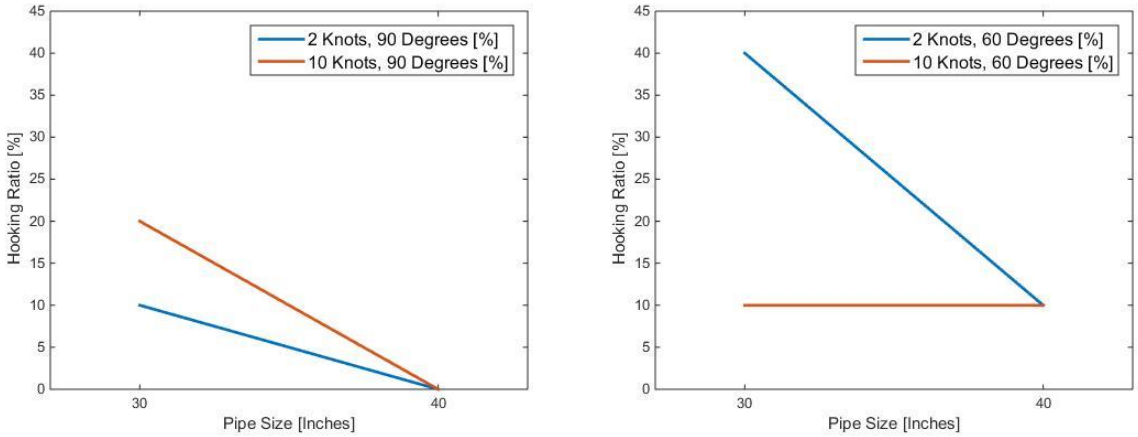

(a) Depending on pipe size and angle of attack (b) Depending on pipe size and vessel velocity

Figure 6.10: Hooking ratio depending on pipe size and vessel velocity

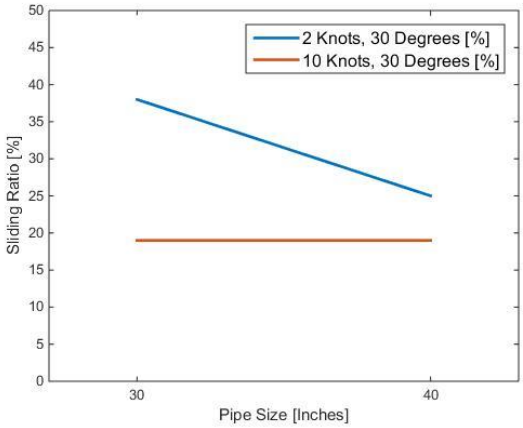

Figure 6.11: Sliding ratio depending on pipe size and vessel velocity

6.1.2 Discussion

General Findings

The general trend points towards an increase in hooking and sliding with increased mass of anchor, lower vessel speed and smaller pipe diameter. The largest amount of hooking occurs for an angle of attack of 60 degrees. All hooking occurrences for the 60 degrees cases were caused by anchor twisting and getting hooked on the side, as seen in Figure 6.3 (b). None of the models displayed a hooking response when the angle of attack was 30 degrees, while all cases of sliding were registered for this angle of attack.

The trend of a higher hooking ratio when larger anchors interact with smaller pipes, at a low velocity, was also found by Vervik (2011) and Wei (2015). However, comparing results do pose several issues as Wei (2015) uses vessel speeds of 6 and 12 knots, and different outer pipe diameter. Despite this, the same conclusion is drawn that more hooking occur for lower velocities, and smaller pipes.

There is some discrepancy when comparing the results with the geometric calculations by Vervik (2011), using Equation (3.13), for the 90 degree angle of attack. According to Vervik (2011), any anchor larger than 4580 kg should hook onto a pipeline with a total diameter of 0.86 meters, and any anchor larger than 13500 kg should hook onto a pipeline with a total outer diameter of 1.12 meter. An outer diameter of 0.86 meters corresponds to a coated 30-inch pipeline, and 1.12 meter corresponds to a coated 40-inch pipeline. The results obtained in the parametric study suggest that 13500 kg would not be sufficient for the 40-inch pipeline, as the 15400 kg anchor did not hook. Furthermore, the smallest anchor to hook onto the 30-inch pipeline was the 7800 kg anchor, which is larger than the predicted 4580 kg anchor. This indicates that geometry alone cannot predict hooking.

A reason for this discrepancy is that the geometry approach done by Vervik (2011) does not consider alternative attack points on the pipeline. Neither does it consider how the attack point for the anchor is influenced by vessel velocity, length of anchor chain, pipe size and soil stiffness. The difference in the anchors' position just before impact, is seen in Figure 6.12. There is a notable difference in how the anchor impacts with the pipeline in Figure 6.12 (b) and (d).

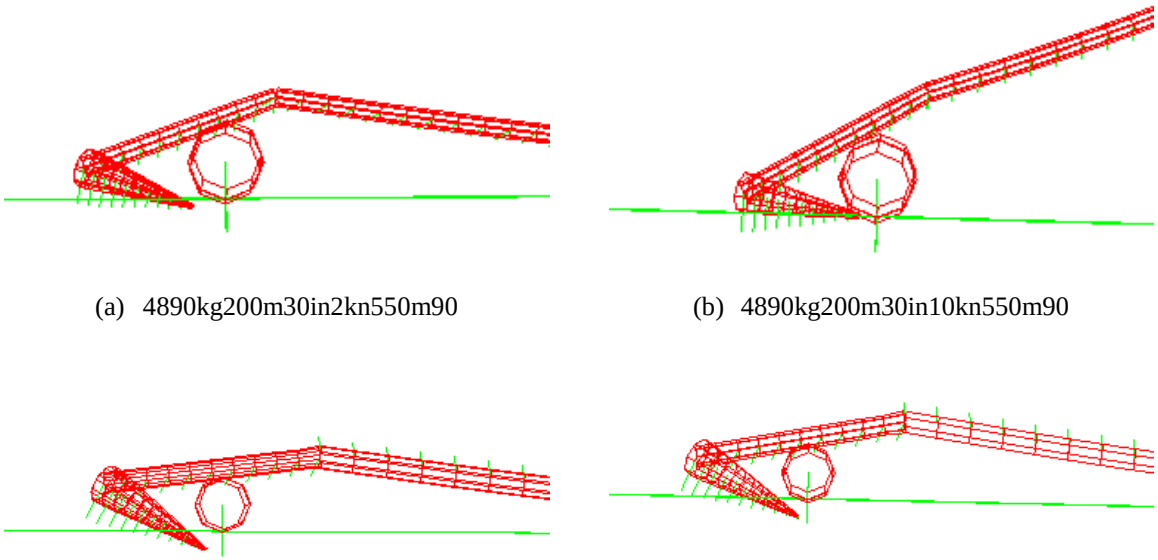

(a) 4890kg200m30in2kn550m90 (b) 4890kg200m30in10kn550m90

(c) 15400kg200m30in2kn743m90 (d) 15400kg200m30in10kn743m90

Figure 6.12: Snapshots showing the effect of size and velocity on attack point

There are also some discrepancies when comparing with Wei (2015), mainly when it comes to the amount of hooking scenarios. When comparing results that are quite similar, Wei (2015) reports hooking for many cases that were not registered as hooking in this study. The fact that Wei (2015) has used different categories makes it problematic to compare the results. It is difficult to pinpoint the reason for the difference in results, as the input files used by Wei (2015) were not available. However, Wei (2015) defined sliding as a hooking response, this may be part of the explanation why Wei (2015) obtained more hooking responses. Furthermore, it is seen that many of the cases Wei (2015) reported as hooking, were categorized as pull over in this study.

The results from this study indicate that the pull over ratio increases with larger anchor mass until the anchor weight reaches 15400 kg. The 15400 kg anchors however, has a drastic increase in hooking ratio, which explains why there were so few cases of pull over. The increase in pull over ratio with increasing mass may be caused by the combination of increased mass of anchor and chain, and the increase in chain length. This combination results in the anchor chain laying on the seabed after having passed the pipeline, and pulling the anchor downwards instead of upwards. The direction of the forces pulling on the anchor, the large distributed mass of the system and the high friction factor between anchor and pipeline, are most likely the reasons for the pull over response.

Despite the difficulties in comparing results, the general trend that hooking increases with anchor geometry, lower vessel velocities and smaller pipe diameter, are the same seen in the theses by Vervik (2011) and Wei (2015)

Sources of Error

There were several sources of error when performing the parametric study. This section is dedicated to describing these, their effects on the result and possible remedies.

The results were gathered by visual inspection of the 3D visualization of the models. This presents a possibility for erroneous classification. This is particularly relevant for the unrealistic models, as the moment where the model went from being realistic to unrealistic had to be located visually. The categorization of the response was then based on the realistic part.

In general, there are more unrealistic responses for the smaller anchors. The short chain length could be the cause of this, as the short length results in the anchors having a different attack point than with longer chain lengths. This effect is enhanced with higher velocities, as seen in Figure 6.12 (a) and (b). Anchors of 3980 kg and 4890 kg had a tendency to reach the pipeline with the flukes first when the velocity was 10 knots, as seen in Figure 6.12 (b). This resulted in the tip of the flukes penetrating the pipewall and deforming in an unrealistic manner. This is also one of the reason there were fewer unrealistic responses for the larger anchors.

The flukes penetrating the pipeline is most likely due to numerical error with SIMLA. The contact element placed on the pipeline does not register the contact between the fluke tips and the pipeline early enough. This effect was one of the main contributors to the unrealistic results, as the flukes would penetrate the pipeline, and be forced back with such a force that the anchor would bounce over and deform. This could possibly have been amended by applying several small roller elements along the circumference of the pipeline, which would be able to register the contact with the fluke tips.

Furthermore, several of the anchors showed signs of small deformation of the flukes. This could have been prevented by applying extra elements along the flukes and shank, with extra bending stiffness, as described in Subchapter 5.5.1. This was not discovered early enough, so the parametric study was performed without the extra elements. However, to investigate if extra elements with extra bending stiffness would solve the problem, seven of the models were reanalysed with the new elements. The general trend of these analyses were that the anchor did not deform, and the anchor displayed the same behaviour as registered.

Another important source of error was related to one of the constraints on the pipeline. The constraint that was supposed to allow for alterations of the span height, had been set to zero, instead of removed when the span height was zero. This results in the pipeline not penetrating the seabed in a realistic manner, but resting on top of the it. This is clearly seen in Figure 6.12. Had this constraint not been present, the pipeline would have settled realistically onto the seabed due to its weight. As the effect of the span height was not studied, this error was not discovered before the end of the project, and was not corrected. It is uncertain how much this affects the results, but it will have had an effect on the attack point on the pipeline.

The chosen run time for the analysis will also have affected the outcome of the study. This is particularly relevant for the sliding scenarios, where a longer time span might have resulted in the anchor beginning to twist and finally pull over, or hook onto the pipeline. However, due to time limits and only applying four roller elements, this was not investigated in the study.

6.2 Minimum Chain Length

A total of 48 models were created and analysed. Each analysis ran for 75 seconds. The nodal velocity for anchors node 40022 in Y- and Z-direction is seen for the 10 knot case in Figure 6.13. The velocities obtain constant values, but become unrealistic the last five seconds. The error, which occurred when towing at both 2 and 10 knots, was caused by towing velocity being defined for 70 seconds in the .sif file. Because of this, all results after 70 seconds are ignored for both the 2 knot and the 10 knot scenario.

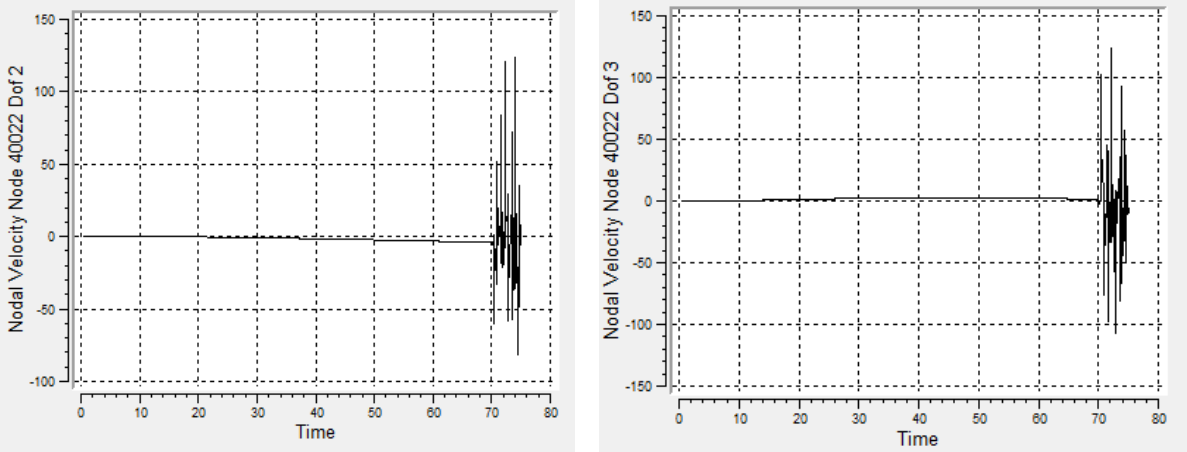

(a) Nodal velocity in Y-direction (b) Nodal velocity in Z-direction

Figure 6.13: Error in nodal velocities in Y- and Z-direction

6.2.1 Results

The general trends in the 2 knot and 10 knot models are seen in Figure 6.14 and Figure 6.15 respectively. The Z-coordinates for the chain element connected to the anchor, at the 70 second mark, are summarized in Table 6.6 and Table 6.7, for 2 and 10 knots, respectively.

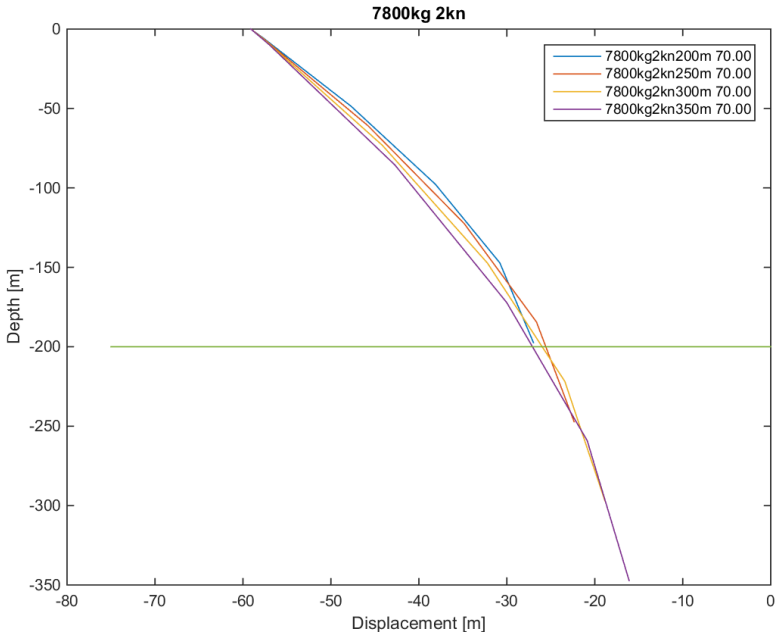

Figure 6.14: Chain shape for different lengths after 70 seconds with 2 knot velocity

Table 6.6: Final Z-coordinate for chain element connected to anchor with 2 knots

Chain Length [m]	Anchor Mass [kg]					
	3870	**4890**	**6000**	**7800**	**9900**	**15400**
200	-196.4	-196.8	-197.1	-197.4	-197.7	-198.3
250	-246.3	-246.6	-246.9	-247.2	-247.5	-248.0
300	-296.4	-296.7	-296.9	-297.2	-297.5	-297.9
350	-346.5	-346.7	-346.9	-347.2	-347.5	-347.9

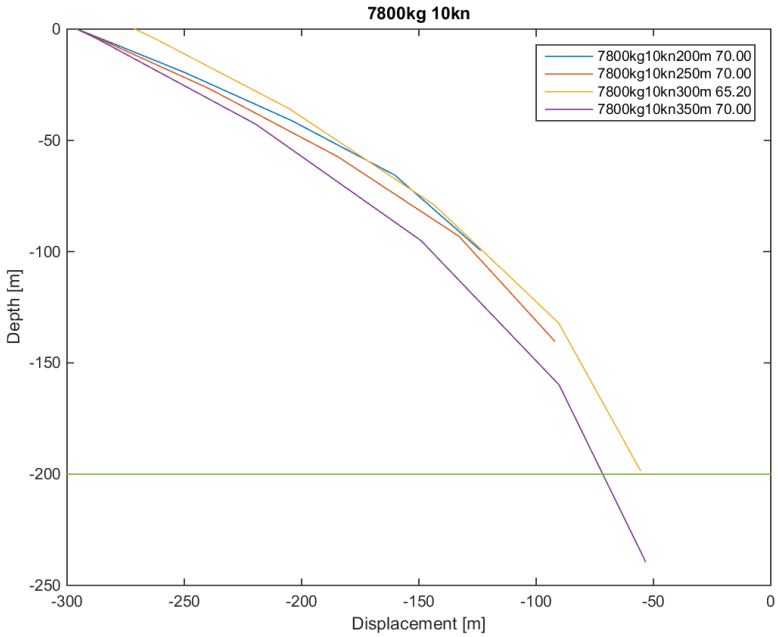

Figure 6.15: Chain shape for different lengths after 70 seconds with 10 knot velocity

Table 6.7: Final Z-coordinates for chain element connected to anchor with 10 knots

Chain Length [m]	Anchor Mass [kg]					
	3870	**4890**	**6000**	**7800**	**9900**	**15400**
200	-96.1	-93.8	-101.7	-99.3	-102.6	-109.1
250	-132.2	-143.8	-137.3	-140.2	-143.9	-150.4
300	-180.4	-182.9	-185.1	-198.4	-191.4	-197.6
350	-240.5	-237.3	-236.5	-239.2	-242.2	-248.0

6.2.2 Discussion

The general trend was, as predicted by Equation (2.2) in Chapter 2.2, that the larger the velocity, the larger the drag forces on the anchor chain. These forces resulted in the anchor being lifted vertically as it was towed. This can be seen in Figure 6.15. This trend was also seen in the work of Vervik (2011) who applied SIMLA, and the same drag coefficients, to study the effect of several velocities on anchor chain being towed.

To estimate the minimum chain length for the anchor to interact with the pipeline, it was assumed that there was a linear connection between the coordinates for the anchor chain above and below the seabed. This is a simplified approach as it completely neglects the shape of the towed chain, and the lumped mass at the end. However, it is adequate for the purpose of finding minimum length of chain. The simplification is seen in Figure 6.16 where (y_0, z_0) are the

coordinates for the anchor chain stopping above the seabed, and (y_1, z_1) for the anchor chain below the seabed.

The recommended new length of the anchor chain was found by use of Equation (6.2). The minimum length for the anchor chain for the two velocities are presented in

Table 6.8.

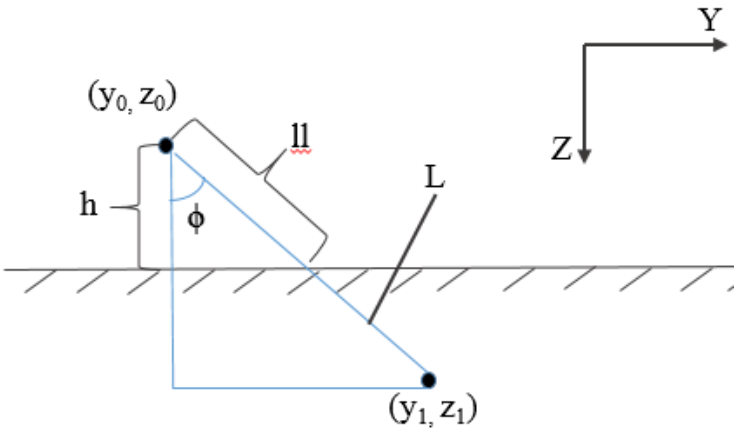

Figure 6.16: Simplified assumption of geometry for two anchor chain coordinates

$$ll = \frac{L}{\cos(\phi)} \tag{6.2}$$

Table 6.8: Minimum required anchor chain length

Minimum length [m]	**Anchor Mass [kg]**					
	3870	**4890**	**6000**	**7800**	**9900**	**15400**
2 Knot	203.62	203.24	202.94	202.58	202.26	201.74
10 Knot	321.05	318.11	315.58	301.62	309.06	302.56

Despite the results showing the same trend as Vervik (2011), the conclusion that 70 seconds was sufficient to get a state of equilibrium in the system, and find the required length of the anchor, has proven to be false. Despite obtaining constant velocity, it was later observed that the results obtained are only applicable if the distance between pipeline and the anchor's starting point is less than 100 meters. In hindsight, the acceleration of the nodes should have been investigated instead of the velocity. The Z-coordinates could then be determined at the time where acceleration in both vertical and horizontal direction was zero, as that would be the time

of equilibrium in the system. However, the results can still be applied as long as the distance between the pipeline and the anchor is less than 100 meters.

6.3 Elastoplastic Case Studies

The eleven cases inspected were chosen based on the results from the previous two studies. There were two motives behind this study. The first, to investigate how well the anchor's response had been predicted in the parametric study. The second, to inspect the pipeline's response, by investigation whether or not the longitudinal strain in the cross-section exceeded DNV's criteria.

The design criteria for local buckling, when the pipeline is exposed to combined loading, is expressed in Equation (3.4) and (3.5). It was assumed that there would be external overpressure, and hence Equation (3.5) was chosen. A conservative assumption was made, assuming that the pressures in Equation (3.5) would be insignificant, and the contribution from these were set to zero. By further assuming a high safety class, and ignoring the contribution from corrosion on the thickness, the characteristic bending strain resistance was calculated using Equation (3.6). The values for the factors needed in this calculation, and the result, can be seen in Table 6.9.

Table 6.9: Calculation of characteristic bending strain resistance

Description	**Symbol**	**Value**
Resistance strain factor	γ_ε	3.3
Material resistance factor	γ_m	1.15
Safety class resistance factor	γ_{SC}	1.26
Train hardening	α_h	0.93
Girth weld factor	α_{gw}	0.82
Thickness/diameter ratio	$\frac{t_2}{D}$	$\frac{1}{35}$
Characteristic bending strain resistance	$\varepsilon_c(t_{2,}0)$	0.01324
Design loads strain	ε_{Sd}	0.00401

The responses were categorized as describe in Subchapter 6.1, with the additional requirement that hooking must result in the pipeline being globally displaced. An example of a hooking scenario in the elastoplastic study, is seen in Figure 6.17 and Figure 6.18. Figure 6.17 shows the configuration of the system before impact, and Figure 6.18 shows the system's configuration during hooking.

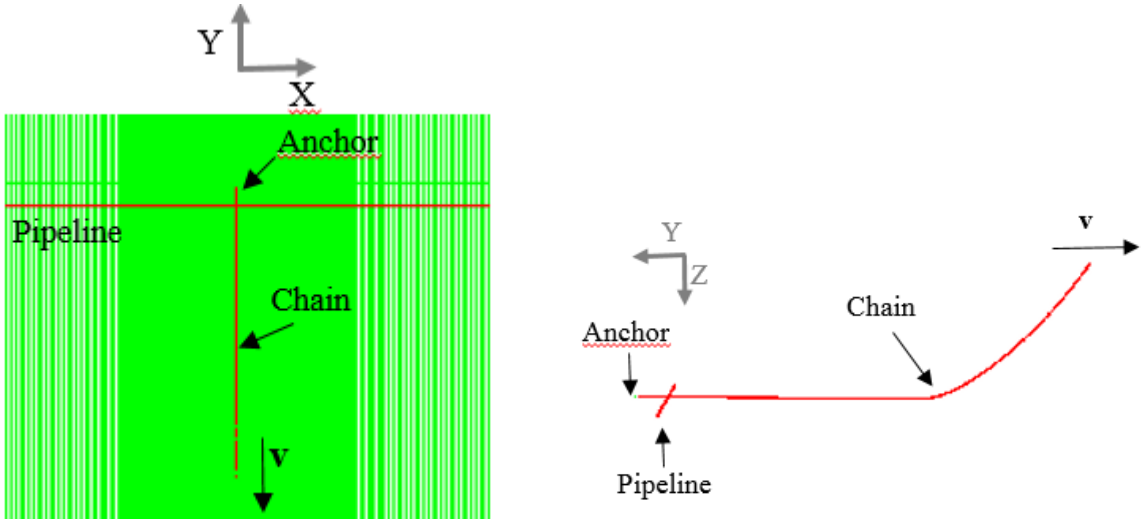

(a) Aerial view (b) Profile view

Figure 6.17: Initial configuration of 15400kg200m30in2kn660m90

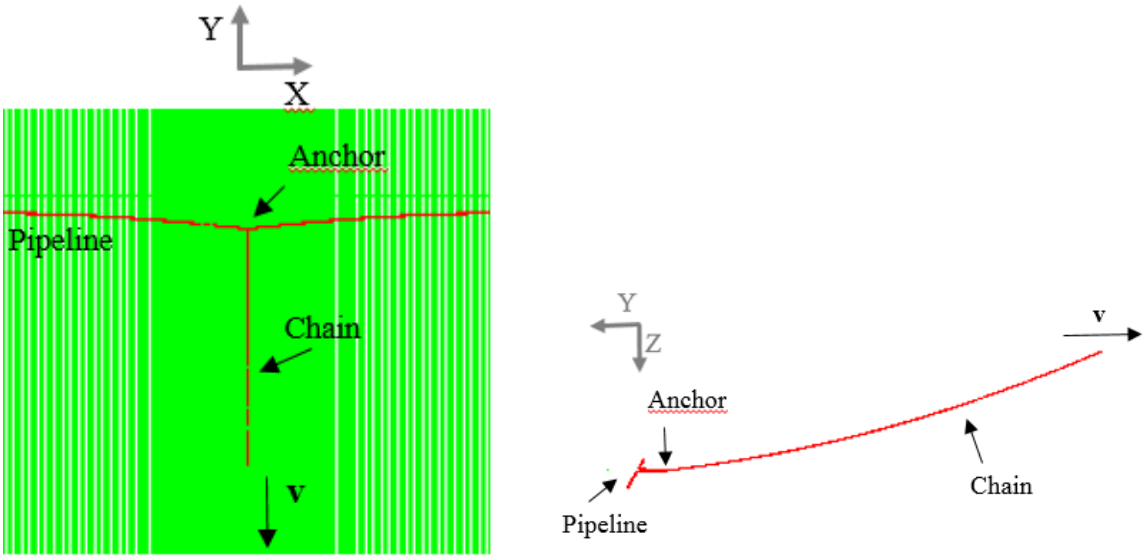

(a) Aerial view (b) Profile view

Figure 6.18: Maximum displacement before reaching chain break load for 15400kg200m30in2kn660m90

6.3.1 Results

The criteria for a realistic response were the same as outlined in the parametric study, and were determined based on inspection of the 3D visualization in Xpost. The distribution of realistic, non-realistic and inconclusive analyses are seen in Table 6.10.

Table 6.10: Overview of usable results in elastoplastic study

	Mass [kg]		
	9900	**15400**	
Anchor Chain Length [m]	**660**	**743**	**350**
Realistic	1	4	2
Non-realistic	3	-	1
Inconclusive	-	-	-
Total cases studied	4	4	3

In all of the non-realistic cases, the anchor penetrated the pipewall. However, this was after a few seconds of contact, which were used as results.

The strain in the pipeline's cross-section, were found from plots created in XPost. Eight Gauss points were applied in the calculations. For the results, strain was inspected at Gauss point 1 and 5, as their location was deemed the most critical for the response. Their location on the cross-section of the pipeline is shown in Figure 6.19, where the anchor is moving in positive Y-direction.

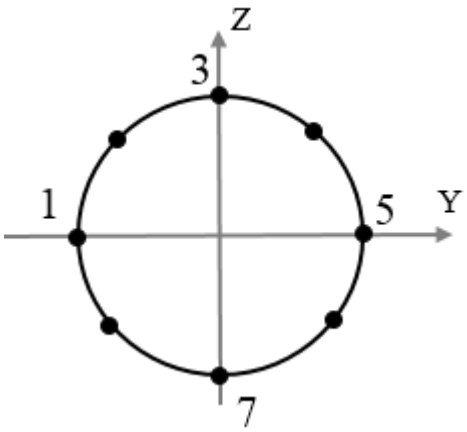

Figure 6.19: Gauss points on the cross-section

The strain plots were compared with the characteristic bending strain resistance, and the design load criteria. If the chain's breaking load was exceeded, the strain values were determined at the time step where the chain would have broken. The response of the anchor and pipeline were documented, and the anchor's response compared to the one found in the parametric study. The longitudinal strain plots, and a complete table containing the results, are found in Appendix E. Table 6.11 summarizes the most important findings.

Table 6.11: Summary of results in Elastoplastic Study

Model Name	Anchor Response	Comparison with parametric study	Strain design load exceeded
9900kg200m30in2kn660m90	Bounce over	Dissimilar	No
-660m60	Twist and slide	Dissimilar	No
9900kg200m30in10kn660m90	Bounce over	Dissimilar	No
9900kg200m40in2kn660m90	Bounce over	Similar	No
15400kg200m30in2kn743m90	Hooks	Similar	Yes
15400kg200m30in10kn743m90	Hooks	Similar	Yes
-743m60	Twist and pull over	Dissimilar	No
15400kg200m30in10kn350m90	Hooks	Similar	Yes
-350m60	Twist and slide	Dissimilar	No
-350m30	Twist and slide	Dissimilar	No
15400kg200m40in2kn743m90	Bounce over	Similar	No

For the three hooking responses, the maximum displacement of the pipeline was found by locating the time step where maximum chain breaking load was reached, and reading of the displacement in Y- and Z-direction from the 3D visualization. The results are presented in Table 6.12.

Table 6.12: Global displacement of roller element

	Global Displacement	
Model Name	**Y-direction [m]**	**Z-direction [m]**
15400kg200m30in2kn660m90	58.94	-0.66
15400kg200m30in10kn743m90	6.50	-1.03
15400kg200m30in10kn350m90	39.29	5.13

6.3.2 Discussion

Ideally, all the parameter combinations inspected in the parametric study should have been studied with a full-length elastoplastic pipeline. The trends that are discussed here are thus based on the eleven cases. It is therefore not possible to draw any overall conclusion about how accurately the parametric study manages to predict the anchor's response.

The general trend of the results imply that in the case of hooking, the longitudinal strain in the pipeline's cross-section will exceed DNV's design load and the characteristic resistance strain. This indicates that hooking exposes the cross-section to local buckling. This is the same trend as observed by Al-Warthan et al. (1993), when inspecting hooking on a 16-inch pipeline.

Furthermore, the results indicate that the strain did not exceed the design load, nor the characteristic strain, before having displaced the pipeline a minimum of 3 meters. This is in accordance with the results obtained by Sriskandarajah and Wilkins (2002).

The hooking scenarios supports the parametric study's conclusion that an anchor of 15400 kg is not large enough to hook onto a 40-inch pipeline, contradicting the results from the geometric consideration done by Vervik (2011). The case studies further support the conclusion from the parametric study that hooking occurs more frequently for smaller pipelines, as no hooking occurred for the cases applying a 40-inch pipeline.

The displacement of the pipeline shown in Table 6.12, indicate that at lower velocities, the pipeline will be displaced farther, before the anchor chain reaches its breaking load of 6.69 MN. This is the same trend reported by Vervik (2011). The 2 knot case shows a slower increase in anchor chain load, as is seen in Figure 6.20 (a), compared to the rapid increase in figure (b) where the anchor is towed at 10 knots. This slow increase in axial force, in the chain element, is due to the low velocity, shape of chain and amount of chain in contact with the seabed.

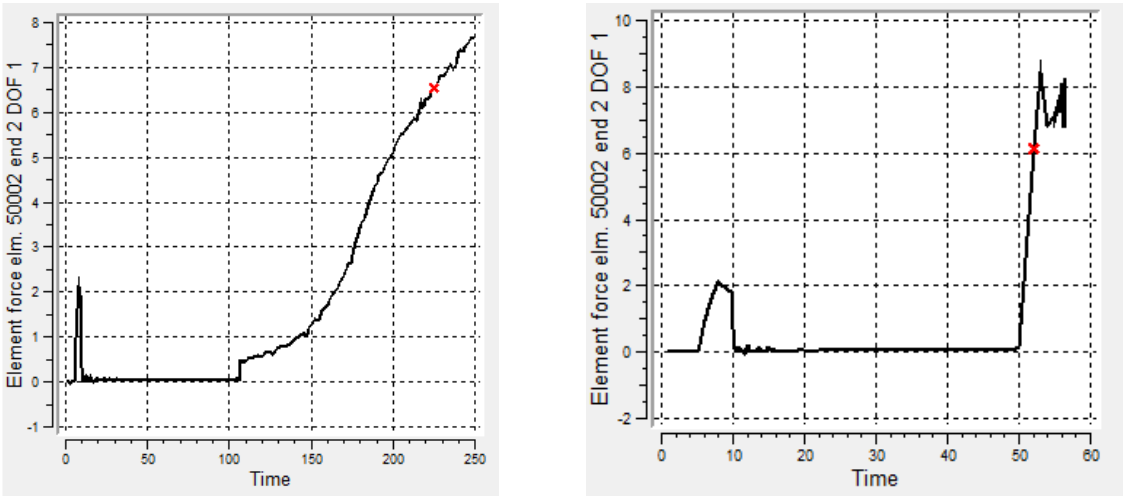

(a) 15400kg200m30in2kn743m90 (b) 15400kg200m30in10kn743m90

Figure 6.20: Element force in anchor chain element 50002
red dot indicates point of anchor chain breaking load

For both of the hooking cases where the chain length was at its maximum, the pipeline was not lifted of the seabed. However, for the case with 350 meter long chain, the pipeline was lifted approximately 5 meters vertically. The 350 meter case also displaced the pipeline further laterally, than the case applying maximum chain length of 743 meters. This indicates that the length of anchor chain is of significance for the pipeline's response. These results support the claim by Sriskandarajah and Wilkins (2002) that the consequences are worse when the anchor is towed without the chain resting on the seabed.

The negative vertical displacement in the hooking scenarios, seen in Table 6.12, indicate that the pipeline was dragged downwards into the soil. Realistic modelling of the soil was outside the scope of this work. Since this response is heavily dependent on the soil properties, it is recommended that the soil modelling should be improved in the future.

Contrary to the parametric study, the cases studied indicate no hooking response for the 60 degrees angle of attack. None of the three cases with this angle displayed any sign of hooking. A possible explanation for this is that in the case studies, pipeline displacement was allowed. The initial impact, combined with the anchor twisting, resulted in the pipeline being displaced, which reduces the pipelines ability to stop the motion of the anchor. The prolonged contact seen in the parametric study was therefore not observed in the elastoplastic cases.

In general, the parametric study was good at predicting hooking, when the angle of attack was 90 degrees. The pull over response was however not seen despite being predicted for the two cases 9900kg200m30in2kn660m90 and 9900kg200m30in10kn660m90. In all cases of brief contact, the anchor appeared to bounce over, rather than pull over. This raises some questions regarding the realism of the pull over response.

Finally, there are two issues regarding the modelling that should be noted. The first is that the friction between the anchor chain and pipeline was removed from the study, as the friction caused the pipeline to roll back and forth on the seabed. This caused instability in the system, and erroneous result. Due to time limitations, the friction between chain and pipeline was hence excluded. This friction could possibly have large effects on the pipelines and anchors response, and should be included in future studies.

The second issue concerns the models showing non-realistic behaviour. These cases all struggle with the same problem as seen in the parametric study, namely that the anchor flukes pierced the pipeline. The proposed remedy in subsection 6.2.2, applying several smaller roller elements along the circumference of the pipe, is also applicable here.

In general, the eleven cases studied support the conclusions drawn in the parametric study, that probability for hooking increases with larger anchor sizes, smaller pipelines and lower velocities. The cases studied also indicate a large probability for local buckling, when the anchor hooks onto the pipeline. This is accordance with the research done by Al-Warthan et al. (1993) and Sriskandarajah and Wilkins (2002). The results did however raise some questions regarding the hooking response, when the angle of attack was 60 degrees, and the pull over response in general.

Chapter 7

Conclusion

The anchor's response to an interaction with the pipeline was categorized as either brief or lasting contact in the parametric study. Brief contact encompasses the pull over and bounce over responses, and lasting contact includes sliding and hooking. Having categorized the responses in the parametric study, certain trends appeared. The results indicate that there is a larger probability for hooking with reduced vessel speed, smaller pipe diameter and larger anchors. This is in accord with the results found by Vervik (2011) and Wei (2015). The results from the eleven elastoplastic cases studied support this finding, by demonstrating that anchor hooking only occurs for the 30-inch pipe size. The results from the parametric study, and the eleven cases studied, also indicate that only inspecting the geometry of the anchor to predict a hooking scenario, as done by Vervik (2011), is not sufficient.

The minimum chain length study displayed that, due to drag forces exerted on the anchor chain, the minimum chain length was much larger at higher velocities. For the vessel towed at 2 knots, a chain approximately 3 meters longer than the water depth is required. For the 10 knot case the drag forces were much greater. The minimum chain length in this case must be at least 110 meters longer than the water depth. These results are however only valid when the anchor is dropped 100 meters away from the pipeline, due to the analyses not being provided enough runtime.

The parametric study indicated that the largest probability for hooking was for an attack angle of 60 degrees. This result was not found in the eleven case studies, where hooking only occurred for an angle of attack of 90 degrees. This might indicate that the hooking response, found in the parametric study, for an angle of attack of 60 degrees, is a result of the rigid body modelling of the pipeline, rather than the actual anchor's response.

All of the cases with full-length pipeline, which resulted in hooking, indicate that the longitudinal cross-sectional strain exceeds DNV's load design criteria, before the axial load in the chain surpasses its breaking load. The longitudinal strain in these cases also exceed the characteristic strain resistance. The exceedance of DNV's design criteria, and characteristic strain resistance, puts the pipeline at risk for local buckling.

The results from the eleven case studies also indicate that the pipeline is displaced laterally, a minimum of 3 meters, before exceeding the characteristic bending strain. This is in accordance with the results of Sriskandarajah and Wilkins (2002), who demonstrated that a much smaller force was needed to initiate lateral displacement, compared to local buckling.

The case studies that resulted in the anchor hooking also reveal that the global displacement of the pipeline is much greater when the anchor is towed at a lower velocity. For higher velocities, the hooking case with minimum chain length, displaced the pipeline farther, both laterally and vertically, than the anchor towed with maximum chain length. This demonstrates that the consequences are worse when the anchor is towed with minimum required chain length, as claimed by Sriskandarajah and Wilkins (2002).

Chapter 8

Further Work

The three hooking cases that exceeded DNV's design load criteria and characteristic resistance strain, indicate that the pipeline's cross-section is exposed to failure mechanisms, such as local buckling. A detailed FEA is necessary to determine which of the failure mechanisms would occur when exceeding the critical strain. The protective effect of the pipeline's coating should be included in such a study of the local effects of the impact.

A more detailed FEA study would allow for the inspection of the effect the attack point of the anchor has on the pipeline's response. That is, how would the pipeline's response differ if the anchor hits with the flukes first, or with the shank. Such a study would also give a better understanding of the dangers of brief contact. The brief contact responses could cause damage to the coating, which after time would develop into leaking or rapturing of the pipeline. A fatigue study of a pipeline damaged by brief contact might therefore be of interest.

It could also be of interest to study the pull over response in more detail. The pull over response was not seen in the eleven cases studied, so it is uncertain if this response is realistic. An analytic study of the pull over response could possible determine the realism of the response.

It is recommended that the focus of future work should be on the study of the pipeline's local response. This should be done by creating a local and detailed FEA, taking in account behaviours such as post-yield and bifurcation, and studying both the immediate reaction to the interaction and the long-term effect.

Bibliography

Al-Warthan, A. I., Chung, J. S., Huttelmaier, H. P., & Mustoe, G. G. W. (1993). *Effect of Ship Anchor Impact In Offshore Pipeline*.

Belytschko, T., Liu, W. K., Moran, B., & Elkhodary, K. I. (2014). *Nonlinear Finite Elements for Continua and Structures - Second Edition*: Wiley.

Damage to Submarine Cables Caused by Anchors. (2009). International Cable Protection Committee.

DNV-OS-E301. (2010). *DNV Offshore Standard - Position Mooring*. Høvik.

DNV-OS-F101. (2013). *DNV Offshore Standard - Submarine Pipeline System*. Høvik.

DNV-RP-F111. (2010). *DNV Recommended Practice - Interference Between Trawl Gear and Pipelines*. Høvik.

DNV Energy Report. (2010). *Recommended Failure Rates for Pipelines* (2009-1115). Retrieved from Høvik: https://www.dnvgl.com/oilgas/publications/reports.html

DNV Rules for Classification of Ships, P. C. (2011). *Hull Equipment and Safety*. Høvik.

Faltinsen, O. M. (1990). *Sea Loads on Ships and Offshore Structures*. Cambridge: Cambridge University Press.

Gjertveit, E., Berge, J. O., & Opheim, B. S. (2010). *The Kvitebjorn Gas Pipeline Repair*. Paper presented at the Offshore Technology Conference Houston, Texas.

HSE. (2009). *Guidelines for Pipeline Operators on Pipeline Anchor Hazards*. Aberdeen.

Kyriakides, S., & Corona, E. (2007). Mechanics of Offshore Pipelines, Volume I: Buckling and Collapse: Elsevier.

Langen, I., & Sigbjörnsson, R. (Eds.). (1986). *Dynamisk Analyse av Konstruksjoner*: Tapir.

MARINTEK. (2012). Fact Sheet - SIMLA. Retrieved from https://www.sintef.no/globalassets/upload/marintek/pdf-filer/factsheets/simla.pdf

Moan, T. (2003a). *TMR4190 Finite Element Modelling and Analysis of Marine Structures*. Trondheim: Department of Marine Technology, Norwegian University of Science and Technology.

Moan, T. (Ed.) (2003b). *TMR4190 Finite Element Modelling and Analysis of Marine Structures - Chapter 12 Nonlinear Analysis*. Trondheim: Department of Marine Technology, Norwegian University of Science and Technology.

SOTRA. (2014a). Stockless Anchors. Retrieved from http://www.sotra.net/products/anchors/stockless-anchors

SOTRA. (2014b). Studlink - Common Link. Retrieved from http://www.sotra.net/products/chains/studlink-common-link

Sriskandarajah, T., & Wilkins, R. (2002). *Assessment of Anchor Dragging On Gas Pipelines*.

Sævik, S. (2008). *SIMLA - Theory Manual* (700254.00.01). Retrieved from Trondheim: MARINTEK

Sævik, S. (2014). *Lecture Notes in Offshore Pipeline Technology*. Trondheim: Department of Marine Technology, Norwegian University of Science and Technology.

Sævik, S., Økland, O. D., Baarholm, G. S., & Gjøsteen, J. K. Ø. (2010). *SIMLA Version 3.15.0 User Manual*. Trondheim: Norwegian Marine Technology Research Institute

Vervik, S. (2011). *Pipeline Accidental Load Analysis.* (Master), NTNU, Trondheim.

Wei, Y. (2015). *Anchor Loads on Pipelines.* (Master), NTNU, Trondheim. (200.10.06.15)

Wong, M. B. (2009). Chapter 2 - Plastic Behavior of Structures *Plastic Analysis and Design of Steel Structures* (pp. 55-80). Boston: Butterworth-Heinemann.

Appendix

Appendix A Alterations done to Wei's Model for Parametric Study

The original short model received from Ying Wei (2015), was a draft, and not the finished product used in Wei's parameter study. This is one of the main reasons it is difficult to compare results obtained in this thesis. What follows is a list of alterations done to create the models in the parameter study. Line numbers listed below refer to the draft received from Wei.

General changes

- Wei performs one static analysis followed by a dynamic analysis. In the parametric study performed in this thesis this has been altered to one static analysis, followed by one static analysis allowing rotation of the pipeline, then one dynamic analysis and lastly sliding is allowed through a new restart of the dynamic analysis. The TIMECO cards were therefore updated to include two static TIMECO cards followed by four dynamic TIMECO cards, instead of one static and three dynamic.

Anchor changes

- Anchor geometry is updated by calculations performed in AnchorCoor.m in accord with anchor mass. Line 20 through 24 is updated with the new information.
- The flukes are modelled as one element group per fluke, instead of as one. Line 26 through 28 is updated to create these element groups. The lines will now have been shifted.
- The distributed mass and outer diameter of the anchor is updated by updating the ELPROP card for the anchor element groups. The calculations necessary are performed in the AnchorCoor.m. Lines 37, 38 and 39 are updated, and a new line is created for the new element group.

- The anchor geometry defined by NODPROP is updated. That is, lines 40-63 are updated.

Cable changes

- The cable is modelled by 1000 elements instead of 230. The cable is divided into three segments instead of four. Each segment is of equal length, but has a different number of elements. In the first segment the first element lengths are equal to 6*chain diameter. The remaining amount of elements are divided in three, 2/3 of the elements are used on the second segment, and 1/3 of the elements are on the last segment. The length of each segment will thus vary. Line 76-86 is altered.
- Line 88, ELCON card is updated as the number of elements are updated from 230 to 1000.
- Lines 94 and 96 are updated, that is the ELPROP card and MATERIAL card. All relevant calculations are performed in CableCoor.m. That is the cable distributed mass and submerged mass, and outer diameter. Bending, axial and torsional stiffness is updated in accord with the calculations.

Pipeline changes

- Lines 115, ELPROP card is updated with correct outer diameter, thickness, distributed dry and submerged mass calculated in PipeMass.m.
- A new line is inserted to model the rotation of the pipeline. This is done with a CONSTR card. A new time history was created for this rotation. The pipeline is fully rotated before the onstart of the dynamic analysis.

Seabed changes

- New contact element groups had to be made for the two fluke segments. In addition, a new contact element was created for the cable.
- The contact elements for the cable were rotated by 90 degrees by use of ELORIENT.
- The friction coefficient defined in the MATERIAL card were altered from 0.3 in X-direction to 1.0.

- The maximum value for the material curve for soily was reduced to make the soil slightly softer.

Roller/Contact element changes

- Ying Wei had for the short model modelled the roller elements as small roller elements along the cross-sectional area of the pipeline. This was replaced with four roller element groups, modelled as 100 meter long and attached to the pipeline.
- The contact between the cable and the pipeline was updated from CONTACT to ISOCONTACT with friction coefficient of 0.38.

Sliding Analysis

- Each model requires a different restart of the sliding analysis.
- To allow sliding boundary conditions and constrains were adjusted. All boundary conditions for the anchor are released, that is lines 71, 72 and 73 had to be altered. The anchor elements are constrained in direction 1 by constraining the fluke to the shank. All cable elements are also released in direction 1, with the exception of the top element.

Appendix B Structure of MATLAB scripts

Parameter Study

An unfinished model created by Wei (2015) was the starting point for the models. This model was altered using FlexEdit and made into a standard input file that could easily be altered using MATLAB. A list of all alterations is presented in Appendix A. What follows is a description of the MATLAB scripts created to perform the parametric study efficiently. These are presented so that if it is desirable to inspect other parameters than those in this study, it is easily done.

The RunSIMLAMainFile.m script is created such that it writes the .sif file by collecting information regarding the parameters from two Excel sheets, performing relevant calculations and substituting lines in the standard input model before executing the SIMLA analysis. The general structure of the MATLAB script is summarised in Figure B.1 and is described below.

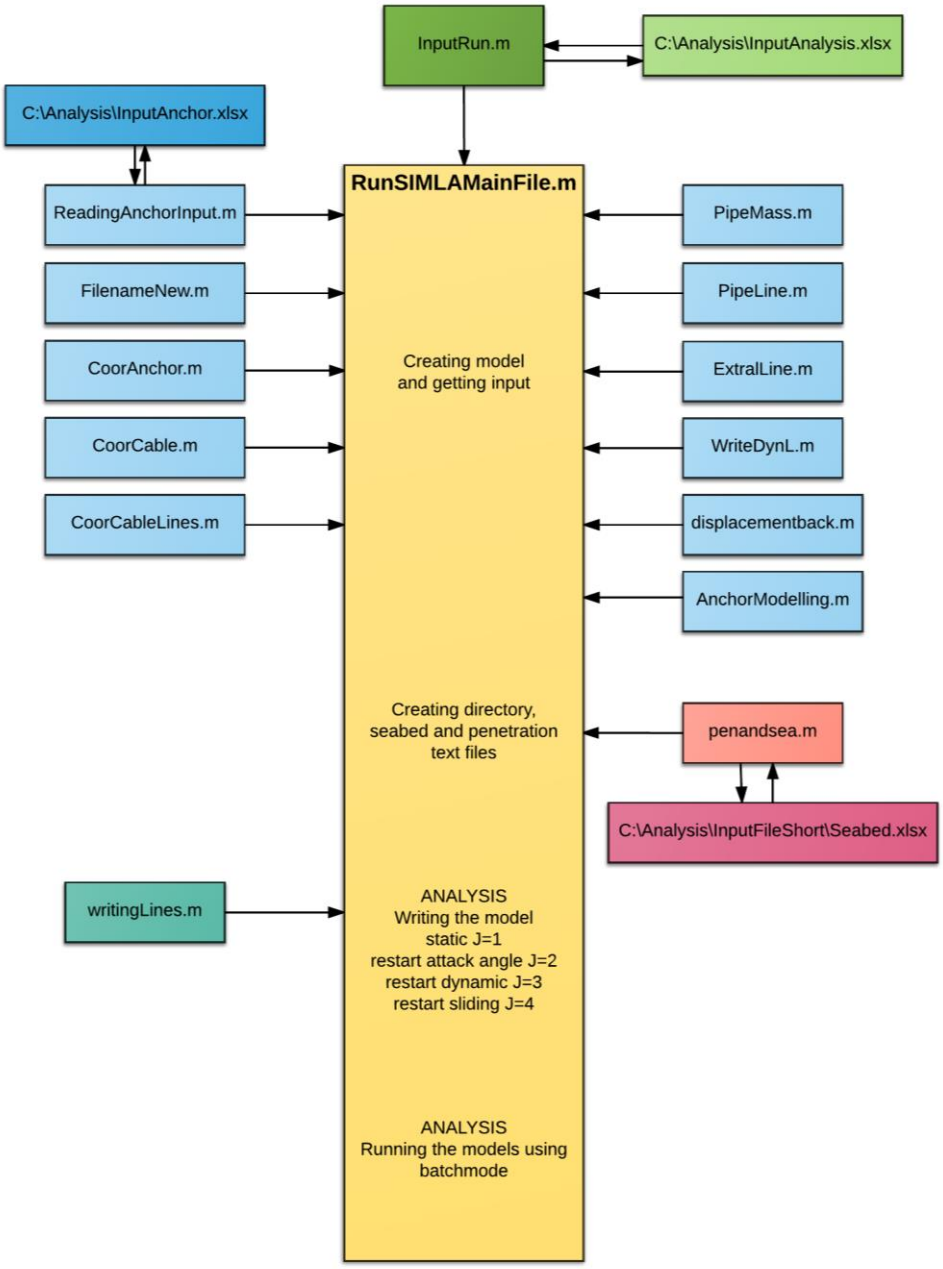

Figure B.1: Structure of MATLAB script, parametric study

InputRun.m starts with collecting relevant information regarding which model to create from "InputAnalysis". This Excel-document contains information about anchor mass, pipe diameter, vessel velocity and angle of attack. Water depth is defined in InputRun.m, and this script also present the possibility for the user to define a chain length. InputRun.m then executes the function RunSIMLAMainFile.m that in return executes ReadingAncorInput.m, which collects the anchor geometry, maximum chain length, chain diameter and breaking load corresponding to anchor mass defined in "InputAnalysis". RunSIMLAMainFile.m then proceeds to execute the other functions seen in Figure B.1.

FilenameNew.m generates the filename in correspondence with Figure 5.3. The anchor geometry is implemented by CoorAnchor.m, which calculates the new coordinates for the anchor. CoorCable.m calculates the coordinates for the cable based on the length of the cable. The new cable coordinates are written into lines using CoorCableLines.m. PipeMass.m and PipeLine.m calculate the mass and buoyancy of the pipe and writes the new lines. ExtraLine.m defines the lines related to vessel speed, rotation and span height of the pipeline. The lines describing the dynamic aspects of the model are created in WriteDynL.m.

After the new lines have been written in MATLAB, a new directory is created with the same name as the model. In this directory, penandsea.m writes the seabed.txt file in accord with chosen water depth, and a penetration.txt file. WritingLines.m then writes the static model and places it in this directory. The model, now a .sif file, is executed by RunSIMLAMainFile.m and creates a .raf file. Once the static analysis is finished, a short analysis of two seconds is carried out to rotate the pipe if the angle of attack is different from 90 degrees. SIMLA is again executed and the new information is written to the .raf file. This procedure is repeated for the dynamic model with a restart command if the angle of attack is different from 90 degrees and sliding is expected. A more detailed description of the calculations done in the scripts are described in the text below, and can be seen in Appendix C.

Minimum Chain Length Study

As with the parametric study a MATLAB script was created. Many of the same functions used in the parametric study were applied. An overview of the MATLAB scripts is shown in Figure B.2. The scripts noted with DvL have been altered slightly to the ones described previously. This mainly to ensure that the anchor chain starts of as a straight line, and only two analysis sequences are carried out. DvLFilenameNew.m generates the filename in correspondence with Figure 5.4.

The last part of the new MATLAB script creates .mpf files with all relevant information regarding the displacement of the nodes in the anchor chain in Y- and Z-direction. This information is then processed and used to create plots of the anchor chain at different time intervals.

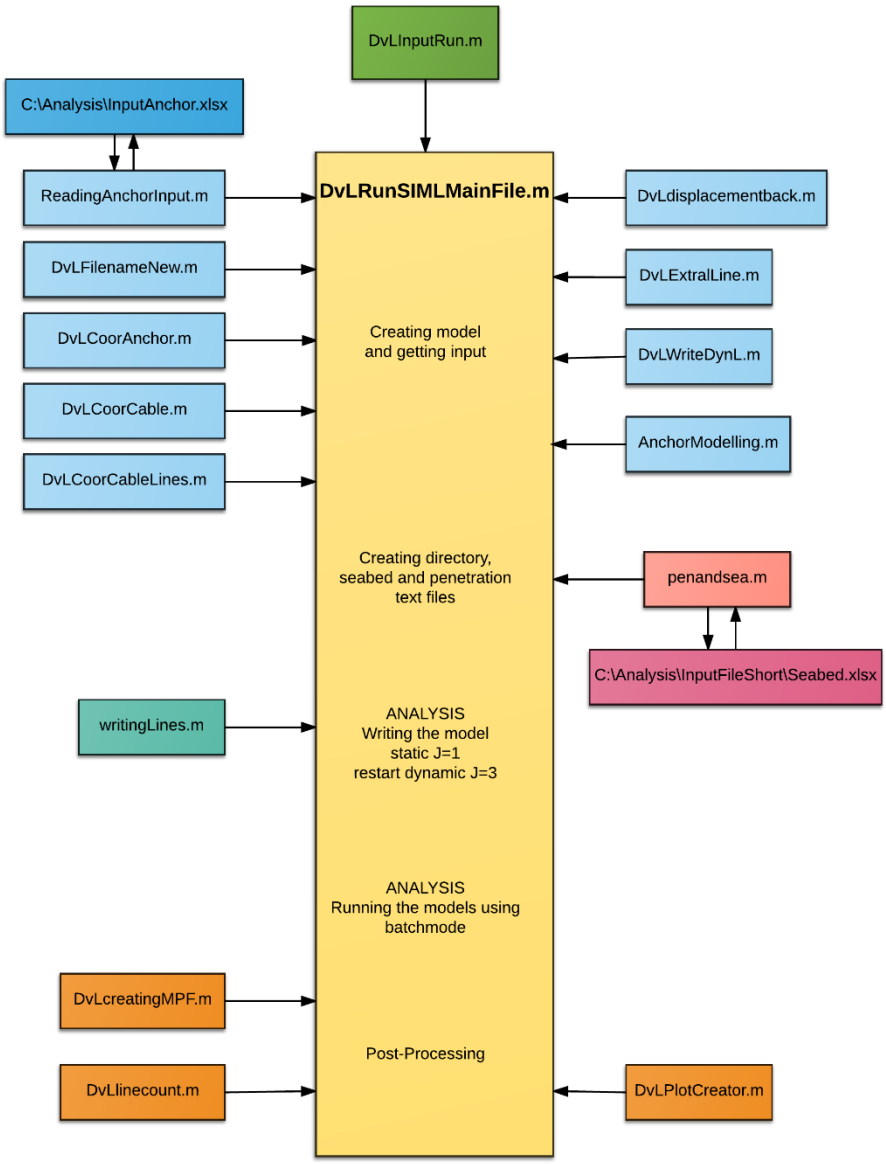

Figure B.2: Structure of MATLAB scripts, minimum chain length study

Appendix C Calculations for Pipe Elements

All of the calculations below are performed in the MATLAB scripts below with the units MN and m. All units of mass are thus given as Mkg/m to ensure that MN is obtained. That is the masses are multiplied with 10^{-6}. This is not shown in the tables below.

Anchor

M_{total} is the total dry mass of the anchor, $\rho_{seawater}$ is the seawaters density and ρ_{steel} is the density of steel. *F*, *E* and *A* are dimensions in accord with SOTRA. Node 40011 has a vertical distance from the seabed of 0.2 meters. The starting location of the anchor is dependent on the vessel velocity. The pipe is located at -100 meters in Y-direction, while the anchor is placed at 100 meters if the vessel velocity is 10 knots, or -25 meters is the vessel velocity is 2 knots. The coordinates for node 40011 is then for the 10 knots case: [100, 100, -(depth-0.2)]. These coordinates are defined as [x0, y0, z0] in the calculations.

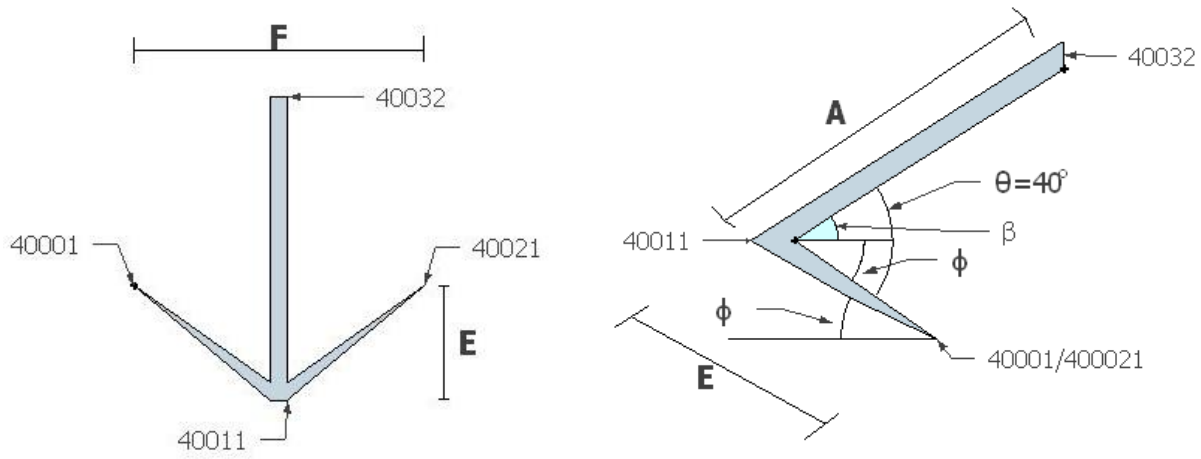

Figure C.1: Simplified Anchor Geometry

Table C.1: Anchor calculations

Description	Calculation	
φ	$\varphi = \sin^{-1}\left(\frac{0.2}{E}\right)$	(C-1)
β	$\beta = 40° - \varphi$	(C-2)
Distributed dry mass of anchor	$m_{dry} = \frac{M_{total}}{\sqrt{\left(\frac{F}{2}\right)^2 + E^2} \cdot 2 + A} \left[\frac{kg}{m}\right]$	(C-3)
Distributed submerged mass of anchor	$m_{submerged} = \frac{M_{total}\left(1 - \frac{\rho_{seawater}}{\rho_{steel}}\right)}{\sqrt{\left(\frac{F}{2}\right)^2 + E^2} \cdot 2 + A} \left[\frac{kg}{m}\right]$	(C-4)
Coordinates 40001	$\left[x0 - \frac{F}{2}\ ,\ \ y0 - E\ , -depth\right]$	(C-5)
Coordinates 40021	$\left[x0 + \frac{F}{2},\ \ y0 - E, -depth\right]$	(C-6)
Coordinates 40011	$[x0,\ \ y0, -depth + 0.2]$	(C-7)

Cable

The area and second moment of inertia are multiplied by two instead of four to not make the chain too stiff when calculating axial, bending and torsion stiffness. This is despite the chain being modelled with a diameter of four times the radius.

Table C.2: Cable calculations

Description	**Calculation**	
Radius of chain $[m]$	$r_c = \frac{ChainDiameter}{2}$	(C-8)
Chain area $[m^2]$	$A_c = 2 \cdot \pi r_c^2$	(C-9)
Second moment of inertia $[m^4]$	$I_c = 2 \cdot \pi \frac{r_c^4}{4}$	(C-10)
Polar moment of inertia $[m^4]$	$I_p = 2 \cdot \frac{\pi r^4}{2}$	(C-11)
Axial stiffness $[N]$	$EA = E_{steel} A_c$	(C-12)
Bending stiffness $[Nm^2]$	$EI = E_{steel} I_c$	(C-13)
Torsion stiffness $[Nm^2]$	$GI = GI_p$	(C-14)
Chain mass $[kg/m]$	M_{dry}	(C-15)
Chain volume $[m^3/m]$	$V_c = \frac{M_{dry}}{\rho_{steel}}$	(C-16)
Buoyancy mass $[kg/m]$	$M_{buoy} = V_c \rho_{seawater}$	(C-17)
Submerged mass $[kg/m]$	$M_{sub} = M_{dry} - M_{buoy}$	(C-18)
Damping ratio [-]	$\xi = \frac{c}{c_{critical}}$	(C-19)
Critical damping	$c_{critical} = 2\sqrt{mk}$	(C-20)
Damping	$c = 2\xi\sqrt{mk}$	(C-21)

Pipeline

Table C.3: Pipeline calculations

Description	Calculation	
Outer diameter steel pipe $[m]$	c	(C-22)
Thickness of steel wall $[m]$	$t = \frac{c}{35}$	(C-23)
Outer radius of steel pipe $[m]$	$r_{sout} = \frac{c}{2}$	(C-24)
Total outer radius of pipe $[m]$	$R_{out} = r_{sout} + t_{corr} + t_{conc}$	(C-25)
Inner radius $[m]$	$r_{in} = r_{sout} - t$	(C-26)
Area steel pipe $[m]$	$A_{pipe} = \pi(r_{sout}^2 - r_{in}^2)$	(C-27)
Second moment of inertia $[m^4]$	$I_x = \frac{\pi}{4}(r_{sout}^4 - r_{in}^4)$	(C-28)
Polar moment of inertia $[m^4]$	$I_p = \frac{\pi}{2}(r_{sout}^4 - r_{in}^4)$	(C-29)
Axial stiffness $[N]$	$EA = E_{steel}A_{pipe}$	(C-30)
Bending stiffness $[Nm^2]$	$EI = E_{steel}I_x$	(C-31)
Torsion stiffness $[Nm^2]$	$GI = GI_p$	(C-32)
Steel pipe mass $[kg/m]$	$m_{steel} = \frac{\pi}{4}(c^2 - (c - 2t)^2)\rho_{steel}$	(C-33)
Corrosion layer mass $[kg/m]$	$m_{corr} = \pi((r_{sout} + t_{corr})^2 - {r_{sout}}^2)\rho_{corr}$	(C-34)
Concrete layer mass $[kg/m]$	$m_{conc} = \pi({R_{out}}^2 - (r_{sout} + t_{corr})^2)\rho_{conc}$	(C-35)

Content mass $[kg/m]$	$m_{cont} = \pi {r_{in}}^2 \rho_{cont}$	(C-36)
Buoyancy mass [kg/m]	$m_{buoy} = \pi {R_{in}}^2 \rho_{seawater}$	(C-37)
Total pipe dry mass $[kg/m]$	$M_{total} = m_{steel} + m_{corr} + m_{conc} + m_{cont}$	(C-38)
Submerged mass $[kg/m]$	$m_{sub} = M_{total} - m_{buoy}$	(C-39)

Appendix D Results from the Parameter Study

Table D.1: Parameter study results

	Realistic Yes/No	**Extra EI**	**Hook Yes/No**	**Sliding Yes/No**	**Twist Yes/No**	**Bounce over Yes/No**	**Pull over Yes/No**
3780kg200m 30in2kn523m90	Yes	-	No	No	-	**Yes**	No
-60	No	-	No	No	-	**Yes**	No
-30	Yes	-	No	**Yes**	No	No	No
3780kg200m 30in10kn523m90	No	-	No	No	-	**Yes**	No
-60	No	-	No	No	-	**Yes**	No
-30	No	-	No	No	-	**Yes**	No
3780kg200m 40in2kn523m90	No	-	No	No	-	No	**Yes**
-60	No	-	No	No	-	**Yes**	No
-30	No	-	No	No	-	**Yes**	No
3780kg200m 40in10kn523m90	No	-	No	No	-	**Yes**	No
-60	No	-	No	No	-	**Yes**	No
-30	No	-	No	No	-	**Yes**	No
4890kg200m 30in2kn550m90	No	-	No	No	-	**Yes**	No
-60	No	-	No	No	-	**Yes**	No
-30	Yes	-	No	**Yes**	No	No	No
4890kg200m 30in10kn550m90	Yes	-	No	No	-	**Yes**	No
-60	No	-	No	No	-	**Yes**	No
-30	No	-	No	No	-	**Yes**	No
4890kg200m 40in2kn550m90	No	-	No	No	-	No	**Yes**
-60	No	-	No	No	-	**Yes**	No
-30	No		Inconclusive				
4890kg200m 40in10kn550m90	No	-	No	No	-	**Yes**	No
-60	No	-	No	No	-	**Yes**	No
-30	No	-	No	No	-	**Yes**	No
6000kg200m 30in2kn578m90	Yes	-	No	No	-	**Yes**	No
-60	Yes	-	**Yes**	-	**Yes**	No	No
-30	Yes	Yes	-	**Yes**	No	No	No
6000kg200m 30in10kn578m90	Yes	-	No	No	-	**Yes**	No

-60	Yes	-	No	No	**Yes**	**Yes**	No
-30	No	-	No	No	-	**Yes**	No
6000kg200m 40in2kn578m90	No	-	No	No	-	No	**Yes**
-60	No		Inconclusive				
-30	Yes	-	-	**Yes**	**Yes**	No	No
6000kg200m 40in10kn578m90	No	Yes	No	No	-	Yes	No
-60	No	Yes	Inconclusive				
-30	No	Yes	Inconclusive				
7800kg200m 30in2kn633m90	Yes	-	No	No	-	**Yes**	No
-60	Yes	-	**Yes**	-	**Yes**	No	No
-30	Yes	-	-	**Yes**	**Yes**	No	No
7800kg200m 30in10kn633m90	Yes	-	**Yes**	-	-	No	No
-60	No	-	No	No	-	No	**Yes**
-30	Yes	-	-	**Yes**	**Yes**	No	**Yes**
7800kg200m 40in2kn633m90	No	-	No	No	-	No	**Yes**
-60	No	-	Inconclusive				
-30	Yes	-	-	**Yes**	No	No	No
7800kg200m 40in10kn633m90	No	-	No	No	-	**Yes**	No
-60		-	Inconclusive				
-30	Yes	-	-	**Yes**	**Yes**	No	**Yes**
9900kg200m 30in2kn660m90	Yes	-	No	No	No	No	**Yes**
-60	Yes	-	**Yes**	-	**Yes**	No	No
-30	Yes	-	-	**Yes**	**Yes**	No	No
9900kg200m 30in10kn660m90	Yes	Yes	No	No	-	No	**Yes**
-60	No	Yes	No	No	-	No	**Yes**
-30	Yes	Yes	No	**Yes**	**Yes**	No	**Yes**
9900kg200m 40in2kn660m90	No	No	No	No	-	No	**Yes**
-60		-	Inconclusive				
-30	Yes	-	-	**Yes**	**Yes**	No	No
9900kg200m 40in10kn660m90	Yes	-	No	No	-	**Yes**	No
-60		-	Inconclusive				
-30	Yes	-	-	**Yes**	**Yes**	No	No
15400kg200m 30in2kn660m90	Yes	-	**Yes**	-	-	No	No
-60	Yes	-	**Yes**	-	**Yes**	No	No
-30	Yes	-	-	**Yes**	No	No	No

15400kg200m 30in10kn660m90	Yes	-	**Yes**	-	-	No	No
-60	Yes	-	**Yes**	-	-	No	No
-30	Yes	-	-	**Yes**	**Yes**	No	**Yes**
15400kg200m 40in2kn660m90	Yes	-	No	No	-	**Yes**	No
-60	Yes	-	**Yes**	-	**Yes**	No	No
-30	Yes	-	-	**Yes**	No	No	No
15400kg200m 40in10kn660m90	Yes	Yes	No	No	-	**Yes**	No
-60	Yes	Yes	**Yes**	-	**Yes**	No	**Yes**
-30	Yes	Yes	-	**Yes**	**Yes**	No	**Yes**

Appendix E Results from Elastoplastic Case Studies

Anchor chain break load for 9900 kg: 4.50 MN
Anchor chain break load for 15400 kg: 6.69 MN

Table E.1: Results for the cases studied

		Response				
	Realistic	**Predicted Anchor**	**Anchor**	**Pipeline**	**Anchor Chain Breaks**	**Exceeds DNVs Strain Criteria**
9900kg200m 30in2kn660m90	Yes	Pull over	Bounce over	Insignificant	No	No
-660m60	No	Hook and twist	Twist and slide	Insignificant	No	No
9900kg200m 30in10kn660m90	No	Pull over	Bounce over	Insignificant	No	No
9900kg200m 40in2kn660m90	No	Bounce over	Bounce over	Bulk	No	No
15400kg200m 30in2kn743m90	Yes	Hooks	Hooks	Globally displaced	Yes	No
15400kg200m 30in10kn743m90	Yes	Hooks	Hooks	Globally displaced	Yes	Yes
-743m60	Yes	Hook	Slide, twist and pull over	Insignificant	No	No
15400kg200m 40in2kn743m90	Yes	Bounce over	Bounce over	Insignificant	No	No
15400kg200m 30in10kn350m90	Yes	Hook	Hook and lift	Globally displaced	No	Yes
-350m60	Yes	Hook	Twist and slide	Very small displacement	No	No
-350m30	No	Slide, twist and pull over	Twist and slide	Small displacement	No	No

The red dot in the plots either signify the moment of maximum breaking load, or the moment the analysis becomes unrealistic.

9900kg200m30in2kn660m90

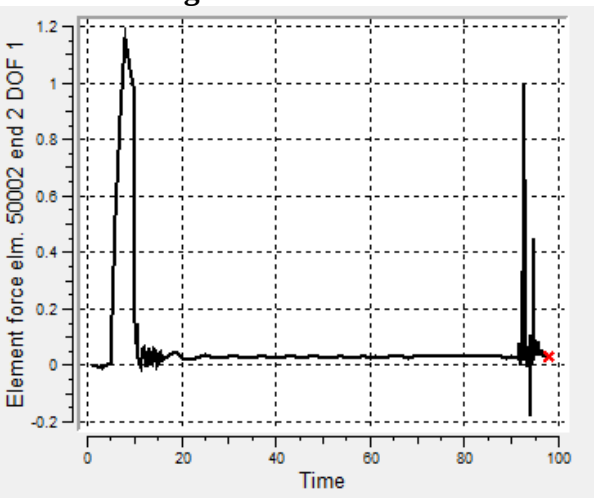

(a) Axial force in anchor chain element 50002

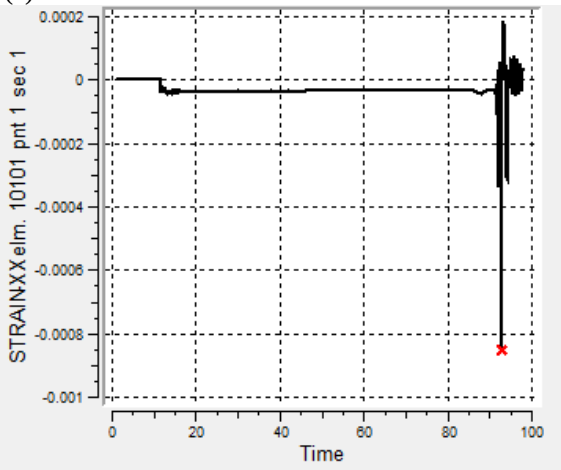

(b) Longitudinal strain in Gauss point 1

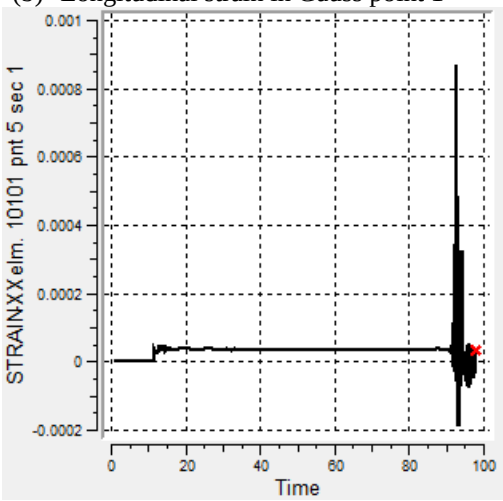

(c) Longitudinal strain in Gauss point 5

9900kg200m30in10kn660m90

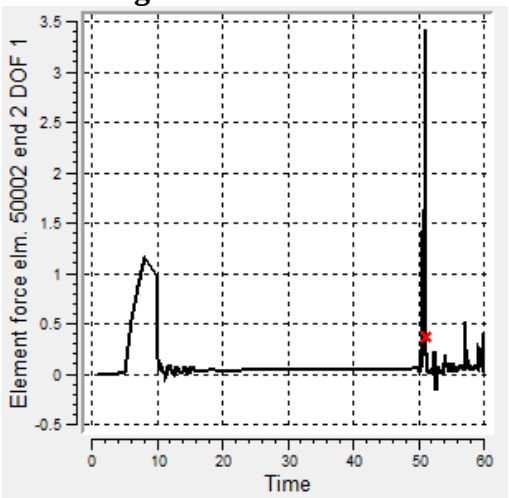

(d) Axial force in anchor chain element 50002

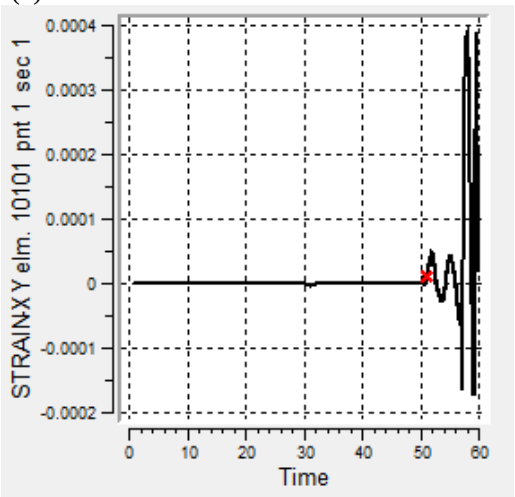

(e) Longitudinal strain in Gauss point 1

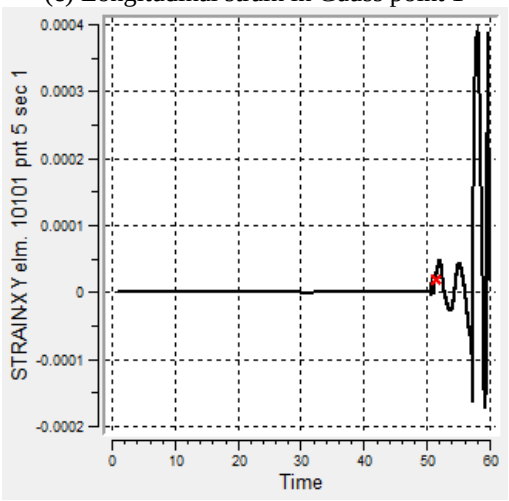

(f) Longitudinal strain in Gauss point 5

Figure E.1: Plots for 9900kg200m30in2kn660m90 & 9900kg200m30in10kn660m90

9900kg200m40in2kn660m90

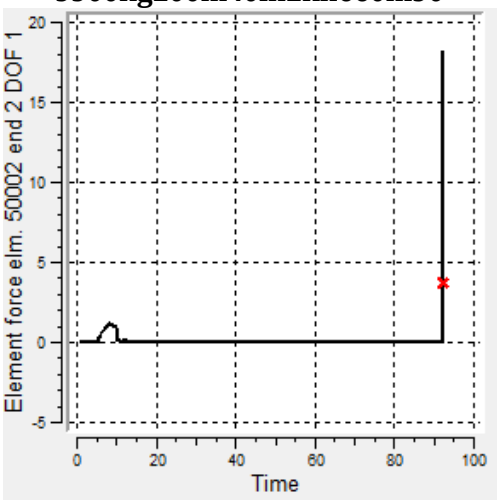

(a) Axial force in anchor chain element 50002

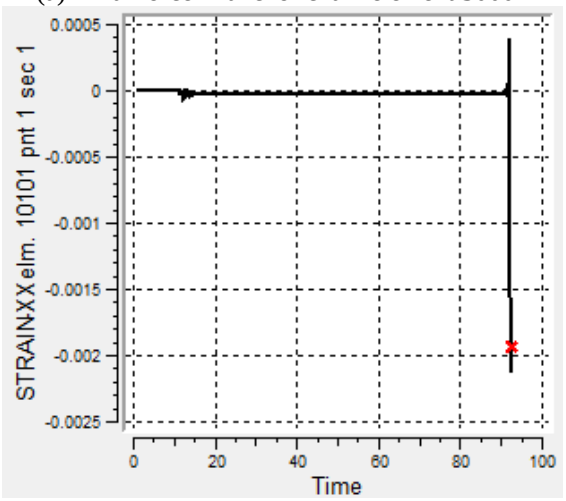

(b) Longitudinal strain in Gauss point 1

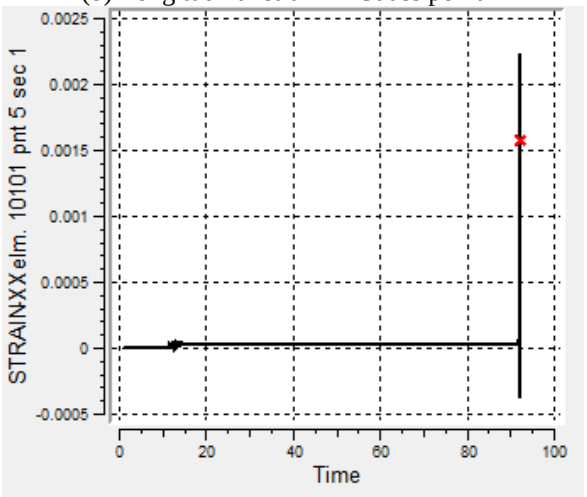

(c) Longitudinal strain in Gauss point 5

9900kg200m30in2kn660m60

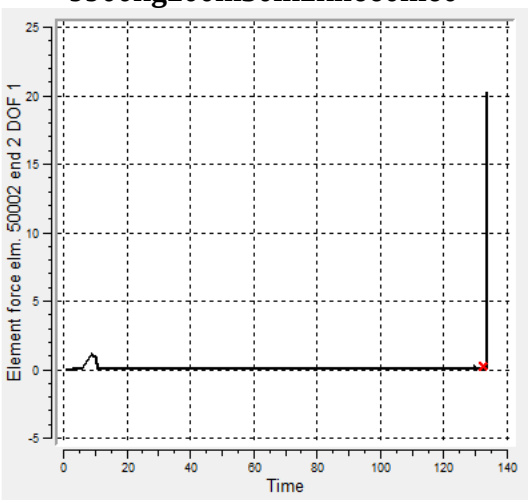

(d) Axial force in anchor chain element 50002

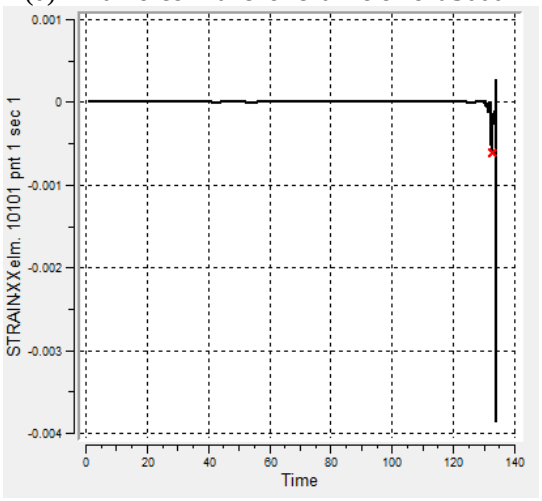

(e) Longitudinal strain in Gauss point 1

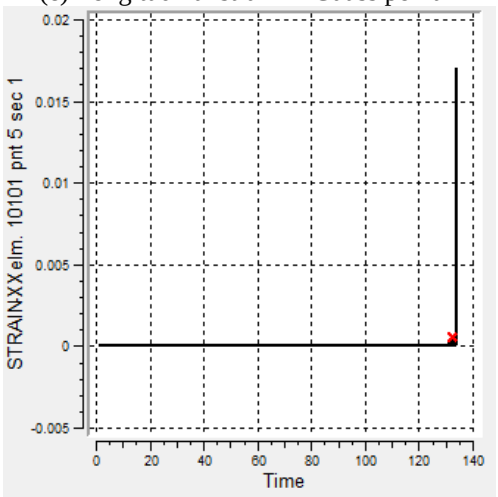

(f) Longitudinal strain in Gauss point 5

Figure E.2: Plots for 9900kg200m40in2kn660m90 & 9900kg200m30in2kn660m60

15400kg200m30in2kn743m90

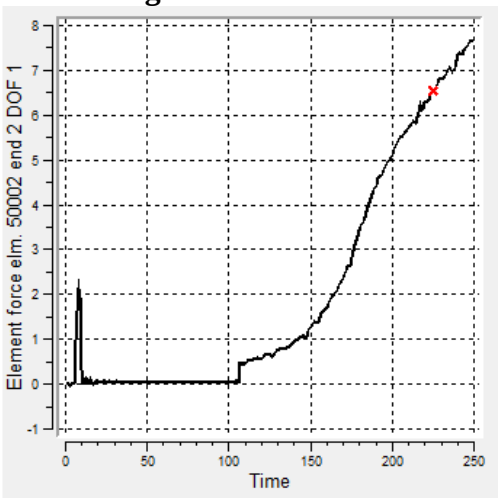

(a) Axial force in anchor chain element 50002

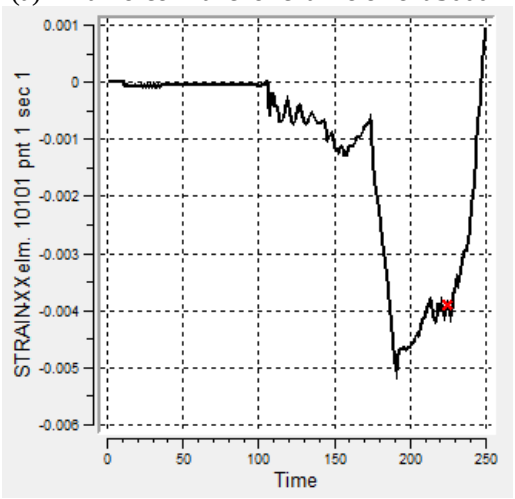

(b) Longitudinal strain in Gauss point 1

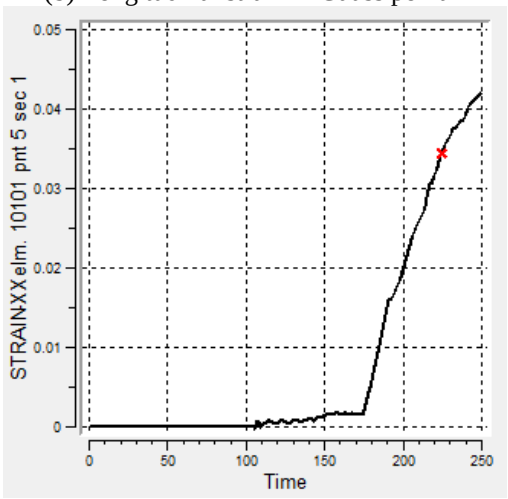

(c) Longitudinal strain in Gauss point 5

15400kg200m30in10kn743m90

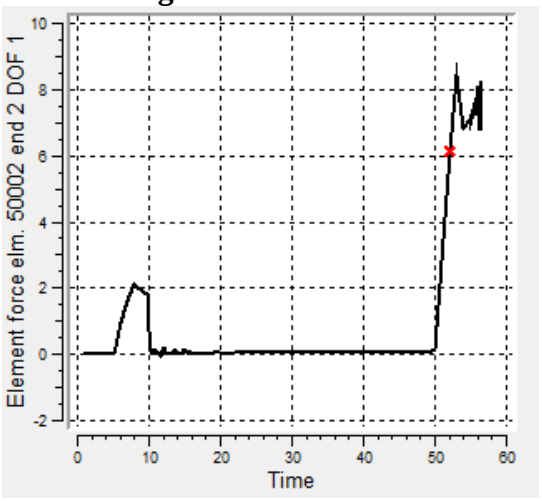

(d) Axial force in anchor chain element 50002

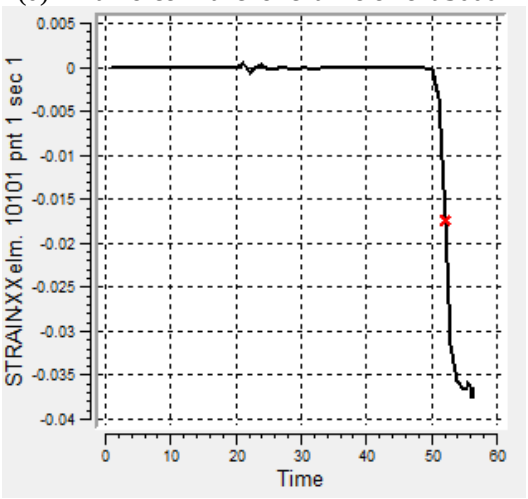

(e) Longitudinal strain in Gauss point 1

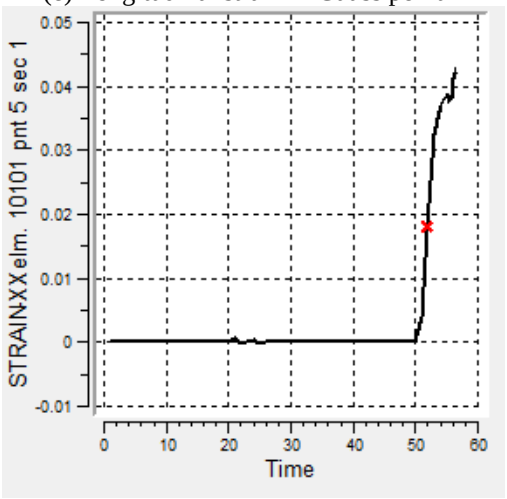

(f) Longitudinal strain in Gauss point 5

Figure E.3: Plots for 15400kg200m30in2kn743m90 & 15400kg200m30in10kn743m90

15400kg200m40in2kn743m90

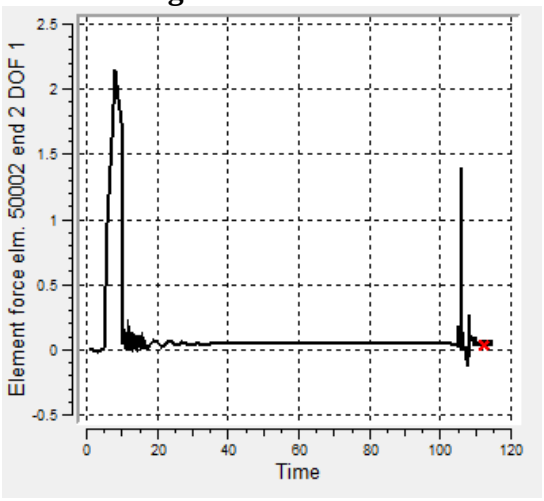

(a) Axial force in anchor chain element 50002

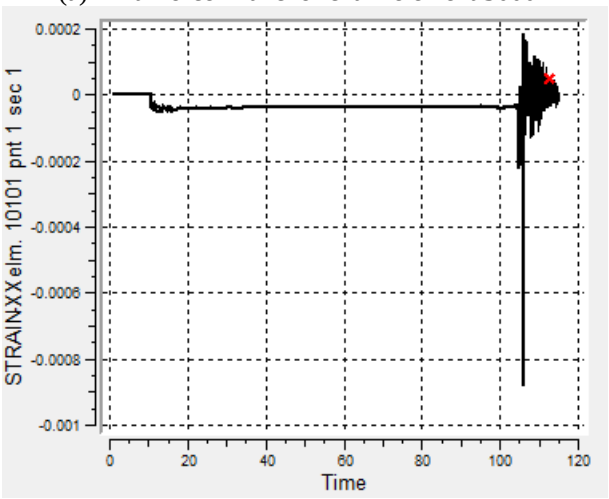

(b) Longitudinal strain in Gauss point 1

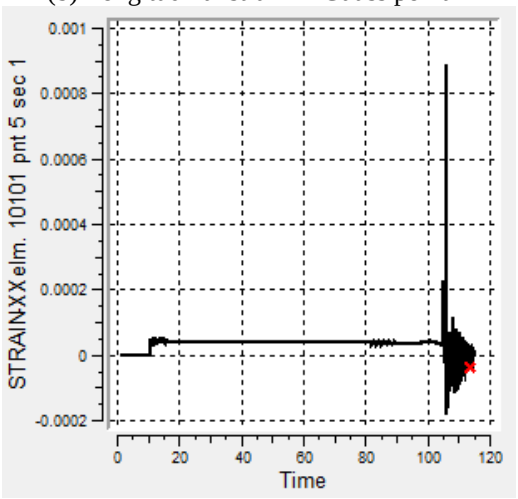

(c) Longitudinal strain in Gauss point 5

15400kg200m30in10kn743m60

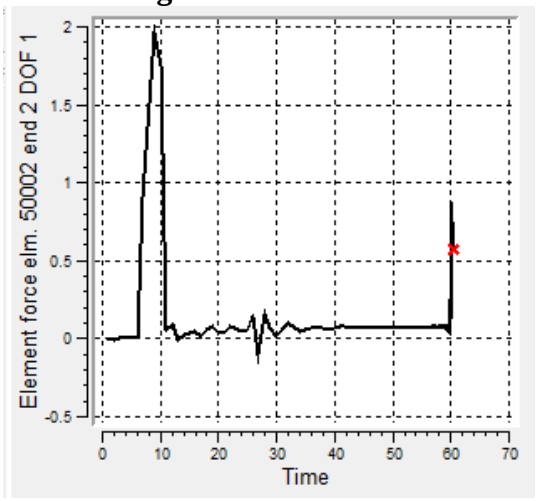

(d) Axial force in anchor chain element 50002

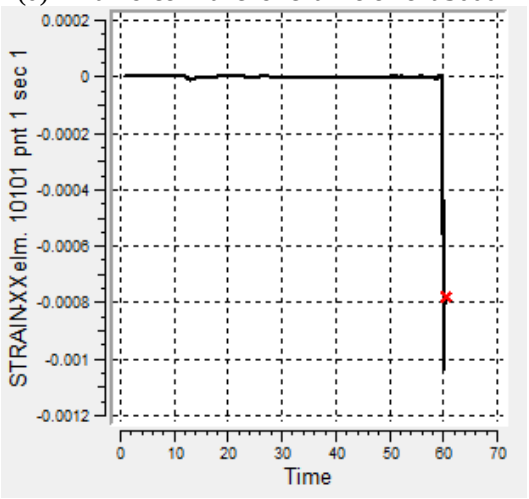

(e) Longitudinal strain in Gauss point 1

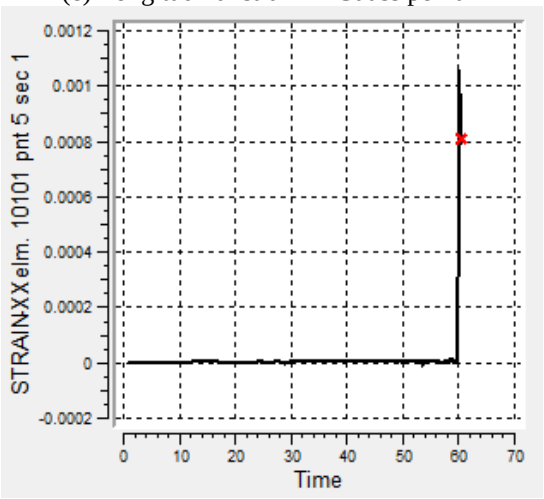

(f) Longitudinal strain in Gauss point 5

Figure E.4: Plots for 15400kg200m40in2kn743m90 & 15400kg200m30in10kn743m60

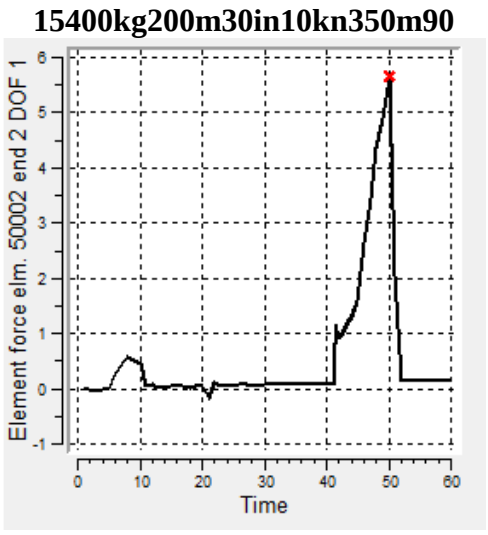

(a) Axial force in anchor chain element 50002

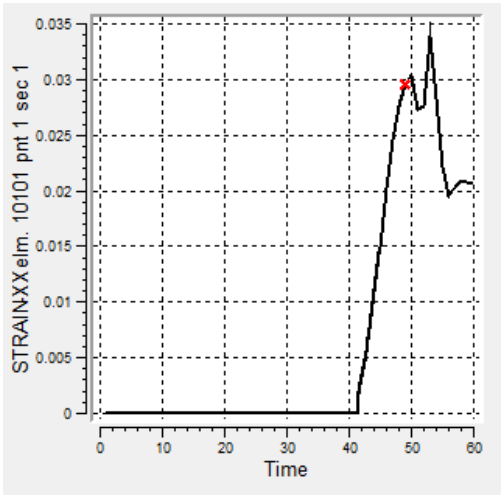

(b) Longitudinal strain in Gauss point 1

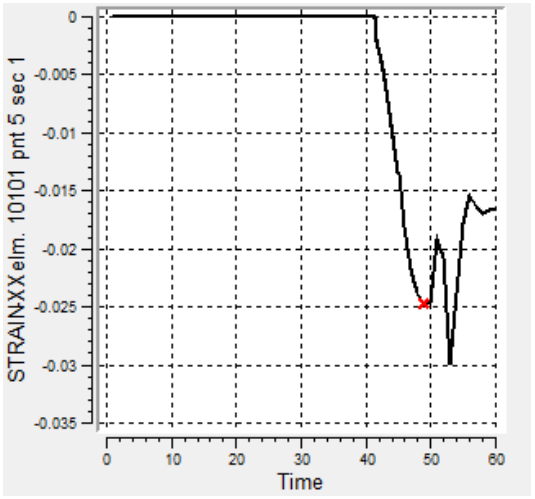

(c) Longitudinal strain in Gauss point 5

Figure E.5: Plots for 15400kg200m30in10kn350m90

15400kg200m30in10kn350m60

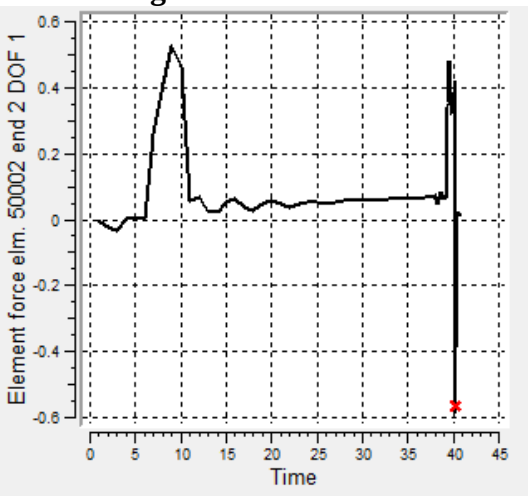

(a) Axial force in anchor chain element 50002

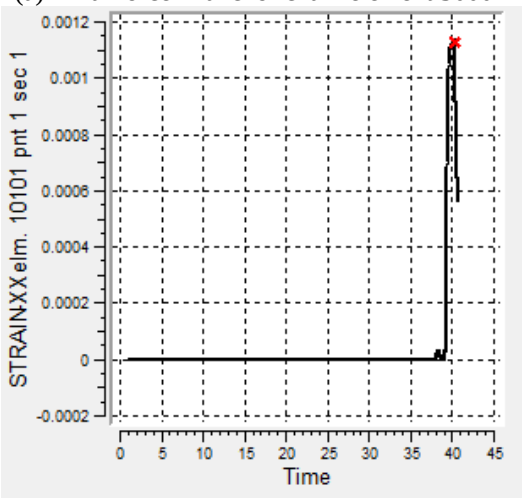

(b) Longitudinal strain in Gauss point 1

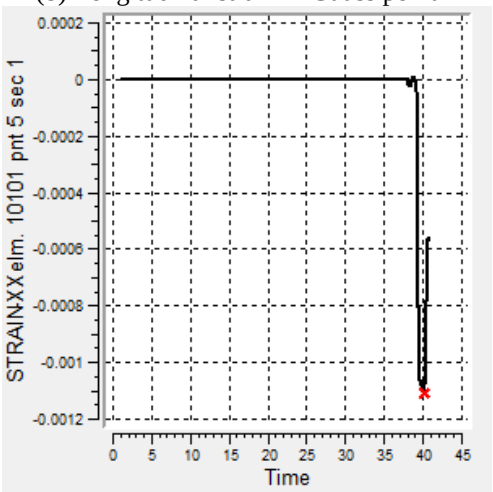

(c) Longitudinal strain in Gauss point 5

15400kg200m30in10kn350m30

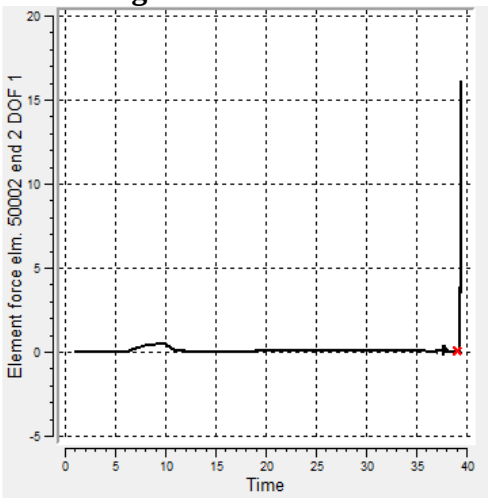

(d) Axial force in anchor chain element 50002

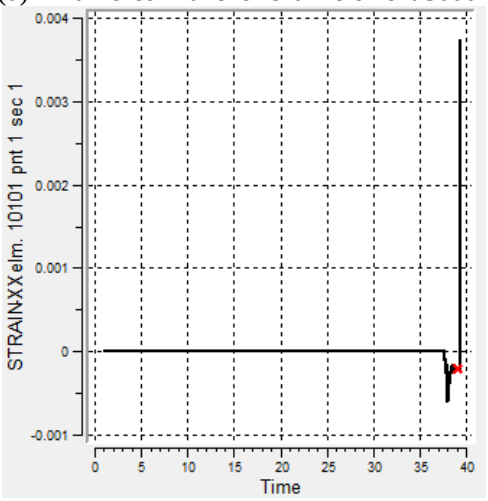

(e) Longitudinal strain in Gauss point 1

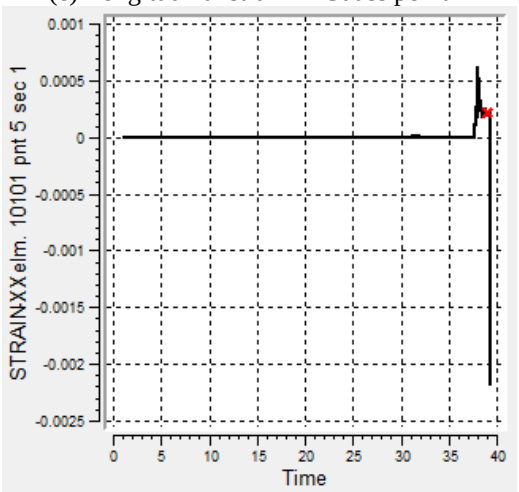

(f) Longitudinal strain in Gauss point 5

Figure E.6: Plots for 15400kg200m30in10kn350m60 & 15400kg200m30in10kn350m30

Appendix F MATLAB scripts and Input Files

The MATLAB scripts, Excel-sheets and Input Files for the case studies have all been uploaded as an electronical appendix on NTNU's DIVA portal. The structure of the MATLAB scripts are explained in Appendix B. Please see NTNU's DIVA for the attached .zip file which contains:

Table F.1: Content of electronical Appendix F, uploaded to DIVA

Folder	**Content**
Case_Studies	All input files to the eleven cases studied. See README.txt in folder on how to run the analyses.
Minimum_Chain_Length	All MATLAB files, and the modified input file, to find minimum chain length. Excel-sheet containing all information relevant for modelling of anchor and anchor chain is also uploaded. See README.txt in folder for more details.
Parametric_Study	All MATLAB files and modified input file to perform the parametric study. Excel-sheet containing all information relevant for modelling of anchor and anchor chain, and the excel-sheet containing all input parameters, are also uploaded. See README.txt in folder for more details.
Poster	Contribution to the poster contest held at Marinteknisk Senter.